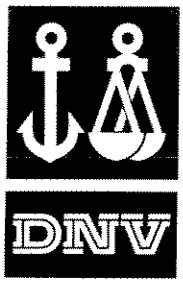

TECHNICAL REPORT

RELIABILITY-BASED RESIDUAL STRENGTH CRITERIA FOR CORRODED PIPES

RESIDUAL STRENGTH OF CORRODED AND DENTED PIPES
JOINT INDUSTRY PROJECT

REPORT NO. 93-3637

DET NORSKE VERITAS INDUSTRY AS

DET NORSKE VERITAS
INDUSTRY AS

TECHNICAL REPORT

Date:	Organisational unit:
25 October 1995	Systems and Components
Approved by: Einar Tore Moe, Head of Section	
Client: Statoil, Phillips, Petrobras, MMS, NPD, NTNF & DNV	Client ref.:
	Project No.: 21410020

Department for Subsea and Structures

Veritasveien 1
N-1322 HØVIK,Norway
Tel. (+47) 67 57 72 50
Fax. (+47) 67 57 74 74

Summary:

This study is carried out in order to provide operators, regulation and classification bodies with refined residual strength criteria for corroded pipes:

Longitudinal corrosion
Modifications to ASME B31G for corroded pipes are suggested to reduce the scatter in the strength prediction and extend its applicability for new problems. Experimental databases are established and finite element analyses are carried out for longitudinally corroded pipes under combined loads.

Circumferential corrosion
Possible residual strength equations for pipes containing girth weld corrosion are discussed and compared with tests and analyses. Finite element analyses are carried out for circumferentially corroded pipes under combined loads.

Safety factors
Procedures for reliability based calibration of safety factors for residual strength assessment are discussed.

In addition, discussions are made on possible applications to:

- Decision of operating pressure
- Re-qualification and life time extension
- Wall-thickness assessment in pipeline design

Report No.:	Subject Group:
93-3637	

Report title:
Reliability-Based Residual Strength Criteria for Corroded Pipes.

Joint Industry Project Residual Strength of Corroded and Dented Pipes

Work carried out by:
Yong Bai and Ola Hallvard Bjørnøy

Work verified by:
Inge Lotsberg and Per Gjerde

Date of last revision:	Rev.No.:	Number of pages:
		174

Indexing terms

Corrosion
Pipelines
Re-qualification
Residual Strength

Table of Contents *Page*

1 SUMMARY AND CONCLUSIONS

This report provides technical evaluations to overcome the limitations of the B31G criterion i.e.: (a) over-conservative estimation of corroded area for long and irregularly shaped corrosion, (b) the projection of defect onto the longitudinal axis for spiral defects, (c) conservative flow stress (=1.1 * SMYS), (d) Folias factor M need to be modified, (e) arbitrary criterion for pits separation and longitudinal grooves separation, (f) not applicable to corroded welds, (g) no consideration for loads other than internal pressure, (h) not applicable to girth weld corrosion.

Modifications to the B31G criterion are suggested in order to reduce the scatter in the strength predictions and extend its applicability for new corrosion problems. ***Modified criteria*** are proposed and their applications are discussed. The proposed modified criterion are summarised below. Details of the proposed criteria are presented in Chapters 8.1 and 8.2.

According to B31G (ASME 1993), pits depth exceeding 80 % of the wall-thickness is not permitted due to the possibility of a leak developing. From strength point of view, leak will not develop until the pit depth is closer to the wall-thickness. The 80 % limitation is mainly due to the fact that the accuracy of inspection tools is approximately 15-20 % of the wall-thickness.

If the ratio of maximum depth and wall-thickness, d/t, is between 10 % and 80 %, the following evaluation should be performed.

(1) For Longitudinally Corroded Pipes, the Safe Maximum Pressure Level P′ is

$$P' = \frac{1}{\gamma}\frac{2\sigma_{flow}t}{D}\frac{1 - Q\,AREA / AREA_0}{1 - M^{-1}\,AREA / AREA_0} \qquad (1.1)$$

where

P'	=	Safe maximum pressure level
σ_{flow}	=	Flow stress of the material
t	=	Wall-thickness of the pipe
D	=	Outside diameter of the pipe
AREA	=	Exact area of the metal lost due to corrosion in the axial direction through-wall-thickness.
$AREA_0$	=	Original area prior to metal loss due to corrosion within the effective area which is L * t
L	=	Defect length of corrosion profile
M	=	Folias factor
Q	=	Spiral correction factor
γ	=	Factor of safety

The predicted bursting pressure level P_b is $\gamma P'$.

The safe maximum pressure level must be less or equal to the Maximum Allowable Design Pressure, which is;

$$P = \frac{2 \cdot SMYS \cdot t}{D} \cdot F \qquad (1.2)$$

Where SMYS = Specified Minimum Yield Stress
F = Design factor which is normally 0.72

The calculation of AREA, spiral correction factor Q, flow stress σ_{flow} and Folias factor M has been improved:

(a) Exact Area AREA

-Complex Shaped Corrosion:

Two levels of AREA assessment are proposed:

(i) Level 1 :

For $L^2/(Dt)<30$: AREA=(2/3)Ld

where d is the maximum depth of corroded area

For $L^2/(Dt)>30$: AREA=0.85Ld

(ii) Level 2 : To calculate the exact area (AREA) of the corrosion profile using Simpson integration Method, see Chapter 5.5.3.

-Closely Spaced Corrosion Pits:

A distance of t (Wall-thickness) is used as a criterion of pit separation for a colony of longitudinally oriented pits separated by a longitudinal distance or parallel longitudinal pits separated by a circumferential distance.

-Interaction of Longitudinal Grooves:

For defects inclined to pipe axis,

(a) If the distance x, between two longitudinal grooves of lengths L_1 and L_2, is greater than either L_1 or L_2, then the length of corrosion L is L_1 or L_2 which ever is greater.

(b) If the distance x, between two longitudinal grooves of lengths L_1 and L_2, is less than L_1 and less than L_2, then the length of corrosion L is the sum of x, L_1 and L_2, $L=L_1+L_2+x$.

For two longitudinal grooves separated by a circumferential distance x, the wall-thickness t could be used as grooves separation criterion.

(b) Spiral Correction Factor:

For long spiral corrosion, the spiral correction factor Q is given by

$$Q = \frac{1 - Q_1}{32} \frac{W}{t} + Q_1 \qquad (1.3)$$

in which W is defect width, and the coefficient Q_1 is a function of the spiral angle ψ ($\psi=90^0$ for longitudinal corrosion, $\psi=0^0$ for circumferential corrosion)

$Q_l = 0.2$ for $0^0<\psi<20^0$
$Q_l = 0.02\psi-0.2$ for $20^0<\psi<60^0$
$Q_l = 1.0$ for $\psi>60^0$

For W/t>32, the value of Q must be taken as 1.0.

(c) Flow Stress σ_{flow}

The flow stress is ultimate tensile stress σ_u or SMTS (Specified Minimum Tensile Stress) if σ_u is unknown.

(d)Folias factor M

The Folias factor is estimated as for $L^2/(Dt) \leq 50$

$$M = \sqrt{1 + \frac{2.51(L/2)^2}{Dt} - \frac{0.054(L/2)^4}{(Dt)^2}} \quad \textbf{(1.4)}$$

and for $L^2/(Dt) > 50$

$$M = 0.032\frac{L^2}{Dt} + 3.3 \quad \textbf{(1.5)}$$

(2) For Circumferential Weld Corrosion, the Safe Maximum Axial Tensile Stress σ'_{AX} is

$$\sigma'_{AX} = \frac{\sigma_{flow}}{\gamma}\frac{\eta[\pi - \beta(1-\eta)]}{\eta\pi + 2(1-\eta)\sin\beta} \quad \textbf{(1.6)}$$

where

σ'_{AX} = safe maximum axial tensile stress
σ_{flow} = the flow stress
d = defect depth
t = wall-thickness
η = 1 - d/t
c = half defect (circumferential) length
R = pipe radius
β = c/R (in radians)
γ = Factor of safety

(3) Practical Corrosion Problems excluded in the B31G criterion have been addressed.

(a) Corroded Welds, Ductile and Low Toughness Pipe

Corrosion in submerged-arc seams (longitudinal welds) should be handled in the same manner as corrosion in the body of the pipe.

Corrosion in (circumferential) girth welds should be assessed using the Kastner's local collapse criterion (see Chapter 6).

A fracture mechanics approach is applied for assessing corroded welds, considering possible cracks in the welds. The effect of material's fracture toughness (in ductile and low toughness pipe) is reflected by the critical fracture toughness of the material used in the fracture assessment criteria.

(b) Corroded Pipe under Combined Pressure, Axial and Bending Loads

For corroded pipe under combined pressure, axial and bending loads, the flow stress in the circumferential direction could be calculated considering the effects of the longitudinal stress, using von Mises yield function. The longitudinal stress in the corroded region is used in the calculation.

Discussions are made on possible applications to decision of operating pressure, re-qualification and wall-thickness assessment.

2 INTRODUCTION

2.1 Introduction

The purpose of this part project is to develop acceptance criteria (limit states) and a finite element approach for assessing residual strength of corroded pipes. This will enable operators and regulation bodies to undertake cost-effective decision on the operating pressure and whether repair/replacement are required or not. To achieve the goal, finite element approach has been developed and compared with the laboratory tests (Bai et al 1993b), existing laboratory test data will be collected, modifications to the respective criteria will be suggested and a 'Model Code' for possible implementation to rules will be proposed.

Leakage of gas and oil from pipelines may lead to ***human and environmental hazards***. In June 1989 a leakage from a gas pipeline between Siberia and Ufa caused explosion where two trains passed the area. In this accident 462 people were killed and 706 were hospitalised (Morgan 1993).

Internal corrosion is a major cause of leakage from offshore pipelines, installed e.g. in the Gulf of Mexico (Mandke 1990) and the North Sea (Jones et al 1992). Such corrosion damages may cause structural failure (bursting) and loss of revenue due to ***reduced operating pressure or stopped production***.

On the other hand, ***repair*** of the damages could be costly because a repair requires shut down periods and removal or replacement of a complete section of the pipe. For example, corrosion in the Trans Alaskan pipeline cost $ 1.5 billion to repair (Keen 1990) and the Forties oil pipeline in the UK North Sea had to be replaced at a cost of $265 million because of corrosion caused by the presence of water in the oil (London 1991). There are therefore considerable economic incentives to continue operation of corroded pipe, provided an acceptable safety level is maintained.

If it is necessary to uprate an in-service pipeline, existing standards require hydrostatic re-testing as the basis for demonstrating that the pipeline contains no damages which could fail at the ***uprated pressure***. An alternative method is on-line inspection to obtain information on the damages in the pipeline followed by burst strength assessment using criteria available from rules and/or finite element analysis.

Re-qualification is necessary in case the design condition has been changed or the design lifetime need to be extended when more oil/gas can be economically taken out from the reservoirs than first assumed in the design phase. For re-qualification of existing pipeline after damage, several levels of analyses of increasing detail and complexity could be applied to document that the pipeline has sufficient strength:

Level 1: To use criteria for strength and loads available from rules or technical reports
Level 2: To apply a non-linear numerical procedure and conduct laboratory tests which accurately predicts strength and loads, *or* to conduct hydrostatic re-testing
Level 3: To carry out reliability-based assessment accounting for uncertainties in loads, damage measurement and strength modelling
Level 4: To make optimum decisions based on balanced risks and costs

The safety and reliability of pipelines and their cost-effective operation and maintenance will therefore largely depend on the availability of tools/methods for evaluation of the significance of corrosion defects under service conditions.

The ASME B31G (1993) criterion for corroded pipe was based on the knowledge ***more than 20 years ago***. This criterion is considered to be quite conservative and inaccurate, with a mean bias of 2.0 and COV 0.56 when AGA (American Gas Association) test database is used for uncertainty assessment (Wang 1991).

Aiming at improving the accuracy of the B31G criterion, recently several research projects have been conducted in the USA (Kiefner and Vieth 1989, 1993), the UK (Hopkins and Jones 1992) and Canada (Mok et al 1991, Chouchaoui and Pick 1993). However, these results have not been utilised in the development of pipeline codes. There is therefore a need to develop a code which implements the latest technology development. Some additional investigations using experimentally validated finite element method are also necessary to formulate the code. In addition, safety factors need to be calibrated considering safety philosophy and model and parameter uncertainties through reliability analysis. These are the subject of the present part project.

The approach adopted is

(1). A large amount of full scale tests are evaluated and utilised.
(2). Guidance on, modifications to, and additional design equations for situations not included in present rules are suggested.
(3). Published finite element analyses and analytical solution are utilised for deriving new criteria.

In Chapter 5, the sources of conservatism in the original B31G criterion are discussed. This includes:

- The parabolic representation of the metal loss (assumed within the B31G limitations)
- The approximation used for the Folias factor
- The expression for flow stress
- The inability to consider the strengthening effect of islands of full thickness or near full thickness pipe at the ends of or between arrays of corrosion pits

The original B31G criterion can not be applied to spiral corrosion, pits/grooves interaction, corrosion in welds and combined loads. The present project provides information on assessment of spiral corrosion (Chapter 5.8), interaction of pits (Chapter 5.6) and longitudinal grooves (Chapter 5.7), corrosion in longitudinal welds (Chapter 5.10) and circumferential welds (Chapter 6) and combined loads(Chapter 5.12 and 6.5).

This part project is carried out within the JIP (Joint Industry Project) on **Residual Strength of Corroded and Dented Pipe.** The results of the JIP project will be available in the following five (5) project reports:

Report No. 93-3531: Finite Element Analysis Considering Ductile Fracture
Report No. 93-3637: Reliability-based Residual Strength Criteria for Corroded Pipes (*This report*)
Report No. 93-3638: Fracture, Fatigue and Buckling of Dented Pipes with Cracks
Report No. 95-3514: Finite Element Analyses of Corroded Pipes
Report No. 95-3594: Summary Report

2.2 Project Participants and Their Representatives

The following organisations participated in the present project during Phase 1 period:

- Statoil (Den Norske stats oljeselskap)
- Phillips (Phillips Petroleum Company Norway)
- Brasoil (On behalf of Petrobras)
- MMS (The US Mineral Management Service)
- NPD (Norwegian Petroleum Directorate)
- NFR (The Research Council of Norway) (NFR was formerly called NTNF)
- DNV (Det Norske Veritas)

Their representatives to the project are:

- Statoil: Richard Verley
- Phillips: Tor G. Tangeland
- Petrobras: Teresinha Alves
- Brasoil: Francisco Massa (On behalf of Petrobras)
- MMS: Charles Smith
- NPD: Kjell Anfinsen
- NFR: Knut Helge Osmundsvåg
- DNVC: Niels-Jørgen Rishøj Nielsen

The supports from the project participants and comments by their representatives are acknowledged.

2.3 Notations and Unit

Notations used in the report are summarised below:

a	=	depth of a crack
A	=	Constant which is $A=0.893L/(Dt)^{1/2}$
AREA	=	Corroded area
$AREA_0$	=	L*t
B	=	Constant which is $B=\{(d/t/(1.1d/t-0.15))^2-1\}^{1/2}$
c	=	W/2 half defect (circumferential) length
COV	=	Coefficient of variance
D	=	Nominal outside diameter of the pipe
d	=	Maximum depth of the corroded area
F	=	Design factor (usually taken as 0.72)
L	=	Axial extent of the defect
L_{allow}	=	Maximum allowable longitudinal length of corrosion defects
M	=	Folias factor
Mean (Bias)	=	Mean bias of the random variable X_m
MAOP	=	Maximum Allowable Operating Pressure
P	=	Maximum allowable design pressure, or design pressure
P_b	=	Burst pressure (safety factor is excluded)
P′	=	Safe maximum pressure level (safety factor is included)
Q	=	Spiral correction factor
R	=	pipe Radius
SMYS	=	Specified Minimum Yield Stress
SMTS	=	Specified Minimum Tensile Stress
t	=	Nominal wall-thickness of the pipe
W	=	width of the corrosion profile
X_M	=	Real strength/predicted strength (Model uncertainty parameter)
σ_{AX}	=	axial stress applied at circumferential weld
σ_{flow}	=	Flow stress of the material
σ_p	=	Predicted hoop stress level at failure
σ_u	=	Ultimate tensile stress
σ_y	=	Yield stress
γ	=	Factor of safety
ψ	=	Spiral angle
β	=	c/R (radian)
η	=	1-d/t

Both the SI units and the US units are used in the project reports. The conversion factors are:

From US units to SI units

length:	1 in (inch)	=	25.40 mm
Mass	1 lb (pound)	=	0.4536 kg
Force	1 lbf (pound force)	=	4.448 N
	1 kip	=	4.448 kN
Stress (Pressure)	1 psi (lbf/in^2)	=	0.006895 MPa (N/mm^2)
	1 ksi (1000 psi)	=	6.895 MPa

From SI units to U. S units

length:	1 mm	=	0.03937 in
Mass	1 kg	=	2.205 lb (pound)
Force	1 N	=	0.2248 lbf (pound force)
	1 kN	=	0.2248 kip
Stress (Pressure)	1 MPa	=	145.0 psi (lbf/in^2)
	1 MPa	=	0.1450 ksi

1 ksi = 1000 psi
10 bar = 1 MPa

3 EXISTING RESIDUAL STRENGTH CRITERIA

3.1 General

The wall-thickness loss due to corrosion causes a local magnification of the stress levels within the remaining wall and a reduction in the applied stress necessary to cause a local overload.

The evaluation methods apply to either internal or external corrosion. When applied to internal corrosion, either the corrosion must be arrested with certainty, or the evaluation must be based on the probable size of defect that will exist by the time of the next inspection. When applied to external corrosion, it is assumed that the pipe will be re-coated and the defect will not further enlarge.

3.2 ANSI/ASME B31G Criterion

In the late 1960s and early 1970s, a criterion was developed through research sponsored by Texas Eastern Transmission Corporation and the Pipeline Research Committee of AGA (American Gas Association) to evaluate the remaining strength of corroded pipe(see Maxey et al 1971, Kiefner and Duffy 1971, Kiefner 1974). This criterion has been embodied in both the B31.4 and B31.8 pipeline design codes and is described in detail in a separate document: "ANSI/ASME B31G - Manual for Determining the Remaining Strength of Corroded Pipelines". The procedure for analysis of corroded pipe strength is illustrated in Figure 3-1 (after Fig. 1-2 of ANSI/ASME 1993).

The B31G criterion can be used by a pipeline operator to assess corroded pipe for rehabilitation purpose. If the calculated remaining strength exceeds the maximum allowable operating pressure of the pipeline by a sufficient safety margin, the corroded segment can remain in service. If not, it must be repaired or replaced.

The main equations and procedures in ANSI/ASME (1993) are summarised in (1)-(3) below.

(1) Maximum Allowable Length

In the B31G (ANSI/ASME 1993), a criterion for the acceptable corroded length is given as below for a corroded area having a maximum depth 'd' of more than 10 % but less than 80 % of the nominal wall-thickness.

$$L_{allow} = 1.12B\sqrt{Dt} \qquad \textbf{(3.1)}$$

where

L_{allow} = Maximum allowable axial extent of the defect
D = Nominal outside diameter of the pipe
t = Nominal wall-thickness of the pipe

and where a constant 'B' is calculated according to the following expression

$$B = \sqrt{\left(\frac{d/t}{1.1d/t - 0.15}\right)^2 - 1} \qquad (3.2)$$

where

d = Maximum depth of the corroded area

B may not exceed the value 4.

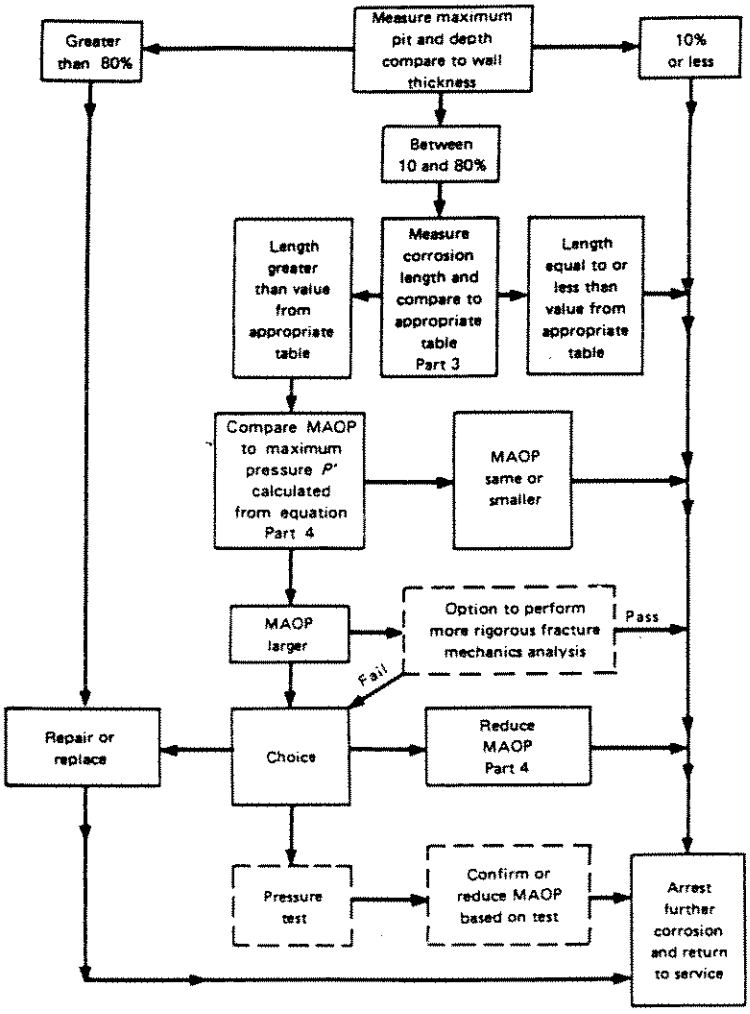

Figure 3-1 Procedure for Analysis of Corroded Pipe Strength as per ANSI/ASME(1993) (MAOP: Maximum Allowable Operating Pressure)

(2) Maximum Allowable Design Pressure P for Uncorroded Pipe

The maximum allowable design pressure is

$$P = \frac{2SMYSt}{D} * F \tag{3.3}$$

where

P = Maximum allowable design pressure
SMYS = Specified Minimum Yield Stress
F = Design factor which is normally 0.72

(3) The Safe Maximum Pressure Level P′

A constant 'A' is calculated from

$$A = 0.893\left(\frac{L}{\sqrt{Dt}}\right) \tag{3.4}$$

The safe maximum pressure level P′ for the corroded area is

(a) For $A \leq 4$

$$P' = 1.1P\left(\frac{1-\frac{2}{3}\left(\frac{d}{t}\right)}{1-\frac{2}{3}\left(\frac{d}{t\sqrt{A^2+1}}\right)}\right) \tag{3.5}$$

except that P′ may not exceed P.

(b) For $A > 4$

$$P' = 1.1P\left(1-\frac{d}{t}\right) \tag{3.6}$$

except that P′ may not exceed P. (If A exceeds 4, the corrosion is so long that there is no effective reinforcement from adjacent uncorroded material. The safe pressure is then directly proportional to the remaining wall thickness).

If P′>P (or MAOP), the maximum safe pressure shall be taken as P (or MAOP). The 1.1 factor accounts for ductile failure at the flow stress of the material.

Because the parabolic representation becomes less and less an accurate representation of the actual area of metal loss as the length increase, it is limited to A values less than or equal to 4.0.

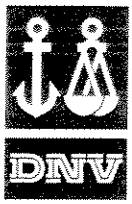

(4) Sources of Excess Conservatism

The sources of excess conservatism in the original B31G criterion are (Kiefner and Vieth 1989)

- The expression for flow stress
- The approximation used for the Folias factor
- The parabolic representation of the metal loss (assumed within the B31G limitations)
- The inability to consider the strengthening effect of islands of full thickness or near full thickness pipe at the ends of or between arrays of corrosion pits

These will be discussed in Chapter 5.

3.3 NG-18 Surface-flaw Equation

The NG-18 surface-flaw equation is the basis of the B31G criterion. It was developed in 1971 for a pipe with a longitudinal corrosion defect(Maxey et al 1971, Kiefner and Duffy 1971):

$$\sigma_p = \sigma_{flow} \frac{1 - AREA / AREA_0}{1 - M^{-1}(AREA / AREA_0)} \tag{3.7}$$

where

σ_p = Predicted hoop stress level at failure
σ_{flow} = Flow stress of the material
AREA = Area of through thickness profile of flaw
$AREA_0$ = L*t
M = Folias factor which is

$$M = \sqrt{1 + \frac{2.51(L/2)^2}{Dt} - \frac{0.054(L/2)^4}{(Dt)^2}} \tag{3.8}$$

Since the definition of M is complex, Kiefner(1974) recommended that it be simplified to

$$M = \sqrt{1 + \frac{0.8 L^2}{Dt}} \tag{3.9}$$

The Folias factor M is shown as a function of the L^2/Dt in Figure 5-2. The relationship between M given by Eq.(3.9) and A defined by Eq.(3.4) is

$$M = \sqrt{1 + A^2} \tag{3.10}$$

For short corrosion defects in which the pit depth is uneven, the through thickness profile area (AREA) can be approximated by a parabolic area as

$$AREA = \frac{2}{3} Ld \tag{3.11}$$

In the original NG-18, the flow stress was 1.11 SMYS (Specified Minimum Yield Stress) and the maximum allowable length L_{allow} was solved from a formula which equates predicted bursting hoop stress σ_p to SMYS (Kiefner 1974):

$$SMYS = 1.11SMYS\frac{1-2/3\,d/t}{1-(2/3\,d/t)\left(1+0.8\frac{L^2}{Dt}\right)^{-1/2}} \qquad (3.12)$$

The obtained L_{allow} can be expressed as Eq.(3.1), with a minor difference in determining the constant B (1.1 and 0.15 in Eq.(3.2) are replaced by 1.11 and 0.167 respectively).

Assuming the flow stress equals to 1.1 SMYS and relating pressure to stress equilibrium, the failure pressure of pipe with a short corrosion pit leads to Eq.(3.5) for A≤4.

For longer defects (e.g. A>4), the parabolic approximation of the defect area tends to give too small an area. A more conservative estimate of the defect area is

$$AREA = Ld \qquad (3.13)$$

For an infinitely long defect where M approaches infinity, the failure pressure is reduced to Eq.(3.6).

It is noted that the NG-18 has been adopted by the Canadian standard CSA-Z184-M86 for Gas Pipeline Systems (CAN/CSA 1986), with a minor modification in determining the constant B (The one used in B31G was adopted instead).

The use of L and AREA in the NG-18 Equation for an array of pits tends to result in a conservative assessment of the remaining strength for several reasons:

First, corrosion pits are seldom lined up along an axial line as assumed in the use of the NG-18 equation. When they are not so lined up, the NG-18 Equation will tend to underestimate the remaining strength.

Secondly, corrosion pits are blunt defects compared to cracks and many other kinds of flaws found in pipelines. It has been demonstrated that blunt surface flaws have appreciably higher failure stress levels than sharp surface flaw. Thus, the NG-18 equation which was developed on the basis of burst tests involving relatively sharp flaws will tend to give conservative predictions for the effects of blunt flaws.

Factors influencing the conservatism of the NG-18 equation which have been addressed in this report are flow stress, and the Folias factor M.

3.4 Modified B31G Criterion - Effective Area

Vieth and Kiefner (1993) proposed two modified B31G criteria (Effective Area and 0.85dL Area) within the AGA PR-218-9205 project "RSTRENG2 User's manual". According to the effective area approach, the safe maximum pressure is predicted as

$$P' = P\left(1 + \frac{10{,}000}{SMYS}\right)\frac{1 - AREA_{eff} / AREA_0}{1 - M^{-1} AREA_{eff} / AREA_0} \qquad \text{US Unit} \qquad \textbf{(3.14)}$$

$$P' = P\left(1 + \frac{69}{SMYS}\right)\frac{1 - AREA_{eff} / AREA_0}{1 - M^{-1} AREA_{eff} / AREA_0} \qquad \text{SI Unit}$$

except that P′ must be less than or equal to P and where

P′ = the safe maximum pressure for the corrosion area
P = the greater of either the pressure determined by the equation in Title 49, Part 192 of the code of Federal Regulation as shown in the Note under paragraph. 4.3 (excluding joint factor) as applied to the pipe containing the corroded area, or the established MAOP.
SMYS = Specified Minimum Yield Strength of the pipe material (psi, MPa)
$AREA_{eff}$ = the effective area of the metal loss due to corrosion in the axial direction through-the-wall thickness based on iterative calculation
$AREA_0$ = original area prior to metal lost due to corrosion within the effective area $L_{eff}t$
L_{eff} = effective axial extent of the corrosion
t = specified wall thickness of the pipe
D = nominal outside diameter of the pipe
M = Folias factor as given below:

for $L_{eff}^2/(Dt) \le 50$

$$M = \left(1 + \frac{1.255}{2}\frac{L_{eff}^2}{Dt} - \frac{0.0135}{4}\frac{L_{eff}^4}{(Dt)^2}\right)^{1/2} \qquad \textbf{(3.15)}$$

which can be rewritten as

$$M = \sqrt{1 + \frac{2.51(L_{eff}/2)^2}{Dt} - \frac{0.054(L_{eff}/2)^4}{(Dt)^2}}$$

and is identical to Eq.(3.8) when $L = L_{eff}$.

For $L_{eff}^2/(Dt) > 50$

$$M = 0.032\frac{L_{eff}^2}{Dt} + 3.3 \qquad \textbf{(3.16)}$$

The effective area of the corrosion is determined through an iterative calculation procedure that results in a minimum predicted pressure. The iterative calculation procedure uses the corresponding lengths and corrosion pit depths to calculate an effective area of missing metal and an effective length. These effective areas and effective lengths are used to calculate a predicted pressure. The minimum predicted pressure that is the result of this iterative calculation procedure is presented as the safe maximum pressure for the corroded area.

There are a number of limitations in using the modified B31G, effective area, as the B31G criterion:

(1) Pit depths exceeding 80 percent of the wall thickness are not permitted due to the possibility of a leak developing.

(2) General corrosion where all of the measured pit depths are less than 20 percent of the wall thickness is permitted. This is slightly less conservative than the 12.5 percent allowed using the B31G.

The predicted burst pressure using the Effective Area Approach is calculated as

$$P_b = \left(\frac{2t}{D}\right)(SMYS + 10{,}000)\frac{1 - AREA_{eff} / AREA_0}{1 - M^{-1}\left(AREA_{eff} / AREA_0\right)} \qquad US\ Unit \qquad (3.17)$$

$$P_b = \left(\frac{2t}{D}\right)(SMYS + 69)\frac{1 - AREA_{eff} / AREA_0}{1 - M^{-1}\left(AREA_{eff} / AREA_0\right)} \qquad SI\ Unit$$

3.5 Modified B31G Criterion - 0.85 dL Area

$$P' = P\left(1 + \frac{10{,}000}{SMYS}\right)\frac{1 - 0.85\frac{d}{t}}{1 - M^{-1}\left(0.85\frac{d}{t}\right)} \qquad US\ Unit \qquad (3.18)$$

$$P' = P\left(1 + \frac{69}{SMYS}\right)\frac{1 - 0.85\frac{d}{t}}{1 - M^{-1}\left(0.85\frac{d}{t}\right)} \qquad SI\ Unit$$

According to the 0.85dL Area approach, the safe maximum pressure is predicted as excepted that P′ must be less than or equal to P and where

P′	=	the safe maximum pressure for the corrosion area
P	=	the greater of either the pressure determined by the equation in Title 49, Part 192 of the code of Federal Regulation as shown in the Note under paragraph. 4.3 (excluding joint factor) as applied to the pipe containing the corroded area, or the established MAOP.
SMYS	=	Specified Minimum Yield Strength of the pipe material (psi / MPa)
d	=	Maximum depth of corroded area
L_{total}	=	effective axial extent of the corrosion
t	=	specified wall thickness of the pipe
D	=	nominal outside diameter of the pipe

M = Folias factor as given below:

for $L_{total}^2/(Dt) \leq 50$

$$M = \left(1 + \frac{1.255}{2}\frac{L_{total}^2}{Dt} - \frac{0.0135}{4}\frac{L_{total}^4}{(Dt)^2}\right)^{1/2} \quad \textbf{(3.19)}$$

for $L_{total}^2/(Dt) > 50$

$$M = 0.032\frac{L_{total}^2}{Dt} + 3.3 \quad \textbf{(3.20)}$$

There are a number of limitations in using the modified B31G, 0.85 dL Area, as the B31G criterion:

(1) Pit depths exceeding 80 percent of the wall thickness are not permitted due to the possibility of a leak developing.

(2) General corrosion where all of the measured pit depths are less than 20 percent of the wall thickness is permitted. This is slightly less conservative than the 12.5 percent allowed using the B31G.

The predicted burst pressure using the 0.85dL Area Approach is calculated

$$P_b = \left(\frac{2t}{D}\right)(SMYS + 10{,}000)\frac{1 - 0.85\frac{d}{t}}{1 - M^{-1}\left(0.85\frac{d}{t}\right)} \quad US\ Unit \quad \textbf{(3.21)}$$

$$P_b = \left(\frac{2t}{D}\right)(SMYS + 69)\frac{1 - 0.85\frac{d}{t}}{1 - M^{-1}\left(0.85\frac{d}{t}\right)} \quad SI\ Unit$$

4 REVIEW OF LABORATORY TESTS OF CORRODED PIPELINES

4.1 AGA Database (Tests No. 1 - No. 86)

The pipeline Research Committee of the American Gas Association published a report on a study to reduce the excessive conservatism of the B31G criterion (Kiefner and Vieth 1989). In Appendix D to this report, 86 burst tests are listed as shown in Appendix A of the present report, Test No. 1 - No. 86. The first 47 of these tests were used to develop the B31G criterion, and were full scale tests conducted at Battelle. The rest of the 86 tests were also full scale and were tests on pipe sections removed from service and containing real corrosion.

4.2 NOVA Tests (Tests No. 87 - No. 106)

The applicability of the B31G criterion to long longitudinal corrosion defects and long spiral corrosion defects was investigated experimentally by Mok et al (1990, 1991) of NOVA. Two series of burst tests of large-diameter pipeline were undertaken by NOVA during 1986 and 1988, see Table 5.5. The pipe was made of grade 414 (X60) steel with an outside diameter of 508 mm and a wall-thickness of 6.35 mm. Longitudinal and spiral corrosion defects were simulated with machined grooves on the outside of the pipe.

In the first series of burst tests, a total of 13 pipes (No. 1-No. 13 of Table 5.5) were burst. In all tests, the simulated corrosion defects were 25.4 mm wide and 2.54 mm deep producing a width to thickness ratio (W/t) of 4 and a depth to thickness ratio (d/t) of 0.4. Various lengths and orientations of the grooves were studied. Angles of 20, 30, 45 and 90 degrees from the circumferential direction, referred to as the spiral angle, were used. In some tests, two adjacent grooves were used to indicate interaction effects. One specimen of plain pipe (no corrosion) was also tested.

In the second series of burst tests, seven pipes were tested(No. 14 - No. 20 of Table 5.5). The defect geometries tested were longitudinal defects, circumferential defects, and corrosion patches of varying W/t and d/t. A corrosion patch refers to a region where the corrosion covers a relatively large area of pipe and the longitudinal and circumferential dimensions are comparable. In some of the pipes, two defects of different sizes were introduced but were kept far enough apart to eliminate any interaction. Again, a plain pipe was tested to provide a reference for the effect of the defect depth on the burst pressure.

In Appendix A, the tests are number No. 87 - No. 106.

4.3 British Gas Tests (Tests No. 107 - No. 124)

Hopkins and Jones (1992) conducted five vessel burst tests and four pipe ring tests. The results of the five vessel tests are summarised in Table 5.3. In Appendix A, the tests are number No. 107 -No. 115.

Jones et al (1992) conducted nine (9) pressurised ring tests. Seven of the nine rings were machined internally over 20% of the circumference, the reduced wall thickness simulating smooth corrosion. All specimens were cut from a single pipe of Grade 5LX60 with the Diameter of 914 mm, and wall-thickness of 22 mm. In Appendix A, the tests are number No. 116 - No. 124.

4.4 Waterloo Tests (Tests No. 125 - No. 151)

13 burst tests of pipes containing Internal Corrosion Pits were reported by Chouchaoui and Pick (1992) at University of Waterloo (Proceedings Int. Conf. on Pipeline Reliability, Calgaly, June 1992). In Appendix A, the tests are number No. 125 -No. 135. The paper is entitled "Residual Burst Strength of Pipe With Internal Corrosion Pits".

8 burst tests of pipes containing Circumferentially Aligned Pits were reported by Chouchaoui and Pick (1992) for publication in Int. J. of Pressure Vessel and Piping. In Appendix A, the tests are number No. 136 -No. 143. The paper is entitled "Behaviour of Circumferentially Aligned Corroded Pits".

8 burst tests of pipes containing Longitudinally Aligned Pits were reported by Chouchaoui and Pick (1992) for publication in Int. J. of Pressure Vessel and Piping. In Appendix A, the tests are number No. 144 -No. 151. The paper is entitled "Behaviour of Longitudinally Aligned Corroded Pits".

5 LONGITUDINAL CORROSION

5.1 Type of Corrosion Defects

Figure 5-1 shows type of corrosion defects as below:

(a) Groove
(b) Pits
(c) Pits containing cracking in their bottom

Corrosion may also occur near or in the weld.

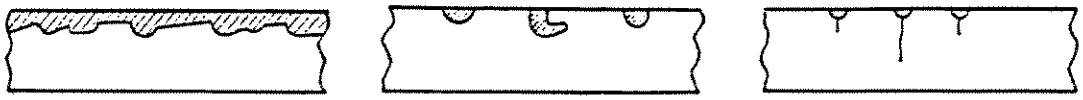

(a) Groove **(b) Pits** **(c) Pits containing cracks in their bottom**

Figure 5-1 Type of Corrosion Defects

Internal corrosion is a major problem in offshore pipeline (Mandke 1990, Jones et al 1992). Many forms of internal corrosion occur, e.g.

(a) girth weld and seam weld corrosion,
(b) massive general corrosion around the whole circumference and
(c) long plateau corrosion at about 6 o'clock position.
(d) Pitting corrosion

External corrosion is normally thought of as being local, covering an irregular area of the pipe. However, in the case where the protective coating has failed, the corrosion may tend to be a pattern of long grooves. For example, failure of the protective coating may occur along the spiral joint in the coating if the pipe has been wrapped. This will produce a long spiral corrosion groove. If the coating has sagged, pulling away from the bottom of the pipe and trapping moisture, along longitudinal corrosion groove may result.

The relation between corrosion modes, operational force and failure modes are summarised in Table 5-1.

Table 5-1 Relation between corrosion modes, operational force and failure modes

Corrosion Mode	Operational Force	Failure Mode
Uniform Corrosion	Internal/External Pressure Axial Tension or Bending	Longitudinal rupture or collapse or transverse fracture
Longitudinal Grooving	Internal Pressure	Longitudinal rupture
Seam Weld Corrosion	Internal Pressure	Longitudinal rupture
Pitting Corrosion		Leak
Girth Weld Corrosion	Internal/External Pressure Axial Tension/Bending	Transverse fracture

Note that girth weld corrosion will be discussed in Chapter 6 and the rest will be considered in this Chapter. Seam weld corrosion is evaluated in the same way as longitudinal grooving.

Pits with depths greater than 0.8 of the wall thickness are not permitted because of the chances that very deep pits would develop leaks even though the criterion predicts that they will not cause ruptures. The factor of 0.8 is also due to the inspection accuracy limitation of pigs (10%-20% of the wall-thickness).

5.2 Material Grades and Flow Stress

5.2.1 Flow Stress Formulae in Literature

Flow stress σ_{flow} is a concept suggested by Hahn et al (1969) to account for the strain-hardening in terms of an equivalent elastic-perfectly-plastic material having a yield stress of σ_{flow}. The flow stress also depends on if it is used for base material or welded region. In this report, flow stress in the hoop direction is considered because bursting is a kind of hoop fracture. Several flow stress formulae have been proposed in literature, and the most relevant ones are listed below.

In the B31G-1993 manual, the flow stress was defined as 1.1 SMYS. In Kiefner and Vieth (1989), the flow stress was re-defined as SMYS plus 69 MPa (10 000 psi). Based on full-scale tests of low strength pipes, Maxey et al (1971) and Kiefner et al (1973) demonstrated that the flow stress could be estimated as:

$$\sigma_{flow} = SMYS + 10\ ksi \qquad \text{US units} \qquad \textbf{(5.1)}$$

$$\sigma_{flow} = SMYS + 69\,MPa \qquad \text{SI units}$$

An accurate and complex definition is to directly relate the flow stress to both yield stress σ_y and hardening parameter n of true stress-true strain curve follows a power law, see Andersen (1991)

$$\sigma_{flow} = \frac{1}{2}\sigma_y \left(1 + \frac{(0.002n)^{\frac{1}{n}}}{e^{\frac{1}{n}}} \right) \qquad \textbf{(5.2)}$$

A more accurate estimation is to account for possible biaxial stress state in addition to the yield stress σ_y, ultimate tensile stress σ_u and hardening parameter n. Klever (1992) investigated the effect of different stress-strain curves on the flow stress. The burst pressure is divided by the yield stress σ_y and the ultimate tensile stress σ_u in Figs. 5 and 6 (of his paper) respectively. It is demonstrated that the ultimate tensile stress σ_u is much more relevant in burst pressure predictions than the yield stress σ_y, since the curves (in Figure 6 of his paper) are almost independent of the type of material. A flow stress equation obtained by Klever (1992) in his theoretical study is

$$\sigma_{flow} = \left(\frac{2}{3}\right)^{\frac{1}{n}} \left(\sqrt{1-\alpha+\alpha^2}\right)^{\frac{1}{n}-1} \sigma_u \tag{5.3}$$

where α is the longitudinal stress to hoop stress ratio and hardening parameter n is

$$n = 1 / \ln[1 + 0.45 \ln\left(\frac{\sigma_u}{\sigma_y}\right)] \tag{5.4}$$

Tests by Hopkins and Jones (1992) indicated that use of a flow stress σ_{flow} of the ultimate tensile stress σ_u gave good estimation of bursting strength(see Table 5.3).

Recently Stewart et al (1994) provides the flow stress calculation on a sound theoretical basis. Figure 5 of the paper confirms that the flow stress is on average the ultimate tensile strength of the material. According to Stewart et al (1994), the flow stress for an uncorroded pipe is

$$\sigma_{flow} = k^{n'+1}\left(\frac{1}{2}\right)^{n'} \sigma_u \tag{5.5}$$

where k is a constant dependent on the yield criterion used in the derivation of the equation. $k=2/(3)^{1/2}$ for von Mises yield criterion and k=1 for Tresca yield criterion. n′ is the hardening parameter which is defined by the Ludwik power law and calculated as

$$n' = \ln(1+\varepsilon_u) \tag{5.6}$$

where ε_u is the engineering ultimate tensile strain.

The average flow stress given by von Mises yield criterion and Tresca yield criterion, is

$$\sigma_{flow} = \left(\left(\frac{1}{\sqrt{3}}\right)^{n'+1} + \left(\frac{1}{2}\right)^{n'+1}\right)\sigma_u \tag{5.7}$$

Applying the average flow stress equation to n′=0.1 - 0.2, the obtained flow stress is 1.01 σ_u - 0.95 σ_u. This means the average flow stress is approximately σ_u. Waterloo test data shown in Appendix A confirmed that the mean value of the flow stresses given by Eq.(5.7) is 0.991 σ_u.

The above flow stress definitions are for base material. For general welded components, a commonly defined flow stress is the average of the yield stress and ultimate tensile stress, e.g. the PD6493 (1991)

$$\sigma_{flow} = \frac{\sigma_y + \sigma_u}{2} \tag{5.8}$$

5.2.2 Flow Stress based on API 5L Specification of SMTS

As indicated by many researchers, such as Hopkins and Jones (1992), Klever (1992) and Stewart et al (1994), for base material, flow stress could be estimated as ultimate tensile stress of the material. However, for ageing pipelines in operation, it is not easy to know the value of ultimate tensile stress of the pipeline in question. An approximation of the ultimate tensile stress is therefore the Specified Minimum Tensile Stress SMTS.

$$\sigma_{flow} = SMTS \tag{5.9}$$

The Specified Minimum Tensile Stress (SMTS) is defined as a statistic minimum of the ultimate tensile stress.

Table 5-2 Values of SMTS from the API 5L specification

Material	ksi		MPa		Calc from eq. (5.10)	
	SMYS	SMTS	SMYS	SMTS	SMTS ksi	error
B	-	60	-	413.7	-	-
X42	42	60	289.6	413.7	58.5	0.024
X46	46	63	317.2	434.4	62.7	0.006
X52	52	66	358.5	455.1	68.3	-0.035
X56	56	71	386.1	489.5	71.8	-0.011
X60	60	75	413.7	517.1	75.0	0.000
X65	65	77	448.2	530.9	78.7	-0.021
X70	70	82	482.7	565.4	81.9	0.001
X80	80	90	551.6	620.6	87.2	0.031

From the above table, it is derived that SMTS can be approximated by an equation as below:

$$SMTS = 1.73\ SMYS - 0.008\ SMYS^2 \quad (ksi) \qquad \text{US units} \tag{5.10}$$

$$SMTS = 1.73\ SMYS - 0.00116\ SMYS^2 \quad (MPa) \qquad \text{SI units}$$

This equation indicates there is a non-linear relationship between SMYS and SMTS/SMYS for the data range listed in the Table 5-2 (for 42 ksi < SMYS < 80 ksi). The calculation of the formula Eq. (5.10)is also included in the table above.

5.2.3 Factors Affecting Flow Stress

It is necessary to indicate that the amount of flow stress is influenced by fabrication process (e.g. hot rolled versus cold expanded) and material ageing. Possible size effect of the steel strength (SMYS, SMTS) should also be accounted for in the assessment of the flow stress. The installation process (e.g. reeling) can also affect the material property, including flow stress.

Furthermore, the flow stress used in the burst strength criteria, is influenced by possible cracks in the pit bottom (see Figure 5-1 (c)), due to e.g. corrosion fatigue. In this case, the value of the flow stress could be determining using the fracture mechanics criteria (e.g. PD 6493) considering crack size.

Since the flow stress could be affected by many factors, in the proposed criterion, use of the actual value of the flow stress is also allowed, provided the value has been obtained through a reliable approach (e.g. testing).

5.3 Folias Factor M

There are three expressions of Folias factor:

(a) The three-term series (Eq.(3.8) (Maxey et al 1971))

The Folias factor M is a geometric factor which was developed from shell theory by Folias (1964) to account for the stress-concentrating effect of a notch. This equation is a truncated series expansion which approximates the exact M of Folias (an infinite-term series). It has been found to give excellent agreement with the exact M for short corrosion defects (Kiefner 1974). However, for very long corrosion defects(when $L^2/(Dt)$ is large), the negative term of the three-term series in Eq.(3.8) starts to dominate and the three-term approximation is no longer valid. Therefore it is necessary to modify Eq.(3.8) such that it is valid for the whole range of the constant $L^2/(Dt)$.

(b) The expression adopted in the B31G criterion (Eq.(3.9)) (Kiefner 1974)

(c) The two formulae expression made in the RSTRENG project (Kiefner and Vieth 1989).

Kiefner and Vieth (1989) adopted Eq.(3.8) for $L^2/(Dt) \leq 50$ and suggested to use the following equation for $L^2/(Dt) > 50$

$$M = 0.032\frac{L^2}{Dt} + 3.3 \qquad \textbf{(5.11)}$$

which is obtained by means of a straight-line tangent to the curve of Eq.(3.8) at $L^2/(Dt)=50$.

The relationship between Folias factor M and $L^2/(Dt)$ due to the above three expressions have been compared in Table 5-3 and shown in Figure 5-2.

Table 5-3 Folias factor M as a function of $L^2/(Dt)$ due to different expressions

Eq.	$L^2/(Dt)$									
	20.0	40.0	60.0	80.0	100.0	120.0	140.0	160.0	180.0	200.0
(3.8)	3.493	4.550	5.148	5.441	5.477	5.236	4.764	3.873	2.145	error
(3.9)	4.123	5.745	7.000	8.062	9.000	9.849	10.63	11.36	12.04	12.69
(5.11)	4.123	5.745	5.220	5.860	6.500	7.140	7.780	8.420	9.060	9.700

It is found that Eq.(3.8) gives a peak value at approximately $L^2/(Dt)=100$ and the term inside the square root is negative when $L^2/(Dt)=200$. Since a combination of Eq.(3.8) and Eq.(5.11) seems to be a better approximation of the Folias factor, it is recommended in the proposed criterion.

The calculation of M could be further modified based on a sound theoretical formulation if refined stress concentration analysis is available (Popelar 1993).

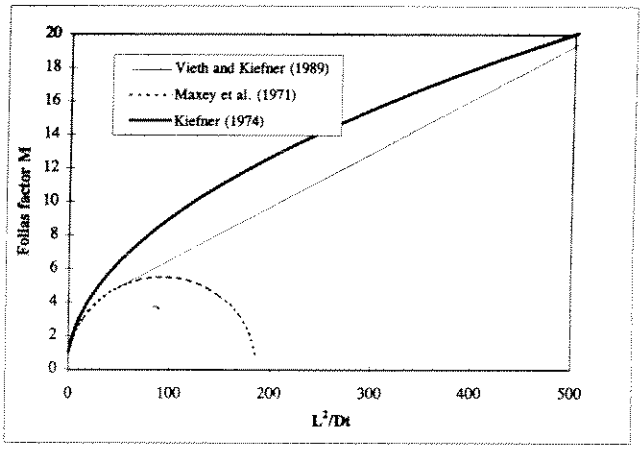

Figure 5-2 Comparison of Folias Factor M given by Alternative Equations

5.4 Short Versus Long Defects

5.4.1 General

The NG-18 equation and B31G criterion were developed based on fracture tests of pipes with relatively short longitudinal corrosion of up to about 25% pipe diameter (Kiefner 1974), but they have not been well validated for longer corrosion. Consequently, there is some concern about applying such methods to long lengths of corrosion, which is increasingly being found in pipelines.

The following three test programs were partly designed to investigate behaviour of long corrosion:

- Hopkins and Jones (1992) (British Gas tests)
- Jones et al (1992) (Shell tests)
- Mok et al (1990) (NOVA tests)

The conclusion from the British Gas, NOVA and Shell tests, is that the failure stress of long defects (>pipe diameter) can be estimated using the NG-18 equation and B31G criterion (Hopkins and Jones 1992).

In Figure 5-3 the maximum allowable operating pressure as given in Eq.(3.5) and Eq.(3.6) is plotted as a function of the corrosion length $L/(D/t)^{1/2}$ for four different corrosion depth d/t=0.2, 0.4, 0.6, 0.8. In Figure 5-4 the corresponding values for the NG-18 equation is shown.

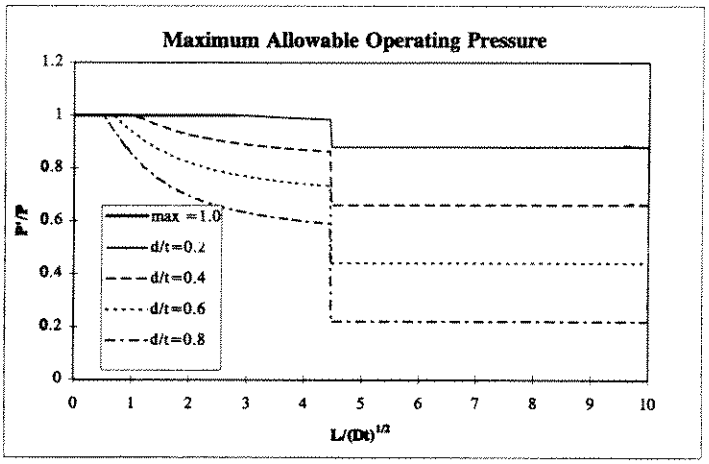

Figure 5-3 P´/P as a Function of Corrosion Length for Different Corrosion Depths According to B31G

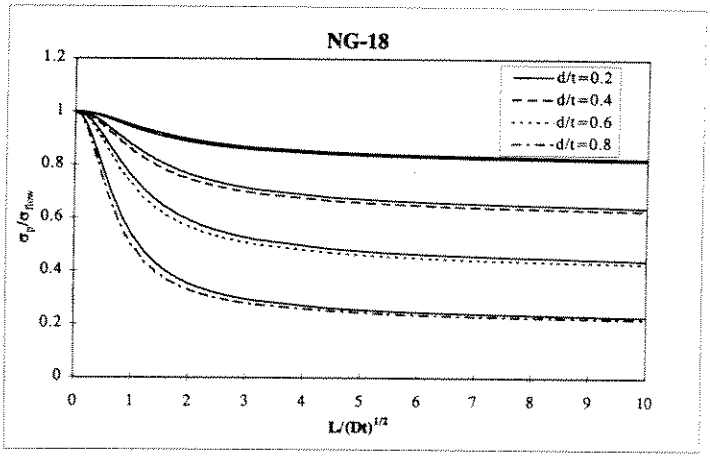

Figure 5-4 Ratio between σ_p and σ_{flow} for the NG-18 equation for different corrosion depths. Both the Folias factors M from Kiefner (1974) and Vieth and Kiefner (1989) are included. $AREA/AREA_0 = d/t$. The lower ones are based on Kiefner (1974).

5.4.2 Hopkins and Jones (1992) Tests

Hopkins and Jones (1992) conducted five vessel burst tests and twelve pipe ring tests. The results of the five vessel tests are summarised in Table 5.3:

In this report, when comparison is made of testing pressure and predictions, safety factors are not applied in the criteria.

Table 5-4 Summary of British Gas Tests (Hopkins and Jones 1992) and Predictions

Test [1) 2) 3) 4)]	Length (mm)	Depth (% of t)	API σ_y (MPa)	API σ_u (MPa)	Burst Stress (MPa)	NG-18 using σ_u (MPa)	B31G Criterion (MPa)	Proposed[5] Criterion (MPa)
1-1	3048	40	451	577	357	351	317	351
2-1	610	40	447	564	346	361	329	361
2-2	305	40	447	564	382	384	350	385
2-3	305	40	447	564	407	384	350	385
2-4	152	40	447	564	456	429	391	431

Note: (1) Diameter was 610 mm;
(2) Wall-thickness was 12.34 mm;
(3) Defect width was 0.15 mm;
(4) Material Grade X52. (SMYS = 358.5 MPa, SMTS = 455.1 MPa)
(5) In the proposed criterion, the flow stress is taken as ultimate tensile stress.

For a long defect, Folias factor M = infinite and AREA/AREA$_0$ = d/t, the NG-18 equation (Eq.(3.7)) leads to:

$$\sigma_p = \sigma_{flow}(1 - \frac{d}{t}) \qquad \textbf{(5.12)}$$

and using σ_{flow} as σ_u = 577 MPa, d/t = 0.4, the predicted σ_p is 346 MPa.

From the table it is seen that

(1) The defects of length exceeding a pipe diameter failed at stresses similar to that of an infinitely long defect.

(2) The prediction based on NG-18, Eq.(3.7) agrees with the test results if the flow stress is taken as ultimate tensile stress σ_u instead of 1.1 SMYS or 1.15 σ_y. This conclusion has also been made by Mok et al (1991) and Jones et al (1992).

(3) The NG-18, Eq.(3.7) is more accurate than Eq.(5.12) (or Eq.(3.6)) since the Folias factor has been included in Eq.(3.7). Therefore in the proposed criterion, Eq.(3.7) is adopted instead of two equations (Eqs.(3.5) and (3.6) in the B31G criterion. The safe maximum pressure level P′ is given by

$$P' = \frac{1}{\gamma}\frac{2\sigma_{flow}t}{D}\frac{1 - AREA/AREA_0}{1 - M^{-1}AREA/AREA_0} \qquad \textbf{(5.13)}$$

where γ = Factor of safety which will be calibrated using reliability methods

5.5 Irregularly Shaped Corrosion - Calculation of Area

5.5.1 General

The major weakness of the existing B31G criterion is its over-conservative estimation of corroded area for long and irregularly shaped corrosion, see Kiefner and Vieth (1990b). Tests of Hopkins and Jones (1992) indicated that irregularly shaped corrosion could be conservatively assessed using Eq.(3.7) when the accurate cross-sectional area of the corrosion defect was used. Therefore the key to the problem of the irregularly shaped corrosion is to accurately calculate AREA.

5.5.2 B31G: Parabolic Area (2/3 dL) and Rectangular Area (dL)

The exact area of metal loss is difficult to represent in terms of simple geometric shapes defined by maximum length and depth. Two shapes which were considered in the development of the original B31G criterion were the rectangle (AREA = Ld) and the parabola (AREA = 2/3 Ld). On the basis of the 47 burst tests of corroded pipe (Kiefner 1974), it was shown that the parabolic method was preferable.

In reality, the parabolic method has significant limitations. Obviously, if the corroded area were very long, the effect of the metal loss would be underestimated and the remaining strength would be over estimated. The fact that the B31G underestimated the strengths in all 47 cases is probably the result of circumstances such as the pits not being lined up axially and the deepest areas being separated by islands of greater remaining wall thickness. To prevent misuse of the criterion in cases where long, deep corroded areas might actually have lower strengths than the criterion would predict, the parabolic method was limited to defects where A values are less than or equal to 4.0. For cases where A becomes larger than 4.0, the rectangular area (dL) is applied.

5.5.3 Modified B31G: 0.85 dL

The 0.85 dL method was proposed by Kiefner and Vieth (1989) to replace the parabolic method (2/3 dL). In both the 0.85dL method and the parabolic method, the total length L_{Total} is used to calculate Folias factor.

The choice of 0.85dL for AREA is arbitrary as was the choice of 2/3 dL in the original criterion. Without the other changes (i.e. flow stress and to the Folias factor) this new area representation would be more conservative than the parabolic representation. However, the 0.85 dL values becomes a reasonable choice because it can be used safely to analyse much longer flaws than the parabolic representation ($A \leq 4$, Kiefner and Vieth 1989).

5.5.4 Exact Area

More realistic representations of the metal loss are available if more detailed measurements of the pit depth profile are made.

Kiefner and Vieth (1989) proposed that the exact area of irregularly shaped corrosion defect can be calculated using

$$AREA = (y_a + y_1)x/2 + (y_1 + y_2)x/2 + \ldots + (y_{n-1} + y_b)x/2 = L_{total}\, d_{avg} \qquad \textbf{(5.14)}$$

in which ***n equal sub-intervals*** have been laid off on the x-axis (in longitudinal direction) by an equal distance x (= L_{Total}/n)

$$y_0, y_1, y_2, \ldots, y_{n-1}, y_n$$

are the respective ordinates (the reduction of the pipe wall-thickness) of these points.

In the proposed criterion, a refined procedure is to calculate AREA of irregularly shaped corrosion defect based on Simpson's rule. The Simpson's rule reads

$$AREA = \frac{b-a}{6n}[y_a + 4y_1 + 2y_2 + 4y_3 + 2y_4 + \ldots + 4y_{2n-1} + y_b] \qquad \textbf{(5.15)}$$

in which *2n equal sub-intervals* have been laid off on the x-axis (in longitudinal direction) by

$$a, x_1, x_2, \ldots, x_{2n-1}, b$$

and

$$y_a, y_1, y_2, \ldots, y_{2n-1}, y_b$$

are the respective ordinates (the reduction of the pipe wall-thickness) of these points.

The Simpson's rule assumes that small arcs of the curve are very nearly coincident with the arc of the parabola through the midpoint and terminal points of the arc. If the curve is not higher order than 3, this formula with n=1, gives the exact area and is called the prismoidal formula. Eq.(3.11) for assessing AREA of short corrosion defect can be obtained from the Simpson's rule by assuming n=1 in Eq.(5.15). It is noted the Simpson's rule has been widely used in engineering calculation, e.g. ship stability calculation.

Thus the exact area is being represented by a rectangular area which is the product of the total length times the average depth. With the parameters L_{Total} and d_{avg} thus defined, one can calculate Folias factor M based upon L_{Total} and NG-18 equation to calculate failure stress. Note that $AREA/AREA_0$ in the NG-18 equation becomes d_{avg}/t.

5.5.5 Equivalent Area

A second method (more accurate than the parabolic method) of analysing the remaining strength on the basis of the corrosion profile is called the equivalent length method. In this method, the metal-loss area, AREA, is defined as

$$AREA = L_{eq}\, d = L_{Total}\, d_{avg} \tag{5.16}$$

where d is the maximum depth. In this method, the area is identical to that of the total length method but L_{eq} is used as the length instead of L_{Total}.

$$L_{eq} = L_{Total}\left(d_{avg} / d\right) \tag{5.17}$$

In this case, the area of the defect is being represented by a rectangle $L_{eq}d$. L_{eq} is used to calculate Folias factor M and the NG-18 equation can be used to calculate failure stress. Note that $AREA/AREA_0$ in the NG-18 equation becomes d/t.

5.5.6 Effective Area

A third more accurate method involves calculations based on various subsections of the total area of metal loss and is called "Effective area method" (Kiefner and Vieth 1989). The regions include all possible subsets of the total area, based on the profile measurement increment. The minimum predicted failure pressure calculated by this approach is usually more accurate than that calculated by B31G, hence the level of conservatism in the defect acceptance criterion is reduced.

The application of the methodology is as follows:

(a) Obtain a composite of the corrosion depth profile along longitudinal meridians that pass through the deepest and the longest areas of corrosion. Several profiles are required to compile a "worst-case" composite profile.

(b) The lengthwise measurement increment should be based on the particular profile being considered. Where it is irregular, the increment should be on the order of 0.1 inch (2.5 mm). In areas without abrupt transitions, larger increments such as 2t are acceptable.

(c) Evaluate each profile. The lowest calculated safe pressure governs.

The Effective Area Method is embodied in the RSTRENG2 program(Kiefner and Vieth 1993).

Since iterative calculation is necessary (this means a computer program is needed), the effective method is not recommended by the present project.

5.6 Closely Spaced Corrosion Pits

Corrosion in pipelines often results in colonies of pits over an area of the pipes. Unfortunately, B31G, based on the length and maximum depth of a corroded area, ignores beneficial effects of circumferential spacing of pits and triaxial stress distributions. No provision exists in the original B31G criterion for considering the effects of interaction between closely spaced corrosion pits. As a result, such areas must either be conservatively treated as being continuous or possibly be non-conservatively considered as separate defects based on an arbitrary criterion of separation. It is therefore necessary to develop a rational criterion of separation.

Kiefner (1974), Kiefner and Vieth (1990b), Hopkins and Jones (1992) and Chouchaoui and Pick (1993) conducted experimental and numerical research on the burst strength of pipe with multiple corrosion pits. Their main conclusions are:

(1) Pits separated by a small distance interacts Figure 5-5 (a)). The distance could be conservatively taken as t based on experimental and numerical data in Hopkins and Jones (1992), and Chouchaoui and Pick (1993). The burst pressure of *circumferentially spaced pits* separated by a distance longer than t, can be accurately predicted by considering the deepest pit within the colonies of pits In such cases, pits lying along spirals behave independently as circumferential spacing eliminates any interaction.

(2) The most critical situation is when pits are oriented *longitudinally* (Chouchaoui and Pick 1992c). The pits lie on the same axial plane but are separated by a distance(See Figure 5-5 (b)). Such pit configurations may alter the hoop stress distribution and promotes bulging, leading to earlier leakage of the pit. According to Table 2 of Chouchaoui and Pick (1993), corrosion pits separated by a critical distance less than about t interact and the failure stress of interacting corrosion can be predicted by neglecting the beneficial effects of the non-corroded area in between. This conclusion is in agreement with Kiefner and Vieth (1990b) who indicated that significant interaction occurred only when the spacing is 1 in. or less, based on Kiefner's earlier tests. Similar conclusion has also been made by Hopkins and Jones (1992) who indicated that pits separated by a distance of t did not interact, and their failure stress could be conservatively predicted using Eq.(3.7).

(3) In many cases, *parallel longitudinal pits are separated by a circumferential distance* but their individual profiles overlap when projected to a single plane through the wall-thickness(see Figure 5-5 (c)). Experiments have suggested that pits can be treated as interacting pits if the circumferential spacing is less than a critical distance. Thus, the projected method as incorporated in the B31G criterion appears adequate for such corrosion configurations. However, pits can be considered separately if the spacing is equal to or greater than the critical distance. According to the tests by Hopkins and Jones (1992) and Chouchaoui and Pick (1993) the critical distance could be conservatively taken as t.

Therefore in the proposed criterion, the criterion of separation is to use a critical distance of t, for parallel longitudinal pits and a colony of longitudinal pits.

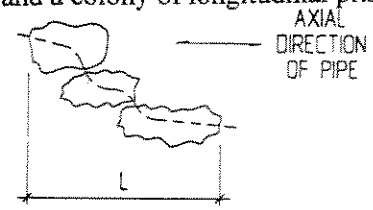

(a) Closely Spaced Pits

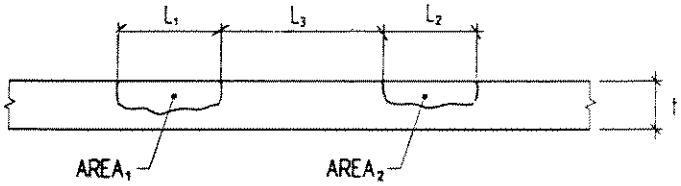

(b) Longitudinally Oriented Pits

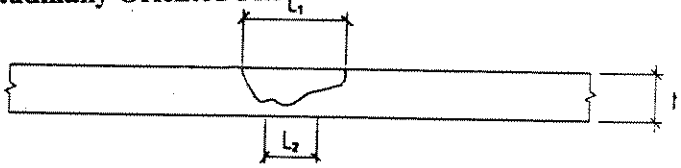

(c) Parallel Longitudinal Pits

Figure 5-5 Closely Spaced Corrosion Pits

5.7 Interaction of Longitudinal Grooves

The length of a pit is within a couple of times pipe wall-thickness. The corrosion defects having longer longitudinal length is called grooves.

According to British Gas Standard BGC/PS/P11,

(1) The effective depth of a longitudinal groove shall be determined as shown in Figure 5-6.

(2) The effective length of longitudinal grooves inclined to the pipe axis shall be determined as shown for a single groove in Figure 5-7 (a). For multiple grooves a similar procedure to that shown in Figure 5-7 (a) shall be applied to the effective length determined as described in (3).

(3) Longitudinal Grooves in close proximity in the longitudinal or circumferential direction may interact. The effective lengths of such grooves shall be determined using the procedures given in Figure 5-7 (b) and (c).

(4) To avoid errors in the determination of effective length or effective depth the procedure specified in (3) shall be used in the order specified in Table 5-5.

Table 5-5 Order of Procedure for the Evaluation of Effective Length and Effective Depth of Longitudinal Grooves

Groove Type	First Step	Second Step	Third Step
Single groove parallel to pipe axis	Figure 5-6	-	-
Single groove inclined to pipe axis	Figure 5-6	Figure 5-7 (a)	-
Multiple grooves parallel to pipe axis	Figure 5-6	Figure 5-7 (b),(c)	-
Multiple grooves inclined to pipe axis	Figure 5-6	Figure 5-7 (b),(c)	Figure 5-7 (a)

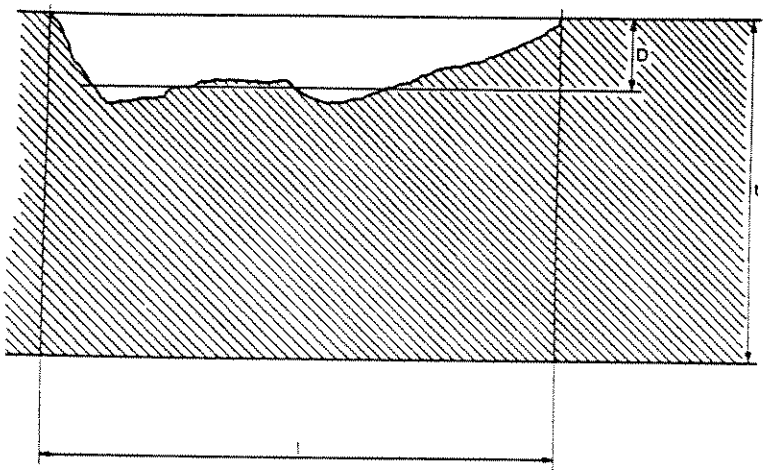

Notes: 1 t is the wall thickness of the pipe. l is the defect length parallel to the axis of the defect

2 A profile gauge or other means shall be used to measure depths along the defect, and hence the sectional area along the axis of the defect shall be calculated. Sufficient depth measurements along the defect length shall be made to ensure an accuracy of ± 10% of the actual area of metal loss.

3 Divide the calculated sectional area (see 2 above) by the defect length (l) to determine the effective depth d. Hence the area given by l x d is equal to the actual area of metal loss measured.

Figure 5-6 Effective depth of a Longitudinal Groove (After Fig.14 of British Gas Standard BGC/PS/P11)

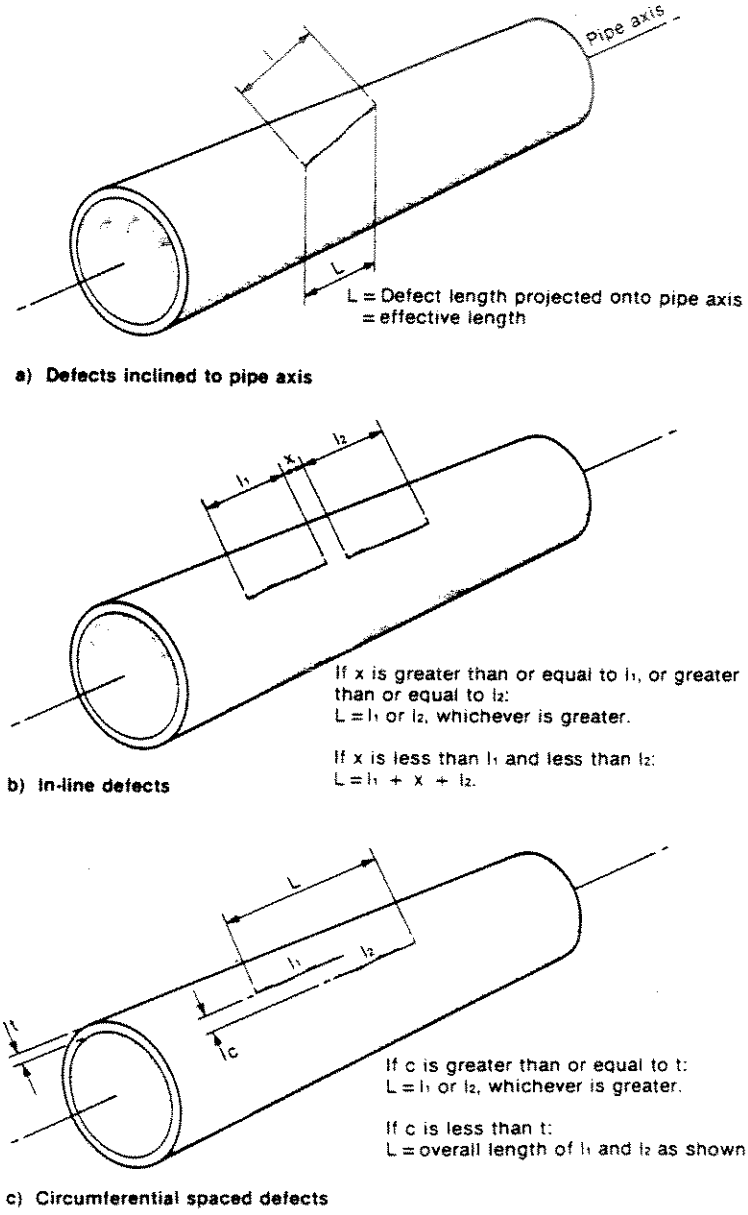

Figure 5-7 Effective Length and Interaction of Longitudinal Grooves (After Fig.15 of British Gas Standard BGC/PS/P11)

5.8 Spiral Corrosion

5.8.1 General

For defects in other orientations, the ANSI/ASME(1993) standard recommends the projection of the defect onto the longitudinal axis of the pipe and treatment as a longitudinal defect. This technique appears adequate for shorter defects, but is conservative for long longitudinal defects and more conservative for long spiral defects. With a longitudinal defect, the full hoop stress is acting over the length of the defect; whereas with a spiral defect, the hoop stress is only acting over the longitudinal width of the defect.

5.8.2 Mok's Tests

The applicability of the B31G criterion to long longitudinal corrosion defects and long spiral corrosion defects was investigated experimentally by Mok et al (1990, 1991) of NOVA. Two series of burst tests of large-diameter pipeline were undertaken by NOVA during 1986 and 1988, see Table 5-6. The pipe was made of grade 414 (X60) steel with an outside diameter of 508 mm and a wall-thickness of 6.35 mm. Longitudinal and spiral corrosion defects were simulated with machined grooves on the outside of the pipe.

In the first series of burst tests, a total of 13 pipes (No. 1 - No. 13 of Table 5-6) were burst. In all tests, the simulated corrosion defects were 25.4 mm wide and 2.54 mm deep producing a width to thickness ratio (W/t) of 4 and a depth to thickness ratio (d/t) of 0.4. Various lengths and orientations of the grooves were studied. Angles of 20, 30, 45 and 90 degrees from the circumferential direction, referred to as the spiral angle, were used. In some tests, two adjacent grooves were used to indicate interaction effects. One specimen of plain pipe (no corrosion) was also tested.

In the second series of burst tests, seven pipes were tested(No. 14 - No. 20 of Table 5-6). The defect geometries tested were longitudinal defects, circumferential defects, and corrosion patches of varying W/t and d/t. A corrosion patch refers to a region where the corrosion covers a relatively large area of pipe and the longitudinal and circumferential dimensions are comparable. In some of the pipes, two defects of different sizes were introduced but were kept far enough apart to eliminate any interaction. Again, a plain pipe was tested to provide a reference for the effect of the defect depth on the burst pressure.

As shown in Table 5-6, the B31G prediction of burst pressure is in most cases conservative, especially in the first series of tests in which the defects were long. The ratio of the experimentally measured burst pressure to the B31G predictions are all (except for No. 18) more than 1; in some cases, a ratio of 2 was observed, which means that B31G under-predicts the actual burst pressure by up to 50%.

For plain pipe without corrosion defects, B31G predicts a burst pressure of 11.38 MPa. The conservative prediction can be contributed to the definition of burst as being when hoop stress reaches a flow stress of 1.1 SMYS. Since this neglects the true stress distribution resulting from bulging and local thinning (or necking) of the material, it can be significantly in error.

For spiral defects with spiral angles other than 0 or 90 degrees, B31G under-predicts the burst pressure by as much as 50 %. The predictions are most conservative for small spiral angles. As indicated earlier, B31G projects a defect with spiral orientation onto the longitudinal axis and treats it as a longitudinal defect. This treatment is adequate for short defects. However, for long defects, it is conservative. This is observed in the burst tests in which the burst pressure of the spiral defects is higher than longitudinal defects (e.g. Test No. 2, 3, and 5). It appears that the stress component perpendicular to the spiral defect is the component that causes failure. Therefore, treating all defects as longitudinal defects would overestimate the stress level, especially for small spiral angles.

Table 5-6 Summary of NOVA Burst Tests and Predictions

Test No. [1),2)]	Spiral Angle	Length (mm) [6)]	Depth (d/t)	Width (W/t)	Burst Pressure MPa	B31G Criterion MPa	Proposed Criterion MPa [5)]
1	20	1114	0.4	4.0	14.54	6.82	11.64
2	30	762	0.4	4.0	13.84	6.82	10.83
3	45	539	0.4	4.0	12.34	6.82	9.56
4	20	558	0.4	4.0	15.84	6.82	11.91
5	90	381	0.4	4.0	11.24	6.82	8.30
6	90	1016	0.4	4.0	11.54	6.82	7.95
7	90	2-152[3)]	0.4	4.0	13.04	9.30	9.17
8	90	2-152[3)]	0.4	4.0	13.04	9.30	9.17
9	90	2-152[3)]	0.4	4.0	13.04	9.30	9.17
10	20	2*950[4)]	0.4	4.0	15.24	6.82	11.69
11	90	2*381[4)]	0.4	4.0	11.04	6.82	8.30
12	90	2*381[4)]	0.4	4.0	10.54	6.82	8.30
13	Plain	Plain	Plain	Plain	15.44	11.37	12.92
14	Plain	900	Plain	Plain	15.25	11.37	12.92
15	90	900	0.54	4.0	8.00	5.23	6.18
16	90 90	900 152	0.34 0.52	4.0 4.0	11.80 -	7.50 -	8.74
17	0 0	- -	0.47 0.20	16.1 32.0	12.50 -	11.31 -	12.79
18	0 0	- -	0.46 0.51	32.0 16.1	9.80 -	11.31 -	12.79
19	Patch Patch	32t 16.1t	0.53 0.50	32.0 16.1	8.45 -	8.22 -	7.21
20	90	1000	0.50	4.0	8.40	5.68	6.67

Note: (1) Pipe Geometry: Outside Diameter = 508 mm; Wall-thickness t=6.35 mm
(2) Pipe Material: X60 Steel
(3) 2-152 indicates two aligned longitudinal defects each with length of 152 mm.
(4) 2*381 indicates two parallel defects each with length of 381 mm.
(5) In the proposed criterion, σ_{flow} is taken as ultimate tensile stress
(6) Nominal length along the spiral corrosion. To get the longitudinal length use sin(angle)*L

5.8.3 Effect of Spiral Angle - Mok's Approach

A finite element approach was applied by Mok et al (1991) to study the effects of the spiral angle and defect width (the extent of corrosion in the circumferential direction)

Figure 5-8 shows the effect of spiral angle (after Fig. 7 of Mok et al 1991), for a case with material grade X60, OD = 508 mm, t=6.35 mm, d/t=0.4, W/t=4).It is shown that the burst pressure decreases as the spiral angle increase from 0^0 (circumferential defect) to 90^0 (longitudinal defect).This is because the longitudinal dimension of a spiral defect perpendicular to the maximum hoop stress increases as the spiral angle increases.

However, the significance of the spiral angle effect depends on the defect depth. Figure 5-9 shows the effect of spiral angle for two defect depths, d/t=0.2 and 0.4 (after Figure 9 of Mok et al 1991), for the case material grade X60, OD = 508 mm, t=6.35 mm, W/t=4).The results for each depth show a similar trend with respect to the spiral angle. The deeper defects fail at lower burst pressures. It is observed that the effect of defect depth is less profound for defects with small spiral angles. In fact, defect depth has almost no effect on circumferential defects.

Mok et al (1991) recommended that the bursting pressure level for spiral long corrosion is

$$P_b = \frac{2\sigma_{flow} t}{D}(1 - Q\frac{d}{t}) \qquad \textbf{(5.18)}$$

where Q is the spiral correction factor, which is estimated by

$$Q = \frac{1 - Q_1}{32}\frac{W}{t} + Q_1 \qquad \textbf{(5.19)}$$

in which the coefficient Q_1 is a function of the spiral angle ψ ($\psi=90^0$ for longitudinal corrosion, $\psi=0^0$ for circumferential corrosion):

$Q_1=$	0.2	for $0^0<\psi<20^0$
$Q_1=$	0.02ψ-0.2	for $20^0<\psi<60^0$
$Q_1=$	1.0	for $\psi>60^0$

It is noted that the value of Q must lie between 0 and 1.0. For W/t>32, the value of Q must be taken as 1.0. Combining Mok's equation with the NG-18 equation, the safe maximum pressure level for long spiral corrosion is proposed by the present project as

$$P' = \frac{1}{\gamma}\frac{2\sigma_{flow} t}{D}\frac{1 - Q\,AREA / AREA_0}{1 - M^{-1}\,AREA / AREA_0} \qquad \textbf{(5.20)}$$

The prediction due to this equation is compared with NOVA's tests in Table 5.5.

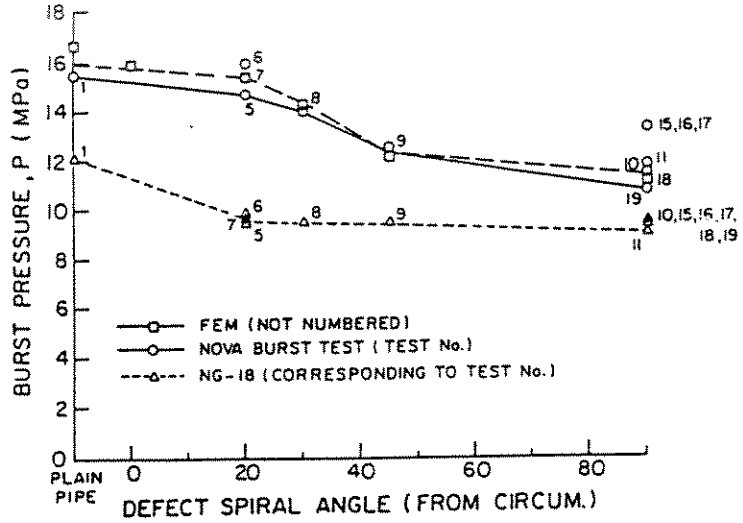

Figure 5-8 The Effect of Spiral Angle

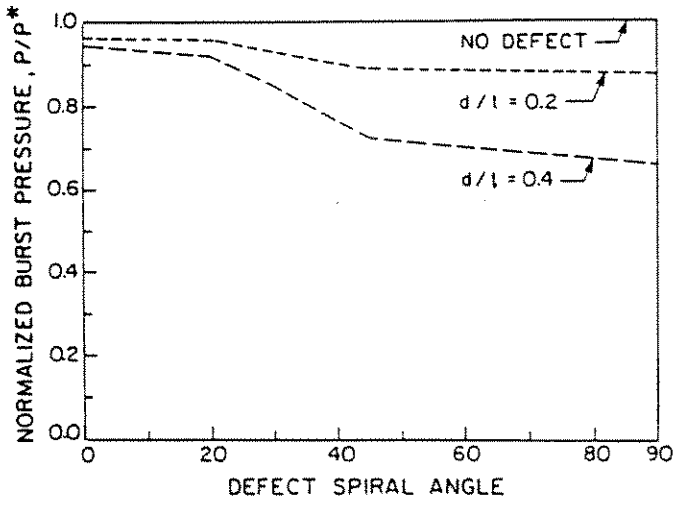

Figure 5-9 The Effect of Spiral Angle
The Significance of the Spiral Angle for Different Defect Depth

5.8.4 Effect of Spiral Angle - Fu and Jones Approach

Fu and Jones (1994) presented a method for predicting the failure pressure of spiral corrosion in pipeline. Fu and Jones (1994) proposed that the failure pressure could be calculated using

$$P_b = \frac{2\sigma_{flow} t}{D} \frac{1 - \frac{d}{t}}{1 - A^{-1} M^{-1} \frac{d}{t}} \tag{5.21}$$

in which Spiral Angle Correction Factor A is obtained from the solid lines in Figure 5-10. In the figure, α is the spiral angle and λ is $0.5(12(1-\nu^2))^{1/4} L/(Rt)^{1/2}$.

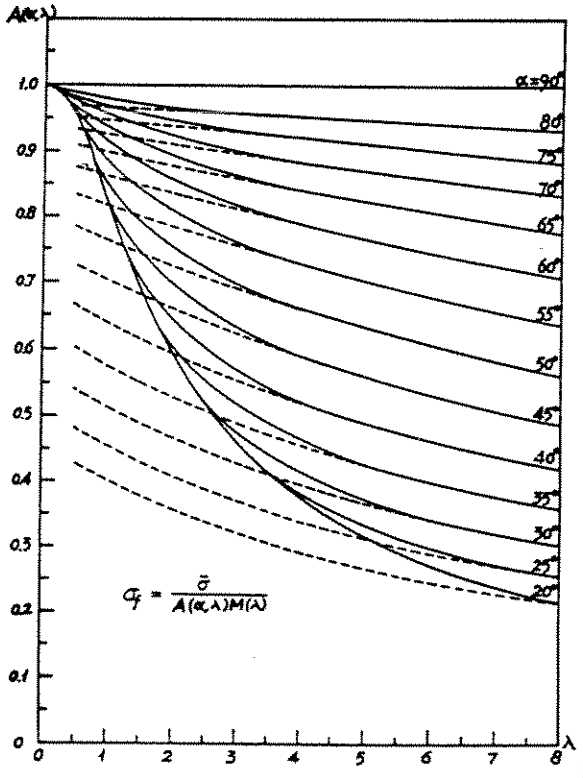

Figure 5-10 Spiral Angle Correction Factor A (After Fig.4 of Fu and Jones (1994))

5.9 Effect of Corrosion Width

The B31G criterion does not include any correction for the width of a defect.

Figure 5-11 shows the effect of defect width on burst pressure of pipe with *a circumferential defect* (after Fig.10 of Mok et al 1991), for the case material grade X60, OD = 508 mm, t=6.35 mm. The burst pressure decreases linearly as the width of the defect increases. For large defect widths (W/t>32, where W is the dimension across the defect width), the pipe with the defect behaves as a plain pipe with wall-thickness equal to the thickness of the defect ligament. For very small defect widths (e.g. a circumferential crack), which were not considered in Figure 5-11, a decrease in burst pressure would be expected because the defect would exhibit crack like behaviour.

Figure 5-12 shows the effect of defect width on burst pressure of pipe with *a longitudinal defect* (after Fig.11 of Mok et al 1991), for the case material grade X52, OD = 508 mm, t=6.35 mm, d/t=0.4. Again, crack like defects (e.g. longitudinal cracks) were not considered in Figure 5-12.

An interesting contribution of Stewart et al (1994) work is that it gives an analytical formula to account for the effect of the circumferential extent of the longitudinal corrosion. The increase due to partial corrosion in the circumferential direction compared with fully corroded pipe is given by the circumferential width correction factor f as

$$f = \left(\frac{2}{1 + \frac{W}{\pi D}} \right)^{n'} \qquad \textbf{(5.22)}$$

in which W is the circumferential width (W=0 for no circumferential extent, W=πD for full circumferential length) and n′ is the hardening parameter which is defined by the Ludwik power law and calculated as

$$n' = \ln(1 + \varepsilon_u) \qquad \textbf{(5.23)}$$

where ε_u is the engineering ultimate tensile strain.

In Figure 5-13, the width correction factor f in Eq.(5.22) is plotted. The curve based on n′=0.1 is plotted as dotted line. This comparison between Figure 5-12 and Figure 5-13 shows that the analytical predictions agree with the finite element results.

Assuming n′=0.1 and n′=0.2, the values of the width correction factor f are 1.04 and 1.09 for W/(πD)=0.3 and 1.02 and 1.05 for W/(πD)=0.6.

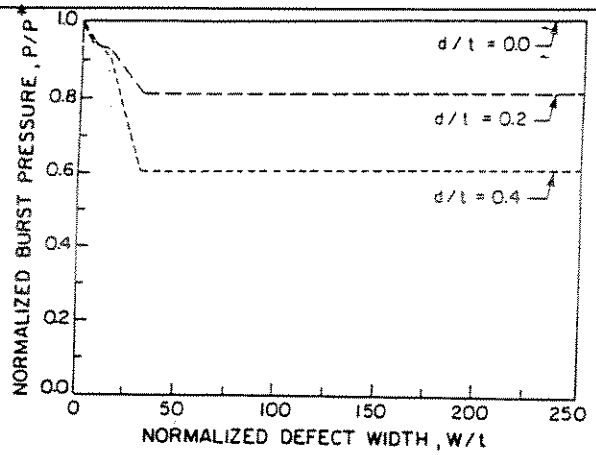

Figure 5-11 The Effect of Defect Width for a Pipe with a Circumferential Defect

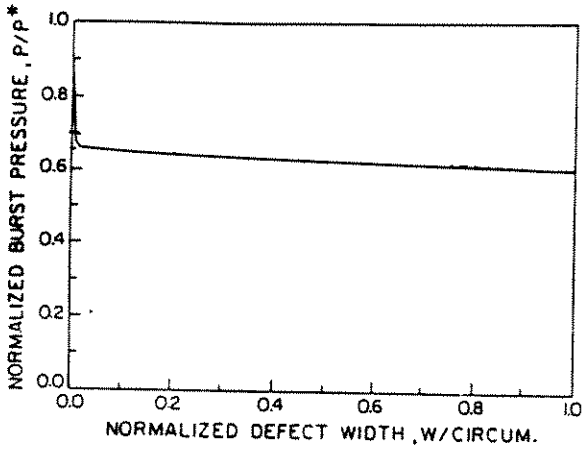

Figure 5-12 The Effect of Defect Width for a Pipe with a Longitudinal Defect (Mok)

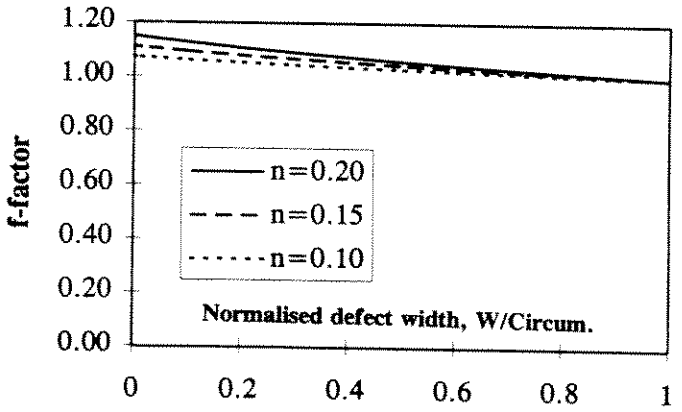

Figure 5-13 The Effect of Defect Width for a Pipe with a Longitudinal Defect (Stewart) for n=0.2, n=0.15 and n=0.1.

5.10 Corroded Welds, Ductile and Low Toughness Pipe

5.10.1 Corroded Welds

It is clearly indicated that the B31G criterion does not cover the corrosion near or in the welds. There is a need to assess the effect of localised corrosion of weld on the fracture resistance of pipeline. Figure 5-14 shows typical patterns of weld corrosion. The fracture mechanics criteria (e.g. PD6493) provide a mathematical relationship between critical combination of external loads(e.g. internal pressure), weld defects and fracture toughness (PD6493 1991).In addition to fracture, fatigue crack growth due to cyclic pressure may also be evaluated using the PD6493 criteria.

In *seam welded* pipes, the hoop stresses will have the greatest effect on a corroded seam weld. Various types of seam welds exist, including double submerged arc welds (DSAW), lap welds (LW), furnace butt welds (FBW), flash welds (FW), electric resistance welds (ERW), and induction welds (IW).

The hoop stress arising from internal pressure loading would act parallel to a corroded *girth weld* and hence would have little effect unless the corrosion was very severe. However, longitudinal stress due to axial and bending loads will act normal to the girth weld, and hence the stress concentration arising from the corrosion groove may be significant. This will be discussed in Chapter 6.

5.10.2 Corrosion in Longitudinal Seams

The existing B31G criterion does not apply to corrosion in any type of seam weld. This situation can be changed as follows: Corrosion in submerged-arc welds should be treated exactly as corrosion in the body of the pipe. Corrosion in ERW or flash-welded seams should not be evaluated on the basis of either the existing B31G criterion or the proposed modified criterion (Kiefner and Vieth 1989).

The justification for treating corrosion in a submerged-arc-seam in the same manner as corrosion in the body of the pipe is that both operating experience and test data show that such seams tend to be at least as resistant to defects as the pipe material itself. Evidence of this was gathered over 20 years ago as shown in Table 5-7 (Kiefner 1969).It involves pairs of tests in which identical through-wall flaws were fabricated into two samples of the same length of pipe. In one sample, the defect was located in the heat-effected zone of the submerged-arc seam or in the fusion line on the ERW seam or flash-welded seam, while in the other sample the defect was located in the body of the pipe. The burst pressures of the flawed specimens were compared as shown in Table 5-7. In every instance the failure stress levels of defects in the submerged-arc welded seams were higher than those of the defects in the body of the pipe. In contrast, defects located in ERW and flash-welded pipe exhibited failures at stress levels below those of the defects in the body of the pipe.

Besides the evidence from these tests, experience has shown that hydrostatic test ruptures and service failures which originate in or near submerged-arc welds seldom propagate preferentially

in the weld or heat-affected zone. More commonly, such fractures tend to move further from the weld as they propagate. In contrast, experience in relation to hydrostatic test failures and service failures originating in or near ERW or flash-welded seams reveals many cases in which the fracture propagated end-to-end in the weld often at obviously higher speeds judging by the lack of fracture arrest. While this experience may not be typical of currently fabricated ERW pipe, it is a major consideration for the vast majority of ERW pipe that has been in service for some time and will be likely to be involved in inspection or revalidation projects.

One other factor which serves to discourage the consideration of corrosion in ERW or flash-welded seams by these methods is the fact that such corrosion is generally "selective" in nature, progressing more deeply and narrowly at the fusion line of the seam that into the surrounding pipe. Thus, a situation is created in which a relatively sharp defect exists in a material with less than optimum toughness. In addition, its crevice-like nature makes it difficult to obtain the critical depth dimensions for the analysis. Given these situations, it is not prudent to use the flow-stress dependent analysis methods of both the existing B31G and the proposed modified criteria to evaluate corrosion in ERW or flash-welded seam.

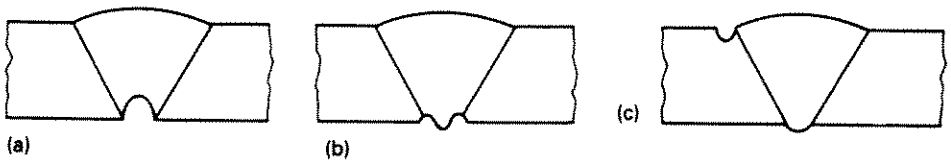

(a) Root Groove **(b) Corrosion of Root HAZ** **(c) Corrosion at Toe of Cap**

Figure 5-14 Typical Patterns of Weld Corrosion (Andrews (1992a)).

Table 5-7 Comparisons of the Failure Pressures of Through-wall Flaws in Longitudinal Welds with Identical Defects in the Pipe Material (After Table 3 of Kiefner and Vieth 1989)

Material	Type of Longitudinal Weld	Flaw Length (inch)	Failure Pressure (psig)	Ratio of Failure Pressure of Weld Flaw to That of Flaw in Pipe Material, percent
30 x 0.328 inch X60				
Pipe		7.00	705	---
Weld	DSA	7.00	870	123
30 x 0.360 inch X60				
Pipe	---	6.00	925	---
Weld	DSA	6.00	995	108
30 x 0.390 inch X60				
Pipe	---	3.00	1265	---
Weld HAZ[a]	DSA	3.00	1334	106
30 x 0.375 inch X52				
Pipe	---	7.00	785	---
Weld	FW	7.00	695	89
30 x 0.360 inch X60				
Pipe	---	5.30	950	---
Weld	FW[b]	5.30	830	88
20 x 0.250 inch X52				
Pipe	---	3.00	1193	---
Weld	ERW	3.00	1102	92

a) Flaw was located approximately in the heat affected zone (HAZ) at mid thickness of the pipe wall. Both inside and outside reinforcements were ground off.
b) Normalised flash welds.

FW = flash welds
ERW = electric resistance welds
DSAW = double submerged arc welds
FBW = furnace butt welds
LW = lap welds
IW = induction welds

5.10.3 Fracture Mechanics Assessment

Conventional fracture mechanics criteria can be applied to assess the risk of fracture. In the following discussion, the level 2 (or level 3) PD6493 procedure is used, as proposed by Andrews (1992a).Details of the procedure of assessing brittle fracture (K_r) and plastic collapse (S_r) are given in PD6493 (1991).

The assessment procedure for the S_r (the ratio of effective net section stress and the flow stress) of the failure assessment diagram (FAD) will be the same for a corroded weld as for a crack, since plastic collapse is not affected by local stress concentrations.

An approach for assessing the stress intensity factor ratio K_r (the ratio of the stress intensity factor to the material fracture toughness) of a corroded weld is to assume the groove as a crack of the same depth and length and use equations written in PD6493(1991).

When a corrosion groove intersects a pre-existing crack, or a fatigue crack may initiate and grow from a groove, a stress intensity factor required for fracture mechanics analysis could be obtained using the stress concentration factors from handbooks (e.g. Peterson 1974) or finite element analysis of the particular geometry (Andrews 1992a).

It is noted that the effect of fracture toughness of the material is accounted for in the calculation of the stress intensity factor ratio K_r according to fracture mechanics criteria(PD6493 1991).

5.10.4 Ductile and Low Toughness Pipe

The methods of flaw assessment presented in this report (Section 5.10.3)are applicable to pipe steels that can be expected to exhibit ductile fracture initiation. Most pipe materials manufactured under API Specification 5L since the First Edition (1927) can be expected to initiate failure in a ductile manner. However, many materials made prior to 1927 and some made afterward are susceptible to brittle failures at low levels of applied stress in the presence of small defects. This may also be the case for many contemporary pipeline materials when exposed to low temperature. Furthermore, ductile failure initiation may transform to brittle fracture propagation even in contemporary materials.

5.11 Effect of Axial Load

The B31G criterion does not distinguish between open and close ended conditions and it was validated from close ended test data. The effect of axial load is not explicitly accounted for in the B31G criterion but it has been developed for pipes with end caps and therefore certain axial tension is applied, which is half of the stress in the circumferential direction in elastic region. The burst pressure for close ended pipe can be higher than the one for open ended pipe.

5.11.1 Causes of Axial Load

The causes of axial load are summarised as bellow:

(a) Differential pressure and Poison effect

The axial force N due to differential pressure for Unrestrained Pipelines, is estimated as

$$N = \frac{\pi}{4}(D-2t)^2 P_i - \frac{\pi}{4} D^2 P_e \qquad \textbf{(5.24)}$$

in which P_i and P_e are internal and external pressure respectively and compressive axial load is positively defined.

(b) Differential Temperature

The axial load due to the difference of the temperature in the outside and the inside of pipe is

$$N_T = -\pi(D-t)tE\alpha_T\Delta T \qquad (5.25)$$

in which α_T denotes thermal expansion coefficient and E is the Young's modulus.

(c) Residual tension after pipeline installation

The amount of the axial load due to pipeline installation depends on the sea bottom and installation methods.

(d) Soil movement

(e) Uniform or concentrated loads on spans

5.11.2 Finite Element Analyses

The effect of various loadpaths on the burst pressure of longitudinally corroded pipes were investigated by means of the finite element methods. Two models were utilised, and a total of 26 analyses were carried out. Three different load paths were evaluated, while two of the load paths were investigated in more details.

A. Operating pressure, succeeded by external axial load until ultimate collapse (burst).

B. Operating pressure, succeeded by a external constant axial compressive strain (displacement), and further additional pressure until ultimate collapse.

C. Operating pressure, succeeded by a external constant axial compressive stress (force), and further additional pressure until ultimate collapse.

The loadpath B and C were investigated in more details.

Problem

In the finite element analysis of the bursting behaviour and ultimate strength of longitudinally corroded pipes under combined internal pressure and axial compression, the pipes shown in Table 5-8 are considered.

Geometry

The bursting behaviour and ultimate strength of the corroded pipes under combined loads are numerically studied for the following two pipes:

Table 5-8 Pipe and Corrosion Geometries - Longitudinally Corroded Pipes under Combined Internal Pressure and Axial Compression

	Outer Diameter D (mm)	Wall-Thickness t (mm)	Defect Depth d(mm)	Defect Length L (mm)	Defect Width W (mm)	d/t	W/(πD)
Pipe-1D	304.8(12 in)	6.35	4.953	infinite	20.0	0.78	0.021
Pipe-2E	914.(36 in)	22.0	6.6	infinite	480	0.3	1/6

Boundary condition
The boundary condition is determined considering symmetric conditions in the axial and circumferential directions.

Load application
A static solution procedure implemented in the finite element program Spectrum (Centric 1995) is applied to study the pre- and ultimate strength behaviour.

Material parameters
A power law curve is used for the true-stress/logarithmic-plastic-strain relationship for strains greater than 1 %. This has the following analytical form for API 5L X60 material:

$$\sigma_0 = C\varepsilon_0^{n'} \quad ; \quad C = \left(\frac{e}{n'}\right)^{n'} \sigma_{ult} \quad for \quad \varepsilon_0 > 1\% \tag{5.26}$$

in which n′=0.13 and σ_{ult} = 563 MPa. σ_0 and ε_0 denotes true-stress and logarithmic-plastic-strain respectively. e is the base of the natural logarithm. The yield stress is 434 MPa. Between zero and 1 % plastic strain, a linear relationship is assumed for the stress/strain curve.

Note that Young's Modulus E is 210000 MPa and Poison's Ratio ν is 0.3.

The analyses and results are included in details in a separate report, DNV report 95-3514 "Finite Element Analyses of Corroded Pipes" (Bjørnøy and Skjolde (1995)).

5.11.3 Bursting Behaviour and Ultimate Strength

In Figure 5-15 to Figure 5-20 the hoop stress versus the longitudinal stress are plotted for both models (Table 5-8) and the three different loadpaths.

In Figure 5-15 results from the analyses using the model with d/t=0.78 are shown. The figure shows the stresses for the loadpath A at a position in the corroded region (local), and at one position far off the corroded region (nominal). The von Mises yield ellipse is also included. The pipe was exposed to internal pressure of 2 MPa, succeeded by axial compressive force until failure. The Figure 5-16 shows the stresses for the analysis with the loadpath B, which was first internal pressure of 2 MPa, then axial compressive strain of 0.133% (displacement control), and succeeded by additional internal pressure until failure. And finally, in Figure 5-17 shows the

stresses for the analysis with loadpath C. First internal pressure was applied, then axial compressive stress of 75 MPa, and succeeded by additional internal pressure until failure.

The Figure 5-18 to Figure 5-20 shows the same results as in Figure 5-15 to Figure 5-17, but for the model with d/t=0.3. The internal pressure was 14.3 MPa (2MPa for the previous model), the applied axial strain was -0.32%, and the applied compressive stress was 197 MPa.

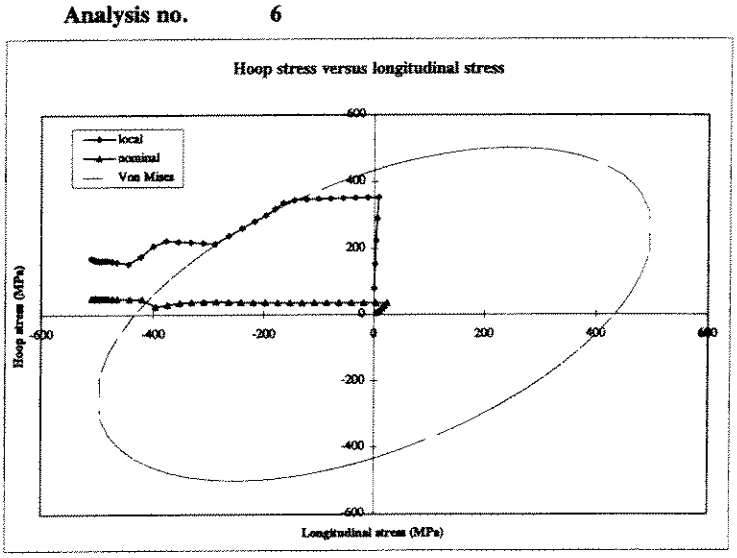

Figure 5-15 Hoop Stress Versus Longitudinal Stress for model Pipe 1D, for loadpath A

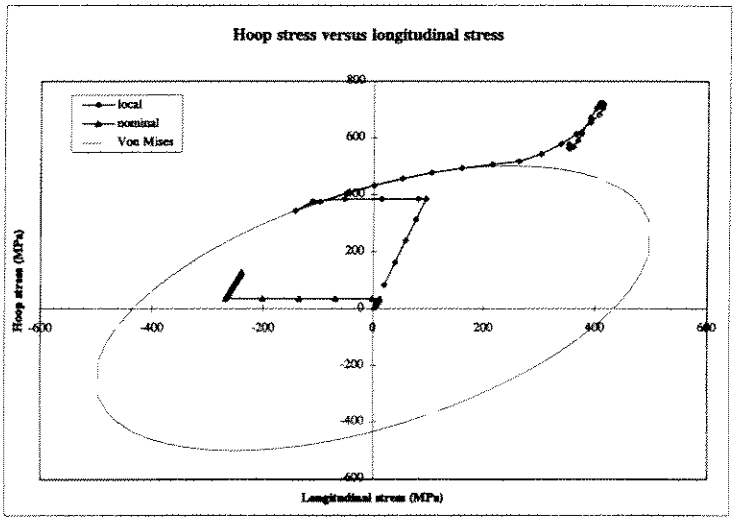

Figure 5-16 Hoop Stress Versus Longitudinal Stress for model Pipe 1D, for loadpath B

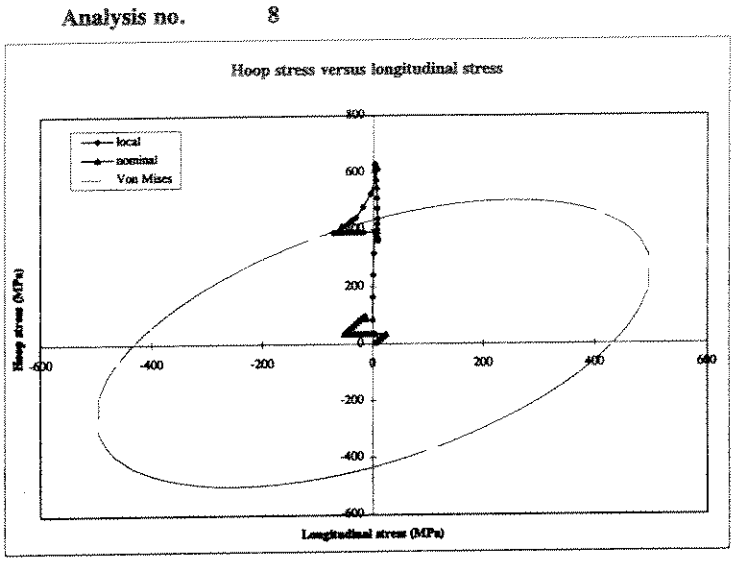

Figure 5-17 Hoop Stress Versus Longitudinal Stress for model Pipe 1D, for loadpath C

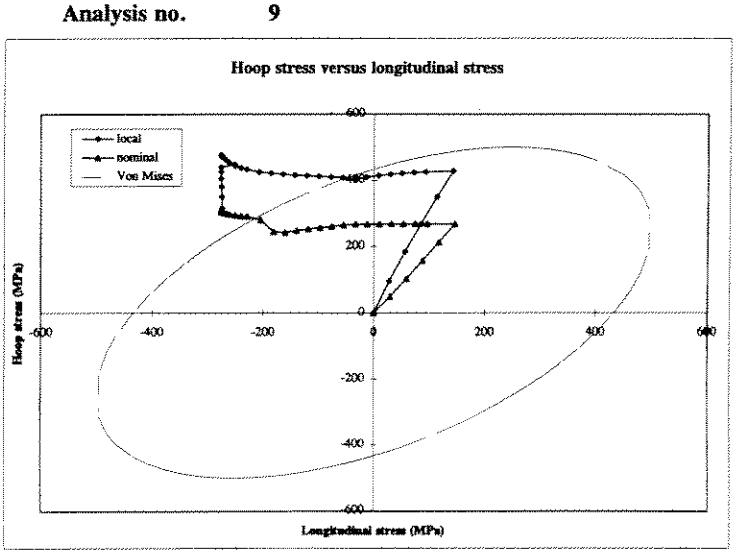

Figure 5-18 Hoop Stress Versus Longitudinal Stress for model Pipe 2E, for loadpath A

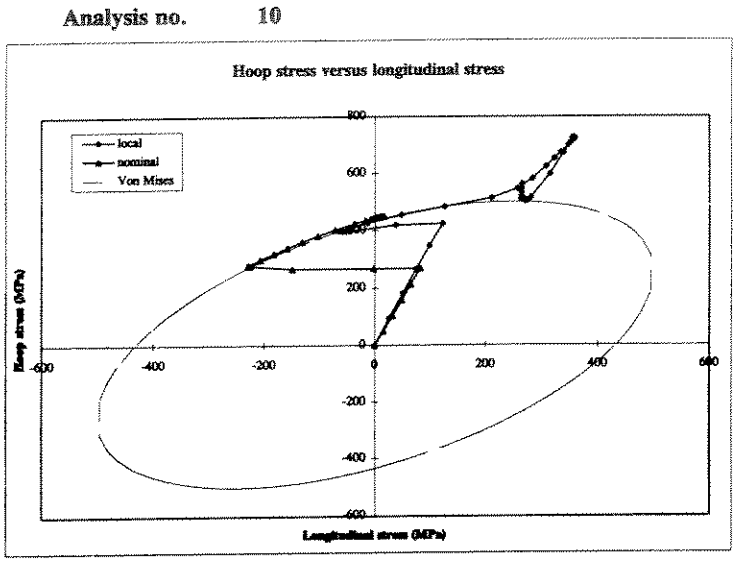

Figure 5-19 Hoop Stress Versus Longitudinal Stress for model Pipe 2E, for loadpath B

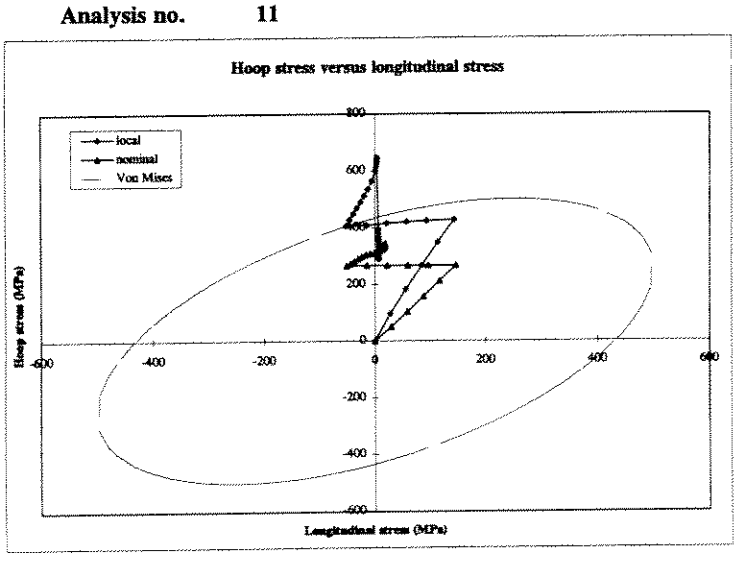

Figure 5-20 Hoop Stress Versus Longitudinal Stress for model Pipe 2E, for loadpath C

5.11.4 Interaction Curves for Selected Loads

For both models described in Table 5-8 several analyses were carried out for the loadpath B and C described in Chapter 5.11.3. The results are shown in Figure 5-21 to Figure 5-24. The figures show the loadpath and the failure point. A von Mises yield interaction curve is also indicated, and the prosedure to calculate the curve is shown in this section.

Part 1: Load path: Design Pressure --> Axial Stress --> Pressure to Burst

Figure 5-21 Interaction between Burst Pressure and Axial Stress for Longitudinally Corroded Pipe (D=914 mm, t=22 mm, d/t=0.3)

Figure 5-22 Interaction between Burst Pressure and Axial Stress for Longitudinally Corroded Pipe (D=304.8 mm, t=6.35 mm, d/t=0.78)

The axial stress is a load type loading (different from that of deformation load). The axial stress is the sum of the stress due to the end cap effect and the applied axial compressive stress. It has been shown that axial stress reduces burst pressure. It is observed that the interaction between compression and bending can be represented by von Mises yield function. A procedure to generate the interaction curve is as follows:

(1) To calculate the point on the Y-axis of the coordinate system using the proposed criterion, reduced to $P_0 = \sigma_{ult} \cdot 2 \cdot t \cdot (1-d/t) / D$ when $M \rightarrow \infty$.
(For example; $P_0 = 563$ MPa·2·6.35 mm·(1-0.78) / 304.8 mm = 5.16 MPa)

(2) The point on the X-axis is calculated as $X_0 = \sigma_{ult} \cdot Area_{corroded} / Area_{uncorroded}$, which is a simple capacity reduction due to the reduced cross section area.
(For example; $X_0 = 563$ MPa · $(\pi Dt - wd)/\pi Dt = 554$ MPa)

(3) The points between these two points are generated using von Mises yield function.

$$\left(\frac{P}{P_0}\right)^2 + \left(\frac{X}{X_0}\right)^2 - \frac{P}{P_0} \cdot \frac{X}{X_0} = 1 \qquad (27)$$

Part 2: Load path: Design Pressure --> Axial Strain --> Pressure to Burst

Figure 5-23 Interaction between Burst Pressure and Axial Strain for Longitudinally Corroded Pipe (D=914 mm, t=22 mm, d/t=0.3)

Figure 5-24 Interaction between Burst Pressure and Axial Strain for Longitudinally Corroded Pipe (D=304.8 mm, t=6.35 mm, d/t=0.78)

The axial strain is a deformation type loading and its value is a constant while applying pressure to burst. It has been shown that the pressure to burst is almost a constant for different levels of axial strain.

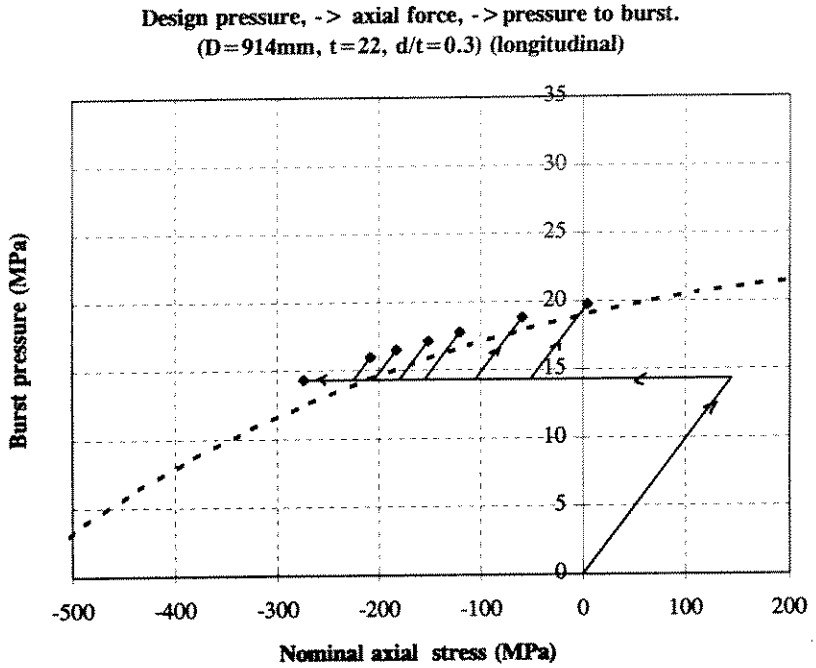

Figure 5-21 Interaction between Burst Pressure and Axial Stress for Longitudinally Corroded Pipe (D=914 mm, t=22 mm, d/t=0.3)

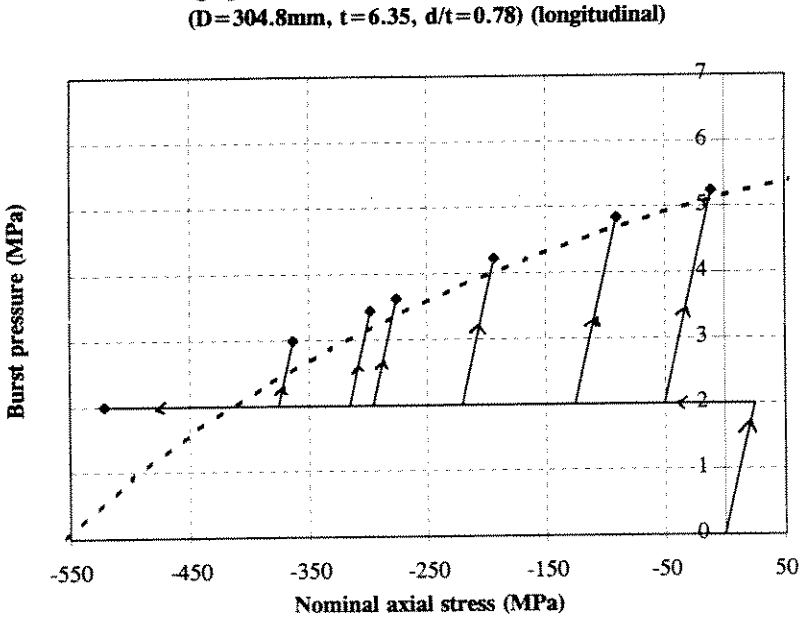

Figure 5-22 Interaction between Burst Pressure and Axial Stress for Longitudinally Corroded Pipe (D=304.8 mm, t=6.35 mm, d/t=0.78)

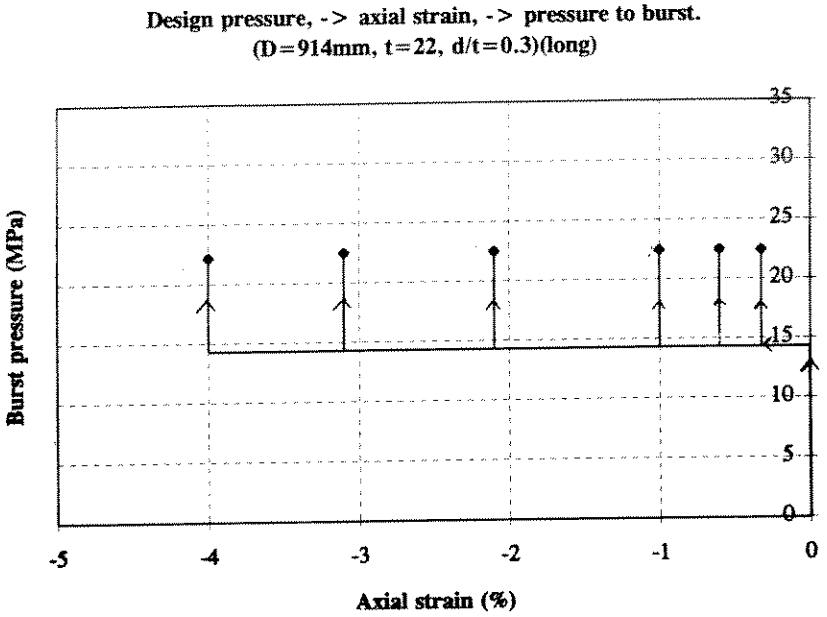

Figure 5-23 Interaction between Burst Pressure and Axial Strain for Longitudinally Corroded Pipe (D=914 mm, t=22 mm, d/t=0.3)

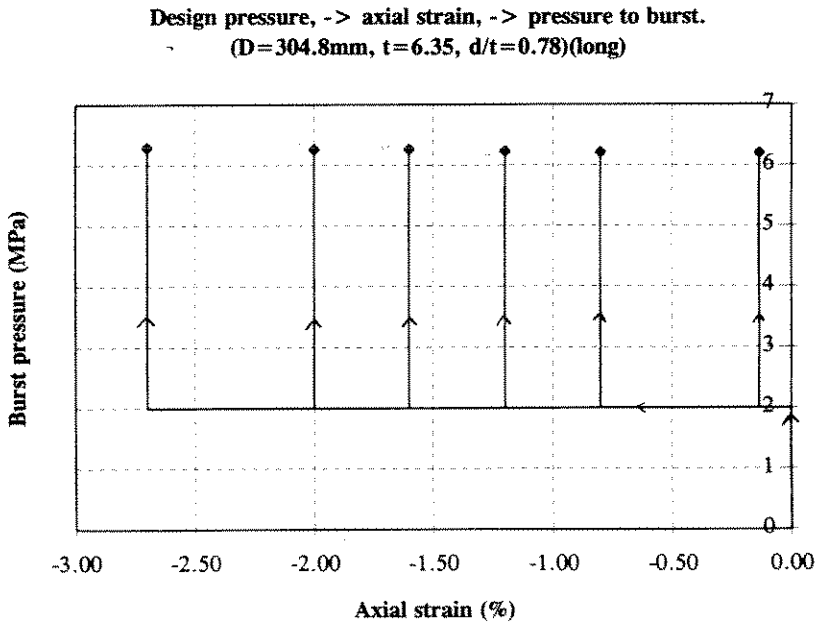

Figure 5-24 Interaction between Burst Pressure and Axial Strain for Longitudinally Corroded Pipe (D=304.8 mm, t=6.35 mm, d/t=0.78)

5.11.5 Proposed Interaction Equations

In the B31G criterion, the effect of axial load has not been discussed. Tensile longitudinal stress may delay yielding and pipe burst. On the other hand, compressive longitudinal stress may accelerate yielding and result in reductions in burst pressure. The effect of axial force and the material yield anisotropy can be considered using Hill's yield function for plastic flow problems (Bai et al 1993a). Note that Hill's yield function is an extension of von Mises function including material yield anisotropy effect.

Radial stresses may be neglected in structural cylinders of usual proportions (whose D/t exceeding about 12, see pp. 502 of Galambos 1988). This topic is concerned with the interaction of the hoop stress caused by pressure and the longitudinal stress resulting from a combination of axial and bending loads.

In Bai et al (1993a), it has been demonstrated through finite element analysis using ABAQUS, that the interaction between axial tension and external pressure can be considered as a problem of material yielding under biaxial loads when plastic flow is involved. It was found that the reduction of hoop buckling strength due to axial tensile load could be estimated using Hill's yield function.

This observation could possibly also be valid for the case when internal pressure is applied together with axial tensile or compressive load. In Figure 5-25 (after Fig.14.13 of Galambos(1988)), the general yield failure of thick-walled pipe based on the maximum strain energy theory is shown. Ellipses have been plotted for Poisson's ratio of 0.3 and 0.5. It was found that Poisson's ratio varied between 0.3 and 0.5 during inelastic action and an average value of 0.4 was recommended through 200 tests of oil well casings. From the figure, it is illustrated that:

- The internal burst pressure is largely reduced by axial compression.
- The effect of axial tension is beneficial, but negligible when it is less than 60 percent of yield strength of the pipe section. However, this effect is significant when axial tension is larger than 60 % of the yield strength.

In fact, this conclusion has also be made by Chouchaoui B.A. and Pick R.J. (1993) through ABAQUS analysis of the effect of end conditions. Since the effect of *axial compression* is significant, this must be of some concern when considering corroded pipes experiencing *bending*.

Due to lack of material yield anisotropy information in connection with application of Hill's yield function, von Mises function is recommended for accounting for the effect of the axial load, in the proposed criterion.

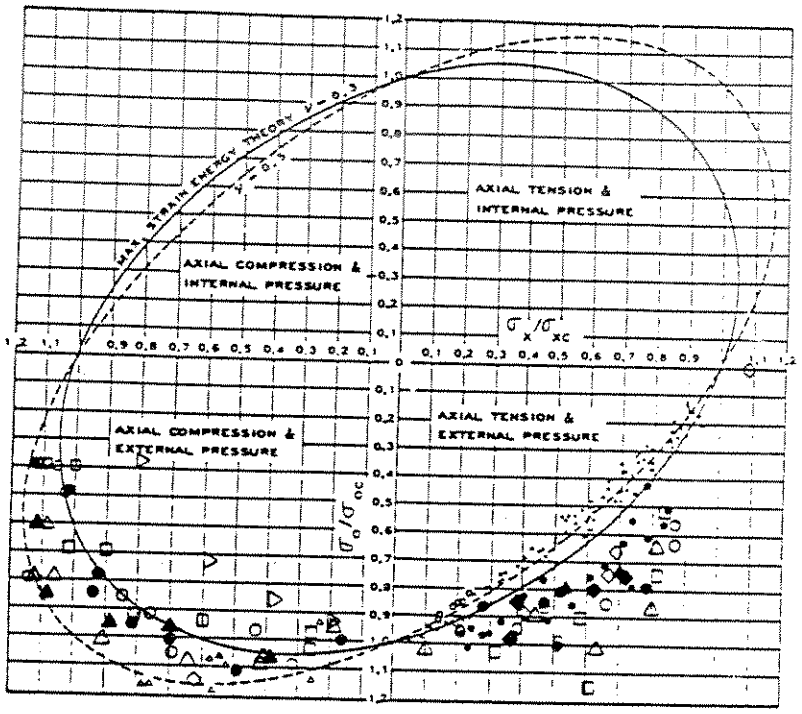

Figure 5-25 Effect of Axial Load on the Collapse Pressure (after Fig.14.13 of Galambos(1988))

5.12 Effect of Axial and Bending Loads

Although longitudinal stresses in pipelines are often insignificant, they may occur under some conditions, such as wave action or vortex shedding on a free span, or loading of a marine riser. However, B31G and its modifications consider internal pressure alone. When large axial and bending stresses are coupled with corrosion, the B31G predictions of burst pressure may be not conservative.

Darlaston and Harrison (1977) experimentally examined ductile failure of pipes with longitudinal defects under combined internal pressure and bending. The interaction of internal pressure and bending on the ductile failure of a pipe containing an axial defect has been demonstrated for a limited range of size.

Since the dominant effect of bending stress is the reduced hoop stress in the corroded region, it is proposed that the flow stress used in the bursting strength assessment, is calculated following the von Mises yield function using the axial (longitudinal) stress in the corroded region.

This conclusion is verified by finite element analysis results, Figure 5-21 and Figure 5-22.

5.13 Proposed Modifications Compared with B31G Criterion

In this section, a criterion is proposed for possible implementation in residual strength and re-qualification assessment.

(1) The NG-18 surface-flaw equation has been adopted for the prediction of hoop stress level at failure.

(2) Calculation of AREA, Spiral correction factor Q, flow stress σ_{flow} and Folias factor M has been improved:

(a) Corrosion AREA

-Irregularly Shaped Corrosion:

Two levels of AREA assessment are proposed.

-Closely Spaced Corrosion Pits:

Criterion for pit separation distance has been proposed which is of vital importance for accurate calculation of AREA for closely spaced corrosion pits.

-Interaction of Longitudinal Grooves

(b) Spiral correction factor Q

(c) Flow Stress σ_{flow}

The flow stress is ultimate tensile stress σ_u or SMTS (Specified Minimum Tensile Stress) if σ_u is unknown.

(d)Folias factor M

The Folias factor used in the modified B31G criterion (Kiefner and Vieth 1989) is adopted.

(3) Corroded Welds, Ductile and Low Toughness Pipe

A fracture mechanics approach for assessing corroded welds is proposed. The effect of material's fracture toughness (in ductile and low toughness pipe) could be taken into account in the assessment procedure.

(4) Corroded Pipe under Combined Pressure, Axial and Bending Loads

For corroded pipe under combined pressure, axial and bending loads, the flow stress in the circumferential direction could be calculated considering the effects of the longitudinal stress, using von Mises yield condition. The longitudinal stress in the corroded region is calculated using beam theory based on the axial and bending loads applied.

Item (2) will reduce the scatter in the predictions and improve the accuracy of the criterion. Items (3) and (4) lead to extension of the application range since these items have not been addressed in the B31G criterion.

6 CIRCUMFERENTIAL WELD CORROSION

Under certain conditions, the longitudinal tensile stress levels caused by external loading (axial and/or bending components) combined with internal pressure may exceed the hoop stress level due to internal pressure. In instances where elevated longitudinal stresses act on a corrosion defect that has greater circumferential than longitudinal extent, circumferential failure is theoretically possible, although it is not known to have occurred in service other than *as a result of defective girth weld.* Girth weld corrosion is primarily confined to the lower part of the pipe, e.g. from 4 o'clock to 8 o'clock at the most. B31G criteria are not suitable for evaluating whether circumferential failure is possible.

The assessment procedure is as follows:

(a) Evaluate the longitudinal defect profile by B31G criteria to verify that the defect is acceptable at the maximum operating pressure.

(b) Evaluate the longitudinal stress state of the pipeline, considering factors such as internal pressure, thermal expansion, spanning loads, and other loading as appropriate. Calculate the ratio of longitudinal stress to circumferential stress $R_s = \sigma_L/\sigma_C$.

(c) Calculate the ratio of the circumferential and longitudinal dimensions of the defect, $R_L = L/b$.

(d) If $R_S \leq 0.5$, or if $R_S \leq R_L$ further evaluation for circumferential failure is unnecessary. If $R_S > 0.5$, and $R_S > R_L$, evaluate the defect for circumferential failure by the methods described in this Chapter.

In this Chapter, existing strength equations for circumferential failure are compared with tests and finite element analysis results.

When this project is closing, a paper by Clyne and Jones (1995) to be published in Sept. 1995 becomes available. The paper is a result of a major research project. Clyne and Jones (1995) also extensively reviewed the work of Miller (1988) (as we did) and extensively collected experimental data for pipes containing circumferential girth weld defects under internal pressure, external bending and combined external bending and internal pressure. A total of 126 tests were collected (but not included in details in the paper): 87 in three or four point bending, 8 under internal pressure and 31 under combined external bending and internal pressure. The paper contains figures comparing tests results and predictions due to alternative criteria. Their conclusions are very similar to this project's achievement. Kastner's equation was recommended (as Miller (1988) suggested) and a safety factor of 2 was proposed.

6.1 Existing Criteria for Plastic Collapse of Circumferentially Corroded Pipe

6.1.1 Kastner's Local Collapse Criterion

The plastic collapse behaviour of girth weld corrosion can be predicted using a failure criterion proposed by Kastner (Kastner et al 1981):

$$\frac{\sigma_{AX}}{\sigma_{flow}} = \frac{\eta[\pi - \beta(1-\eta)]}{\eta\pi + 2(1-\eta)\sin\beta} \qquad (6.1)$$

where

d = defect depth
t = wall-thickness
$\eta = 1 - d/t$
c = half defect (circumferential) length
R = pipe radius
$\beta = c/R$ (in radians)
σ_{flow} = flow stress

and in which σ_{AX} denotes the total axial stress.

This equation is derived below:

The centre of gravity of the flawed pipe is

$$e_1 = -R_m\eta\frac{\sin\beta}{\pi - \eta\beta} \qquad (6.2)$$

The pressure p then causes a bending moment

$$M = p R_i^2 R_m\eta\frac{\sin\beta}{\pi - \eta\beta} \qquad (6.3)$$

This bending moment is not only acting in the flawed cross-section but also some distance ahead, causing a bending stress at $\phi=0$

$$\sigma'_2 = 2\eta\frac{\sin\beta}{\pi - \eta\beta}\frac{p R_i}{2tp}\frac{R_i}{R_m} = \frac{2\eta\sin\beta}{\pi - \eta\beta}\sigma_{AX} \qquad (6.4)$$

In the flawed cross-section this stress in the unflawed pipe is augmented by the ratio of wall thickness and ligament thickness, thus

$$\sigma_2 = \frac{2\eta}{1-\eta}\frac{\sin\beta}{\pi - \eta\beta}\sigma_{AX} \qquad (6.5)$$

This stress has to be added to the stress caused by the internal pressure

$$\sigma_1 = \frac{\pi}{\pi - \eta\beta}\sigma_{AX} \tag{6.6}$$

Equating the sum of σ_1 and σ_2 to the flow stress σ_{flow}, the critical crack-angle for a certain flaw depth is given by

$$\frac{\sigma_{AX}}{\sigma_{flow}} = \frac{\eta[\pi - \beta(1-\eta)]}{\eta\pi + 2(1-\eta)\sin\beta} \tag{6.7}$$

6.1.2 Schulze's Global Collapse Criterion

Schulze et al (1980) proposed a net-section collapse formula (global collapse):

$$\frac{\sigma_{AX}}{\sigma_{flow}} = 1 - \frac{\beta(1-\eta) + 2\sin^{-1}[0.5(1-\eta)\sin\beta]}{\pi} \tag{6.8}$$

6.1.3 Chell Method

A conservative method for estimating the strength of pipe with circumferential corrosion is the Chell method (Chell 1979).The minimum longitudinal tensile stress to cause failure is calculated as

$$\sigma_{AX} = \sigma_{flow}\left(1 - \frac{d_{eff}}{t}\right) \tag{6.9}$$

where

$$d_{eff} = d\frac{1 - \frac{1}{f}}{1 - \frac{d}{t}\frac{1}{f}} \tag{6.10}$$

$$f = \sqrt{1 + \frac{(W/t)^2}{2}} \tag{6.11}$$

and d = depth of corrosion
W = circumferential width of corrosion

Chell method can be rewritten as

$$\frac{\sigma_{AX}}{\sigma_{flow}} = \frac{\eta}{1 - (1-\eta)/f} \tag{6.12}$$

6.2 Circumferentially Corroded Pipes under Internal Pressure

It is assumed that brittle fracture of the girth weld corrosion is not conceivable. Consequently, failure of the girth weld corrosion by plastic collapse only is considered. The girth weld corrosion is assessed in terms of its depth and circumferential length.

Since a girth weld defect is very short in longitudinal direction (of typically pipe wall-thickness), its influence on burst pressure is negligible and the influence can be assessed using B31G. Failure of a corroded girth weld is controlled by the axial tensile stresses.

The axial stress due to internal pressure is conservatively assumed to be 0.5 * hoop stress (which is obtained for unrestrained pipelines):

$$\sigma_{AX} = \frac{PD}{4t} \qquad \textbf{(6.13)}$$

where

P = internal pressure
D = pipe diameter
t = pipe wall thickness at girth weld location

We note that the axial stress is reduced to 0.3 * hoop stress in a fully restrained pipeline. The total axial stress is the sum of the axial stress due to internal pressure and the axial stress result from:

- thermal expansion
- elastic curvature
- uniform weight over spans
- concentrated load on span
- soil movement

Consequently the approach adopted in the assessment is to determine the maximum axial stress that the girth weld corrosion can survive.

The plastic collapse behaviour of girth weld corrosion can be predicted by comparing the total axial stress with equations given in Chapter 6.1 (i.e. Kastner's equation).

Figure 6-1 compares tests and the prediction due to Schulze's global (= net-section) collapse value and Kastner's local collapse value. A comparison of limit pressure solutions due to Schulze and Kastner is shown in Table 6-1.

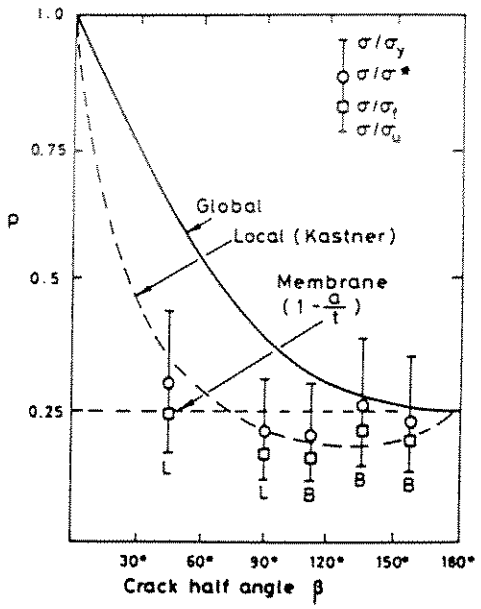

Figure 6-1 **Circumferentially Corroded Pipe under Pressure (with end cap) with experimental results from Eiber et al (1971), L=Leak, B=Break, a/t=0.75, $\sigma^* = \sigma_f/1.2$, p=(PD)/(4tσ_{flow}), From Fig.69 of Miller (1988)**

a/t =	0·1		0·3		0·5		0·7		0·9	
β/π	G	L	G	L	G	L	G	L	G	L
0·00	1·00	1·00	1·00	1·00	1·00	1·00	1·00	1·00	1·00	1·00
0·05	0·99	0·98	0·97	0·95	0·95	0·89	0·93	0·78	0·91	0·50
0·10	0·98	0·97	0·94	0·90	0·90	0·79	0·86	0·64	0·82	0·33
0·15	0·97	0·95	0·91	0·85	0·85	0·72	0·79	0·54	0·73	0·24
0·20	0·96	0·94	0·88	0·81	0·81	0·66	0·73	0·46	0·65	0·19
0·25	0·95	0·93	0·86	0·78	0·76	0·60	0·67	0·40	0·57	0·15
0·30	0·94	0·92	0·83	0·75	0·72	0·56	0·61	0·36	0·49	0·13
0·35	0·93	0·91	0·81	0·72	0·68	0·53	0·55	0·33	0·42	0·11
0·40	0·92	0·90	0·79	0·70	0·65	0·50	0·50	0·30	0·36	0·10
0·45	0·92	0·89	0·77	0·68	0·62	0·48	0·46	0·28	0·30	0·089
0·50	0·91	0·89	0·75	0·67	0·59	0·46	0·42	0·26	0·25	0·082
0·55	0·91	0·88	0·74	0·66	0·57	0·45	0·39	0·25	0·21	0·076
0·60	0·91	0·88	0·73	0·65	0·55	0·44	0·36	0·24	0·18	0·071
0·65	0·90	0·88	0·72	0·65	0·53	0·43	0·34	0·24	0·15	0·068
0·70	0·90	0·88	0·71	0·65	0·52	0·43	0·33	0·23	0·13	0·066
0·75	0·90	0·88	0·71	0·65	0·51	0·43	0·32	0·23	0·12	0·064
0·80	0·90	0·88	0·70	0·66	0·51	0·44	0·31	0·24	0·11	0·064
0·85	0·90	0·89	0·70	0·66	0·50	0·45	0·30	0·24	0·10	0·065
0·90	0·90	0·89	0·70	0·67	0·50	0·46	0·30	0·25	0·10	0·069
0·95	0·90	0·90	0·70	0·69	0·50	0·48	0·30	0·27	0·10	0·077
1·00	0·90	0·90	0·70	0·70	0·50	0·50	0·30	0·30	0·10	0·10

G, global (= net-section) collapse values of *p*; *L*, local (Kastner) collapse values of *p*

Table 6-1 **Comparison of Limit Pressure Solutions due to Schulze and Kastner The table show p which is p=(PD)/(4tσ_{flow}), From Table 15 of Miller (1988**

Figure 6-2 illustrates the relationship between ultimate axial stress and d/t, based on criteria by Kastner, Schulze, Chell and B31G.

Figure 6-3 shows the relationship between ultimate axial stress and β (=c/R, where c is half defect circumferential length), based on criteria by Kastner, Schulze, Chell and B31G.

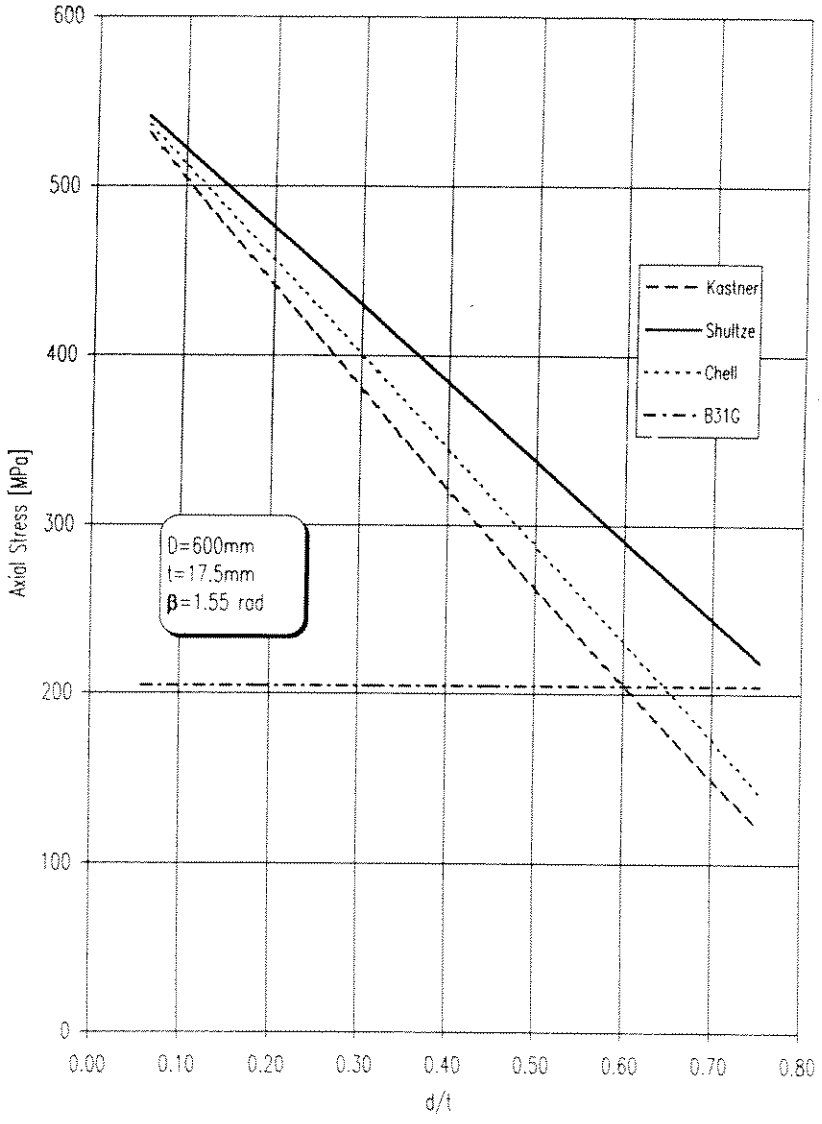

Figure 6-2 Ultimate Axial Strength of Circumferentially Corroded Pipes as a Function of d/t, based on criteria by Kastner, Schulze, Chell and B31G

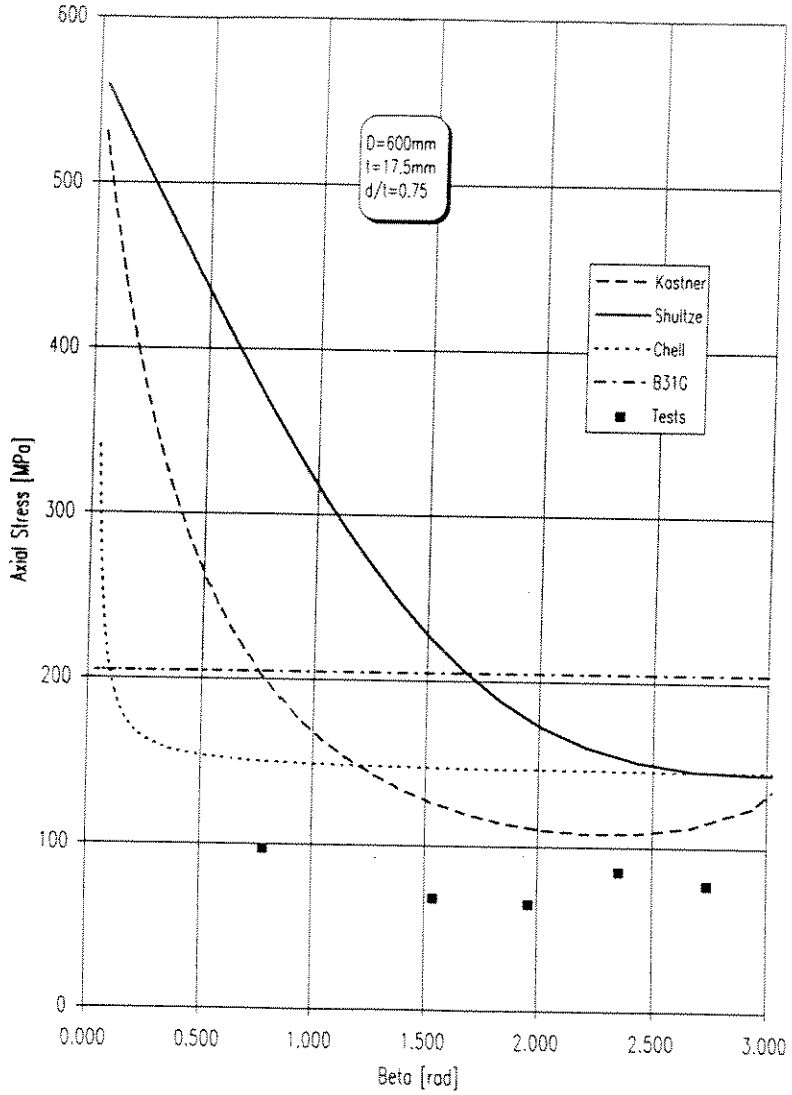

Figure 6-3 Ultimate Strength of Circumferentially Corroded Pipes under Internal Pressure with End Cap Effect as a Function of β (=c/R, where c is half defect circumferential length), based on criteria by Kastner, Schulze, Chell and B31G. The tests plotted are listed in Table 6-2 named Test 1C - Test 1G.

6.2.1 Comparisons of Existing Criteria and Tests of Pipes, Internal Pressure

Kastner et al (1981) collected laboratory tests by Watanabe et al (1977) (Table 6-2, Test 1A, Test-1B) and Eiber et al (1971) (Test-1C - Test-1G).

Table 6-2 Pipe and Corrosion Geometries and Material Properties Circumferentially Corroded Pipes under Internal Pressure

Number	Out. Diam. D (mm)	Wall-Thickness t (mm)	Defect Depth d (mm)	Defect Width W (mm)	d/t	W/(pD)	Yield Stress (MPa)	Ult. Stress (MPa)
Test-1A	100	5.7	3.42	37	0.60	0.24	304	576
Test-1B	100	5.7	4	37	0.70	0.24	304	576
Test-1C	600	17.4	13	471	0.75	0.25	219	568
Test-1D	600	17.25	12.87	942	0.75	0.50	219	568
Test-1E	600	17.5	13.1	1178	0.75	0.625	219	568
Test-1F	600	17.55	13.17	1413	0.75	0.75	219	568
Test-1G	600	17.45	13	1644	0.75	0.87	219	568

In Table 6-3 and Table 6-4, the flow stress equal to ultimate tensile stress has been assumed for the analysis. When B31G is applied, the axial stress at failure is 0.5 times of the burst hoop stress. In all calculations, safety factors are not applied and characteristic values are compared.

Table 6-3 Comparison of Laboratory Test Results and Existing Criteria - Bursting of Circumferentially Corroded Pipes under Internal Pressure

(The table shows mean axial stress in MPa)

Number	Labo. Test Results	Kastner Local Collapse	Schulze Global Collapse	Chell Method	B31G Criterion
Test-1A	210.	396.	494.	264.	288.
Test-1B	173.	341.	480.	201.	288.
Test-1C	97.	198.	365.	149.	284.
Test-1D	68.	126.	222.	149.	284.
Test-1E	65.	110.	175.	145.	284.
Test-1F	85.	106.	151.	144.	284.
Test-1G	77.	115.	146.	146.	284.

Test-1C - Test-1G are plotted in Figure 6-3, in which test results are compared with Kastner's local collapse criterion and Schulze's global collapse criterion.

The mean bias and COV for alternative criteria are shown in Table 6-4.

Table 6-4 Comparison of Laboratory Test Results and Existing Criteria - Mean Bias and COV

	Kastner Local Collapse	Schulze Global Collapse	Chell Method	B31G Criterion
Bias	0.591	0.403	0.619	0.387
COV	0.190	0.272	0.258	0.509

The choice of the flow stress has a great influence on the estimation of critical crack size. In Table 6-5 and Table 6-6, the flow stress equal to the mean of yield stress and ultimate tensile stress has been assumed for the analysis. When B31G is applied, the axial stress at failure is 0.5 times of the burst hoop stress. In all calculations, safety factors are not applied and characteristic values are compared.

Table 6-5 Comparison of Laboratory Test Results and Existing Criteria - Bursting of Circumferentially Corroded Pipes under Internal Pressure

(The table shows mean axial stress in MPa)

Number	Labo. Test Results	Kastner Local Collapse	Schulze Global Collapse	Chell Method	B31G Criterion
Test-1A	210.	303.	378.	201.	151.
Test-1B	173.	260.	367.	154.	151.
Test-1C	97.	137.	353.	104.	110.
Test-1D	68.	87.	154.	102.	110.
Test-1E	65.	76.	121.	101.	110.
Test-1F	85.	73.	105.	100.	110.
Test-1G	77.	80.	101.	101.	110.

The mean bias and COV for alternative criteria are shown below:

Table 6-6 Comparison of Laboratory Test Results and Existing Criteria - Mean Bias and COV

	Kastner Local Collapse	Schulze Global Collapse	Chell Method	B31G Criterion
Bias	0.833	0.566	0.861	1.68
COV	0.215	0.285	0.213	0.334

6.2.2 Finite Element Analysis of Bursting under Internal Pressure

6.2.2.1 Bursting Behaviour and Ultimate Strength

Problem

The purpose of the finite element analyses is to generate numerical data for the comparison of the accuracy of various analytical predictions.

Geometry and mesh

In the finite element analysis of the bursting behaviour and ultimate strength of circumferentially corroded pipes under internal pressure, the following pipes shown in Table 6-7 are considered.

Table 6-7 Pipe and Corrosion Geometries and Material Properties - Circumferentially Corroded Pipes under Internal Pressure

	Outer Diameter D (mm)	Wall-Thickness t (mm)	Defect Depth d (mm)	Defect Length L (mm)	Defect Width W (mm)	d/t	W/(pD)
Pipe-2G	914.0	22.0	13.2	20.0	479	0.6	0.167
Pipe-2H	914.0	22.0	13.2	20.0	957	0.6	0.333
Pipe-2I	914.0	22.0	13.2	20.0	1915	0.6	0.667
Pipe-2J	914.0	22.0	13.2	20.0	2872	0.6	1.0
Pipe-2K	914.0	22.0	6.6	40.0	957	0.3	0.333

Boundary condition

The boundary condition is determined considering symmetric conditions in the axial and circumferential directions.

Load application

A static solution procedure implemented in Spectrum (Centric 1995) is applied to study the pre- and ultimate strength behaviour.

Material parameters

A power law curve is used for the true-stress/logarithmic-plastic-strain relationship for strains greater than 1 %. This has the following analytical form for API 5L X60 material:

$$\sigma_0 = C\varepsilon_0^{n'} \quad ; \quad C = \left(\frac{e}{n'}\right)^{n'} \sigma_{ult} \quad for \quad \varepsilon_0 > 1\% \tag{6.14}$$

in which n_=0.13 and σ_{ult} = 563 MPa. σ_0 and ε_0 denotes true-stress and logarithmic-plastic-strain respectively. e is the base of the natural logarithm. The yield stress is 434 MPa. Between zero and 1 % plastic strain, a linear relationship is assumed for the stress/strain curve.

Note that Young's Modulus E is 210000 MPa and Poison's ratio ν is 0.3 in the linear range.

The analyses are described in details in the project report 95-3514, "Finite Element Analyses of Corroded Pipes", (Bjørnøy and Skjolde, 1995).

6.2.2.2 Comparisons of Finite Element Results and Existing Criteria

Table 6-8 compares the finite element analysis results with the existing prediction equations. In all calculations based on analytical formulae, the flow stress is taken as the ultimate tensile stress of the material σ_u. The axial stress σ_{AX} from the finite element analysis is taken as half of the hoop stress from the internal pressure: $\sigma_{AX} = (PD)/(4t)$.

Table 6-8 Comparison of Finite Element Analysis Results and Existing Criteria - Burst Pressure of Circumferentially Corroded Pipes under Internal Pressure

	Finite Element Results	Kastner Local Collapse	Schulze Global Collapse	Chell Method	B31G Criterion
Pipe-2G	301	343	453	234	203
Pipe-2H	280	247	356	230	203
Pipe-2I	267	185	244	227	203
Pipe-2J	269	225	225	227	203
Pipe-2K	312	247	356	230	203

(The table shows axial stress σ_{AX} in MPa)

Table 6-9 shows the mean bias and COV for alternative strength equations as compared to the finite element results.

Table 6-9 Comparison of Finite Element Analysis Results and Existing Criteria - Mean Bias and COV

	Kastner Local Collapse	Schulze Global Collapse	Chell Method	B31G Criterion
Bias	1.18	0.92	1.25	1.41
COV	0.174	0.236	0.061	0.069

The comparison is also shown in the following figure in which the analytical predictions are compared with Pipe-2B - Pipe-2E

Prediction based on the following strength equations are compared in Appendix C.

- Kastner's Local Collapse Criterion
- Schulze's Global Collapse Criterion
- Chell Method
- B31G criterion

B31G criterion is for longitudinal rupture due to internal pressure, while the other equations are for transverse fracture. While B31G criterion is compared, σ_{AX} is taken as 0.5 times the hoop stress (as for unrestrained pipes).

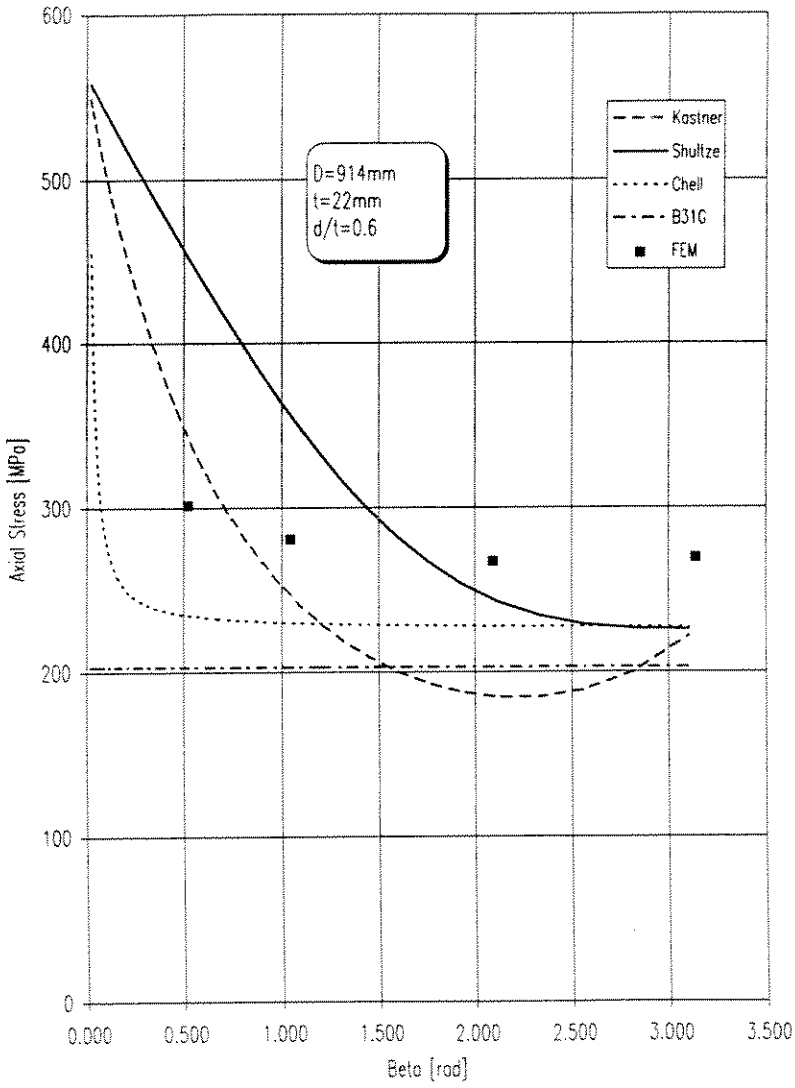

Figure 6-4 Burst Pressure as a Function of Circumferential Width (Angle) - Comparison of Finite Element Results with Analytical Prediction. The FEM results are listed in Table 6-8.

6.3 Circumferentially Corroded Pipe under Bending

6.3.1 Anderson's Equation

Plastic collapse of pipes with loss of material in circumferential direction had been investigated in a study on the failure of pipes containing girth weld repair grooves subjected to offshore laying stresses by Anderson et al (1988). A plastic collapse solution for circumferentially notched pipes in bending was derived. This analysis can be used to predict failure in pipes containing part-wall or through-wall repair grooves at various circumferential positions. Four-point bending tests on small scale pipe sections were performed to validate the analysis experimentally. The agreement between theory and experiment was reasonably good in most cases. The theoretical collapse solution is summarised below:

Consider a pipe containing a groove of length L and depth d, as shown in Figure 6-5. The neutral axis will shift owing to the presence of the notch. This shift Y_1 is given by

$$Y_1 = -\frac{R_g^2 d(\cos\alpha_1 - \cos\alpha_2)}{2\pi(R_m t - R_g dX)} \qquad (6.15)$$

where X is the fraction of cracked circumference:

$$X = \frac{L}{\pi D} \qquad (6.16)$$

The radius to the mid-thickness of the groove, R_g, and the angles α_1 and α_2 are defined in Figure 6-5.

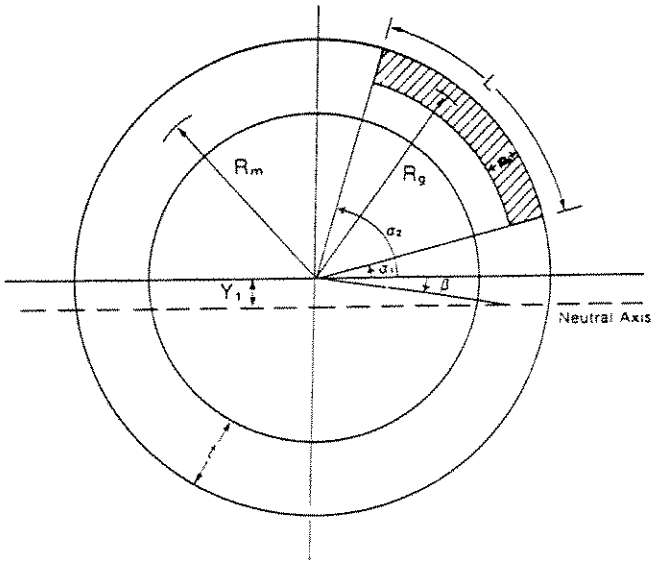

Figure 6-5 Definition of Terms in the Plastic Collapse Analysis of a Notched Pipe in Bending, From Fig.4 of Anderson et al (1988).

Consideration of moment equilibrium on the section below the neutral axis resulted in the following equation for collapse:

$$\frac{M'}{M_0} = \frac{1}{2}(\pi - 2\beta)\left(\frac{\cos\beta}{\frac{\pi}{2} - \beta} - \frac{Y_1}{R_m}\right) \tag{6.17}$$

Where

$$\beta = \sin^{-1}\left(\frac{Y_1}{R_m}\right) \tag{6.18}$$

(For the sake of mathematical convenience, angular dimensions in all equations are expressed in terms of radians).

M_0 is the collapse moment in un-noticed pipe and is computed from:

$$M_0 = 4 R_m^2 t \sigma_{flow} \tag{6.19}$$

Eq. (6.17) is not valid if the grooves intersects the neutral axis, i.e. if $\alpha_1 < \beta$. In such cases a correction factor must be subtracted from Eq.(6.17):

$$\frac{M}{M_0} = \frac{M'}{M_0} - \frac{1}{2}\left(\frac{R_g}{R_m}\right)^2\left(\frac{d}{t}\right)\left(\frac{\cos\alpha_1 - \cos\beta}{\alpha_1 - \beta} - \frac{Y_1}{R_g}\right)(\beta - \alpha_1) \tag{6.20}$$

Where M'/M_0 is the value obtained from Eq.(6.17).

Figure 6-6 and Figure 6-7 are plots of predicted collapse moment in thin wall pipes ($R_m = R_g$) as a function of notch length and of circumferential position, respectively. The θ values correspond to the angle from the centre of the flaw to the 12 o'clock or 6 o'clock position.

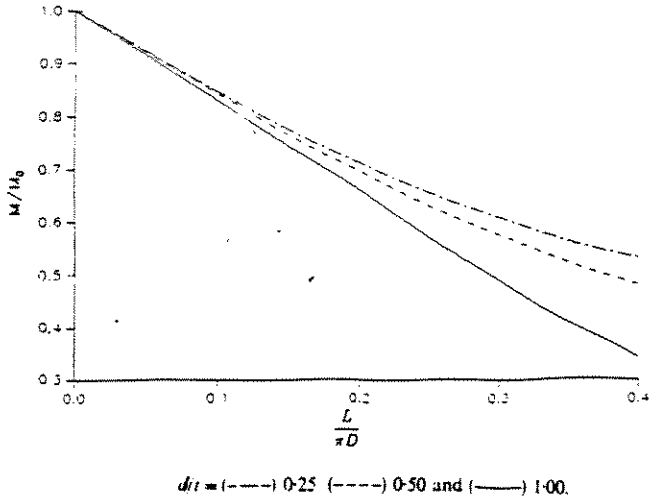

Figure 6-6 Predicted Collapse Moment vs. Notch Length for Thin-Wall Pipe From Fig.9 of Anderson et al (1988)

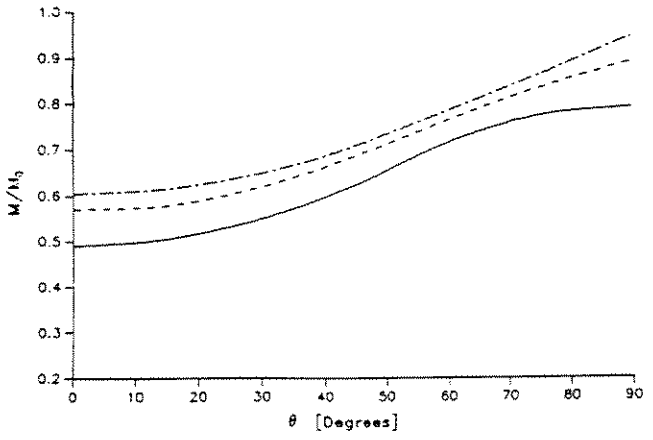

Figure 6-7 Predicted Collapse Moment vs. Circumferential Position for Thin-Wall Pipe From Fig.10 of Anderson et al (1988)

6.3.2 Net-section Collapse Formula

$$m = \frac{M}{4R^2 t \sigma_{flow}} = \cos\left(\frac{(1-\eta)\beta}{2}\right) - \frac{(1-\eta)\sin\beta}{2} \qquad \eta < \frac{\pi - \beta}{\beta} \quad or \quad \beta < \frac{\pi}{1+\eta} \tag{6.21}$$

The net-section collapse formula (Miller 1988) is:

and

$$m = \frac{M}{4R^2 t \sigma_{flow}} = \eta \sin\left(\frac{\pi - \beta(1-\eta)}{2\eta}\right) + \frac{(1-\eta)\sin\beta}{2} \qquad \eta > \frac{\pi - \beta}{\beta} \quad or \quad \beta > \frac{\pi}{1+\eta} \tag{6.22}$$

The formula is plotted in Figure 6-8. Different expressions are needed according to whether the neutral axis is in the flaw or not. If the flaw is in a compressive region, then it might be assumed that it did not have a weakening effect and uncracked result would be used instead.

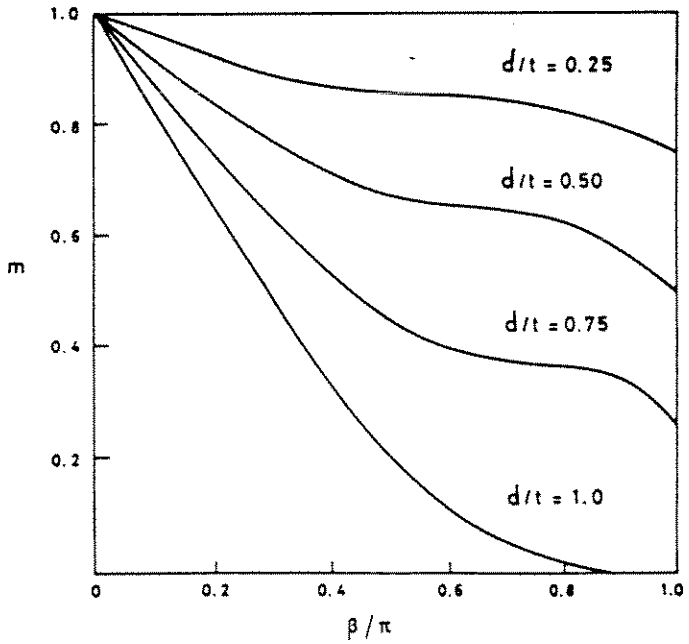

Figure 6-8 Net-section Collapse for Surface Circumferential Defects in Bending From Fig.66 of Miller (1988)

6.3.3 Wilkowski and Eiber's Formula

Wilkowski and Eiber (1981) conducted a large number of bend test on small scale and full scale pipe sections which contain simulated repair grooves. From these data, they derived critical semi-empirical relationships between applied stress, flow stress, repair groove dimensions and pipe geometry. An empirical result given by Wilkowski and Eiber (1981) for a local collapse expression is

$$\frac{M}{\pi R^2 t \sigma_{flow}} = \frac{\eta}{1-(1-\eta)\left(1+0.26(\beta/\pi)+47(\beta/\pi)^2-59(\beta/\pi)^3\right)^{1/2}} \tag{6.23}$$

6.3.4 Willoughby's Empirical Lower Bound

Willoughby (1982) gave an empirical lower bound

$$\frac{M}{\pi R^2 t \sigma_{flow}} = 1-1.6(1-\eta)\beta \tag{6.24}$$

Experimental verification is limited to $\eta>0.2$. Comparison between experiment and theory is given in Figure 6-9.

Miller (1985) compared test results with the theoretical expressions and concluded that the net-section collapse given in Section 6.3.2 function better than Wilkowski and Eiber (1981) formula and Willoughby 's empirical lower bound.

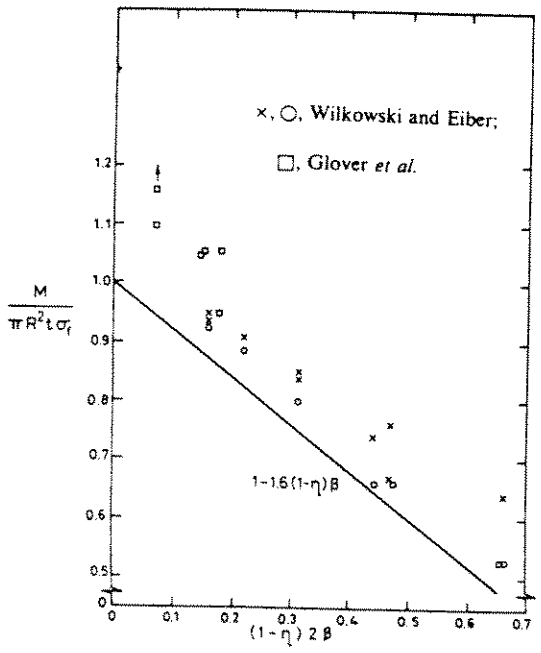

Figure 6-9 Comparison between Failure Stress and β for Circumferential Defects in Pipes under Bending, From Fig.67 of Miller (1988)

6.4 Circumferentially Corroded Pipes, Bending and Pressure

Circumferentially Corroded Pipes under Combined Bending and Internal Pressure, the net-section collapse formula, (Miller 1988)

$$\frac{M}{4R^2 t\sigma_{flow}} = \cos\left(\frac{\pi p + (1-\eta)\beta}{2}\right) - \frac{(1-\eta)\sin\beta}{2} \qquad p = \frac{PR}{2\sigma_{flow} t} \qquad \beta < \frac{\pi(1+p)}{1+\eta} \tag{6.25}$$

and

$$\frac{M}{4R^2 t\sigma_{flow}} = \eta\sin\left(\frac{\pi(1+p)-(1-\eta)\beta}{2\eta}\right) + \frac{(1-\eta)\sin\beta}{2} \qquad p = \frac{PR}{2\sigma_{flow} t} \qquad \beta > \frac{\pi(1+p)}{1+\eta} \tag{6.26}$$

The second pair of expressions apply when the neutral axis is in the defect. When part of the crack is in compression, it is probably unduly conservative to neglect its load-carrying capacity.

Miller (1985) review published experimental results and concluded that they were in reasonable agreement with the net-section collapse result.

Stress result from bending moment M is $M/(\pi R^2 t)$. Kastner (1981) proposed that a lower bound expression for the local collapse load is to add the axial stress due to bending to the axial stress due to internal pressure and then equal the total stress to the flow stress. This is based on an elastic stress distribution, and the limit moment is independent of crack size in pure bending.

In other words, Kastner (1981) proposed a linear interaction between internal pressure and bending.

6.5 Circumferentially Corroded Pipes under Axial Load and Pressure

6.5.1 Finite Element Analysis

The effect of various loadpaths on the burst pressure of circumferentially corroded pipes were investigated by means of the finite element methods. Two models were utilised, and a total of 28 analyses were carried out. Three different load paths were evaluated, while two of the load paths were investigated in more details.

A. Operating pressure, succeeded by external axial load until ultimate collapse (burst).

B. Operating pressure, succeeded by a external constant axial compressive strain (displacement), and further additional pressure until ultimate collapse.

C. Operating pressure, succeeded by a external constant axial compressive stress (force), and further additional pressure until ultimate collapse.

The loadpath B and C were investigated in more details.

Problem
Kastner (1981) proposed a linear interaction between axial load and axial stress due to internal pressure.

It is also reasonable to assume that the interaction between axial tension and internal pressure is same as the interaction between bending and internal pressure due to net-section collapse.

The main purpose of this section is to investigate the interaction numerically.

Geometry and mesh
The bursting behaviour and ultimate strength of the corroded pipes under combined loads are studied for the two pipes shown in Table 6-10.

Table 6-10 Pipe and Corrosion Geometries and Material Properties - Circumferentially Corroded Pipes under Internal Pressure and Axial Loads

	Outer Diameter D (mm)	Wall-Thickness t (mm)	Defect Depth d (mm)	Defect Length L (mm)	Defect Width W (mm)	d/t	W/(πD)
Pipe-2H	914.0	22.0	13.2	20.0	904	0.6	0.333
Pipe-2K	914.0	22.0	6.6	20.0	904	0.3	0.333

Boundary condition
The boundary condition is determined considering symmetric conditions in the axial and circumferential directions.

Load application
A static solution procedure implemented in Spectrum (Centric 1995) is applied to study the pre- and ultimate strength behaviour.

Material parameters
A power law curve is to be taken for the true-stress/logarithmic-plastic-strain relationship for strains greater than 1 %. This has the following analytical form for API 5L X60 material:

$$\sigma_0 = C\varepsilon_0^{n'} \;\; ; \;\; C = \left(\frac{e}{n'}\right)^{n'} \sigma_{ult} \quad for \quad \varepsilon_0 > 1\% \tag{6.27}$$

in which n_{-}=0.13 and σ_{ult} = 563 MPa. σ_0 and ε_0 denotes true-stress and logarithmic-plastic-strain respectively. e is the base of the natural logarithm. The yield stress is 434 MPa. Between zero and 1 % plastic strain, a linear relationship is assumed for the stress/strain curve.

Note that Young's Modulus E is 206000 MPa, and Poison's ratio ν is 0.3 in the linear range.

The analyses are described in details in the project report 95-3514, "Finite Element Analyses of Corroded Pipes", (Bjørnøy and Skjolde, 1995).

6.5.2 Bursting Behaviour and Ultimate Strength

In Figure 6-10 to Figure 6-19 the hoop stress versus the longitudinal stress are plotted for both models (Table 6-10) and the three different loadpaths.

In Figure 6-10 results from the analyses using the model with d/t=0.3 are shown. The figure shows the stresses for the loadpath A at a position in the corroded region at both the inner surface, and the outer surface (inside/ouside), and at one position far off the corroded region (nominal). The von Mises yield ellipse is also included. The pipe was exposed to internal pressure of 14.3 MPa, succeeded by axial compressive force until failure. Figure 6-11 shows the stresses for the analysis with the loadpath B, which was first internal pressure of 14.3 MPa, then axial compressive strain of 0.15% (displacement control), and succeeded by additional internal pressure until failure. And finally, Figure 6-12 shows the stresses for the analysis with loadpath C. First internal pressure was applied, then axial compressive stress of 330 MPa, and succeeded by additional internal pressure until failure.

The Figure 6-13 to Figure 6-19 show the same results as in Figure 6-10 to Figure 6-13, but for the model with d/t=0.6. The loading was also identical.

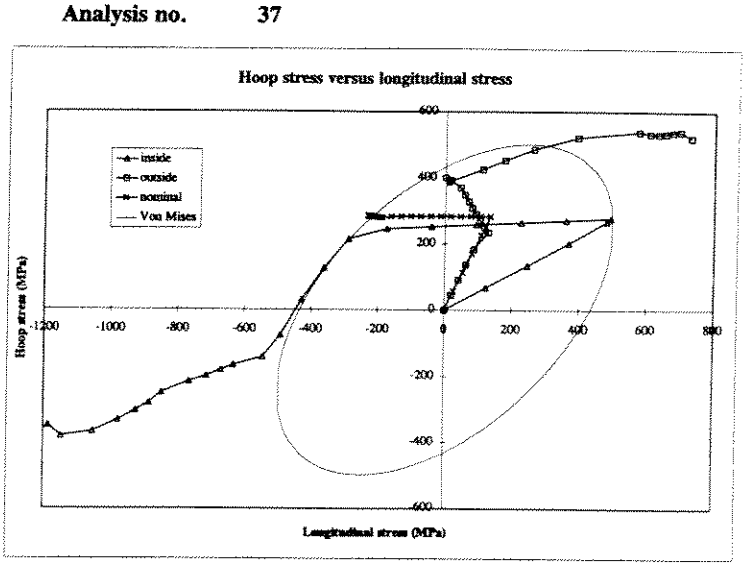

Figure 6-10 Hoop Stress Versus Longitudinal Stress, Pipe-2H, d/t =0.6, for loadpath A

Analysis no. 38

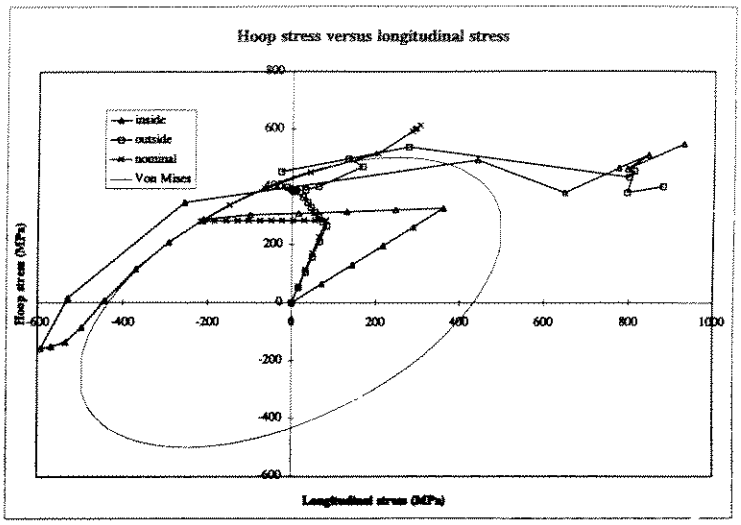

Figure 6-11 Hoop Stress Versus Longitudinal Stress, Pipe-2H, d/t =0.6, for loadpath B

Analysis no. 39

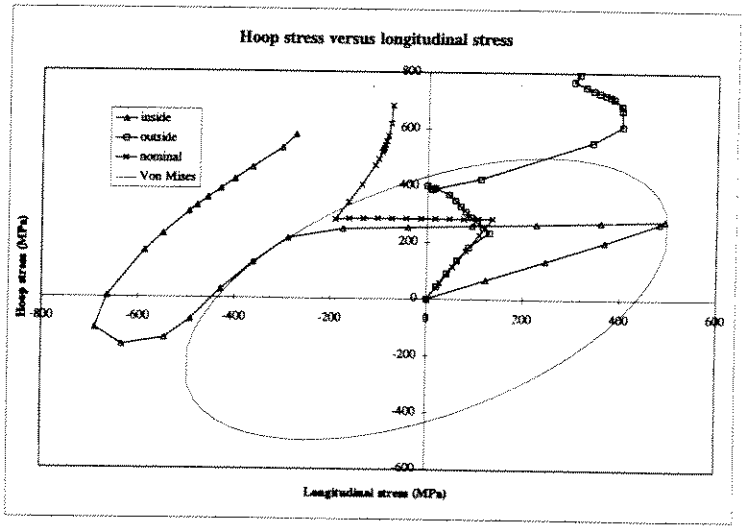

Figure 6-12 Hoop Stress Versus Longitudinal Stress, Pipe-2H, d/t =0.6, for loadpath C

Analysis no. 40

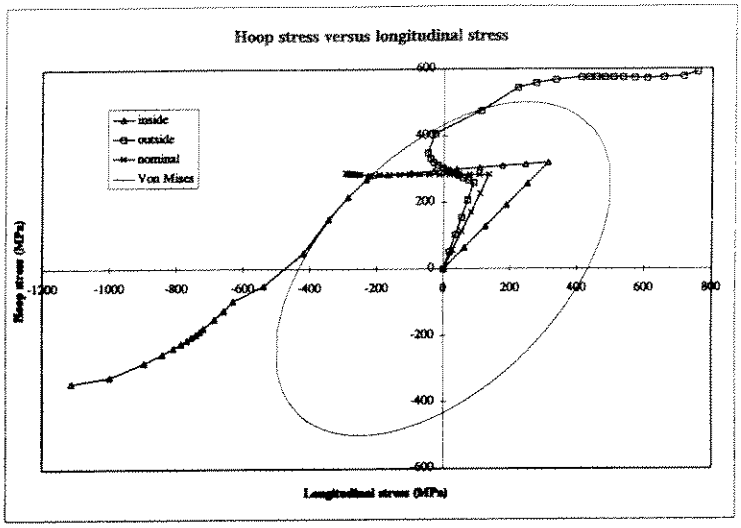

Figure 6-13 Hoop Stress Versus Longitudinal Stress, Pipe 2K, d/t =0.3, for loadpath A

Analysis no. 41

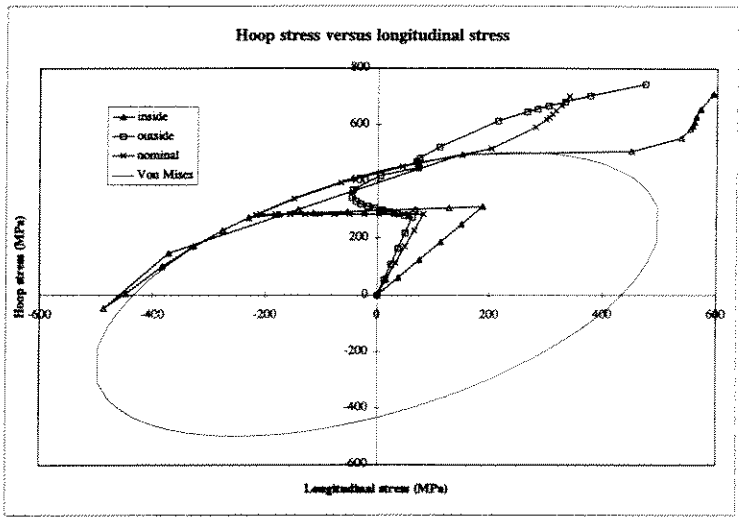

Figure 6-14 Hoop Stress Versus Longitudinal Stress, Pipe 2K, d/t =0.3, for loadpath B

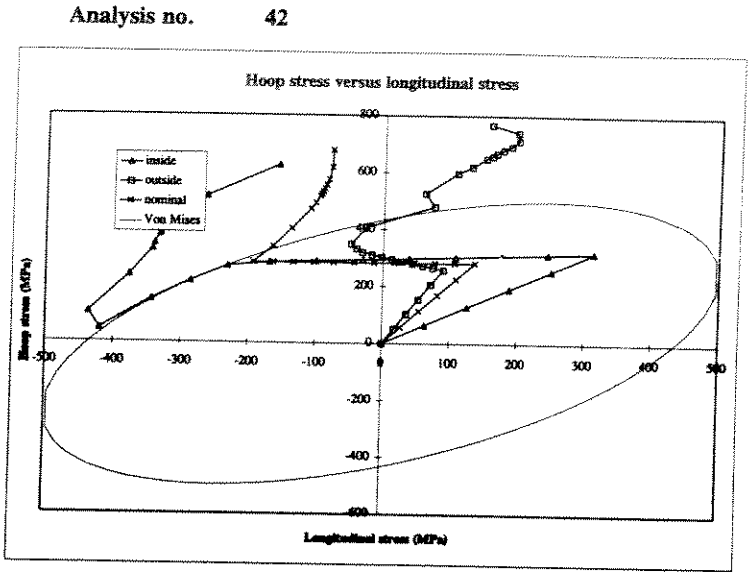

Figure 6-15 Hoop Stress Versus Longitudinal Stress, Pipe 2K, d/t =0.3, for loadpath C

6.5.3 Interaction Curves for Selected Loads

For both models described in Table 6-10 several analyses were carried out for the loadpath B and C described in Chapter 5.11.3. The results are shown in Figure 6-16 to Figure 6-19. The figures show the loadpath and the failure point. A von Mises yield interaction curve is also indicated, and the procedure to calculate the curve is shown in this section.

Part 1: Load path: Design Pressure --> Axial Stress --> Pressure to Burst

Figure 6-16 Interaction between Burst Pressure and Axial Stress for Circumferentially Corroded Pipe (D=914 mm, t=22 mm, d/t=0.6)

Figure 6-17 Interaction between Burst Pressure and Axial Stress for Circumferentially Corroded Pipe (D=914 mm, t=22 mm, d/t=0.3)

The axial stress is a load type loading and its value is a constant while applying pressure to burst. It has been shown that axial stress reduces burst pressure. The axial stress is the sum of the stress due to the end cap effect and the applied axial compressive stress. It is observed that the interaction between compression and bending can be represented by von Mises yield function. A procedure to generate the interaction curve is as follows:

(1) To calculate the point on the Y-axis of the coordinate system using the hoop stress formula criterion, $P_0 = \sigma_{ult} \cdot 2 \cdot t / D$.
(For this example; P_0 = 563MPa ·2·22.0/ 914 = 27.1 MPa)

(2) The axial stress is applied in the centre of the pipe circle. The point on the X-axis of the coordinate system is obtained by equating the ultimate tensile stress of the material to the sum of the axial stress and the bending stress due to the eccentricity of the axial stress. (Anderson's equation, Eq. (6.15). For this example, D=914 mm, t=22 mm, d/t=0.6 and w=904 mm.

$$e = \frac{\left(\frac{D}{2} - t + \frac{d}{2}\right)^2 \cdot d \cdot (\cos 30 - \cos 150)}{2\pi \cdot \left(\left(\frac{D}{2} - \frac{t}{2}\right) \cdot t - \left(\frac{D}{2} - t + \frac{d}{2}\right) \cdot d \cdot \frac{w}{\pi D}\right)} = 90\ mm \qquad \textbf{(6.28)}$$

The additional stresses due to the axial stresses and the eccentricity is calculated as $\sigma_{bending} = 4\sigma_{ax}e/D$. The cross section reduction factor is $Area_{corroded} / Area_{uncorroded} = 0.8$. The stresses are set equal to the ultimate stress;

$$\frac{1}{0.8}\sigma_{ax} + \sigma_{bending} = \left(\frac{1}{0.8} + \frac{4e}{D}\right)\sigma_{ax} = \sigma_{ult} \qquad \textbf{(6.29)}$$

When solving the equation the σ_{ax} = 342 MPa. (σ_{ult} = 563 MPa)

(3) The points between these two points are generated using von Mises yield function,

$$\left(\frac{P}{P_0}\right)^2 + \left(\frac{X}{X_0}\right)^2 - \frac{P}{P_0} \cdot \frac{X}{X_0} = 1 \qquad \textbf{(6.30)}$$

It is noted that local buckling can be a failure mode for pipes under high axial stress and low internal pressure. Local buckling can be assessed as discussed in Chapter 6.6.

From Figure 6-16 and Figure 6-17, it is also observed that the effect of tensile axial stress is negligible.

Part 2: Load path: Design Pressure --> Axial Strain --> Pressure to Burst

Figure 6-18 Interaction between Burst Pressure and Axial Strain for Circumferentially Corroded Pipe (D=914 mm, t=22 mm, d/t=0.6)

Figure 6-19 Interaction between Burst Pressure and Axial Strain for Circumferentially Corroded Pipe (D=914 mm, t=22 mm, d/t=0.3)

The axial strain is a deformation type loading and its value is a constant while applying pressure to burst. It has been shown that the pressure to burst is almost a constant for different levels of axial strain.

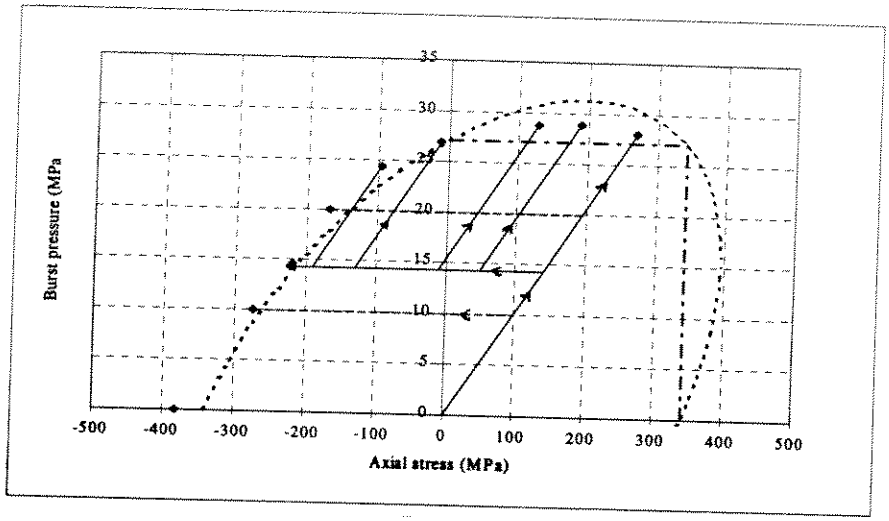

Figure 6-16 Interaction between Burst Pressure and Axial Stress for Circumferentially Corroded Pipe (Pipe-2H, D=914 mm, t=22 mm, d/t=0.6)

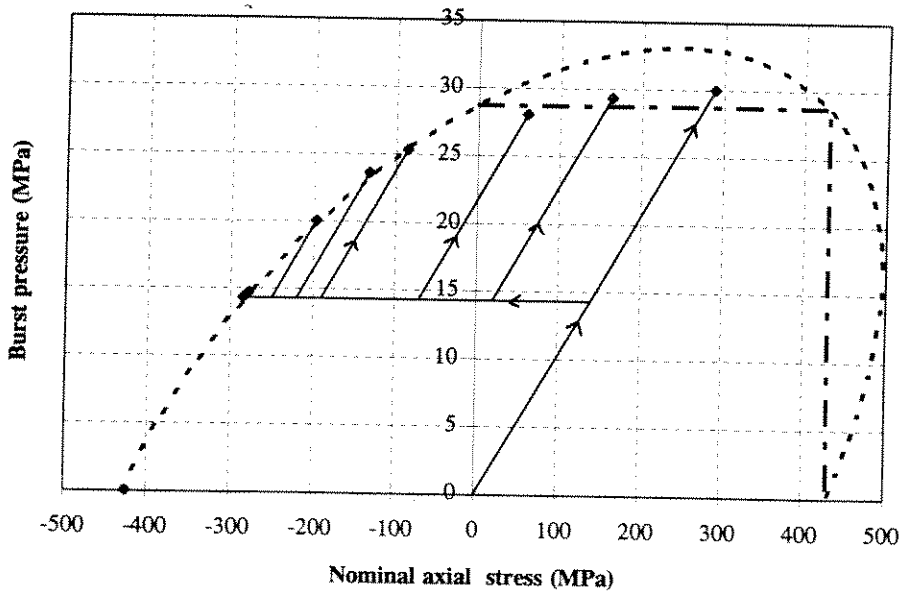

Figure 6-17 Interaction between Burst Pressure and Axial Stress for Circumferentially Corroded Pipe (Pipe-2K, D=914 mm, t=22 mm, d/t=0.3)

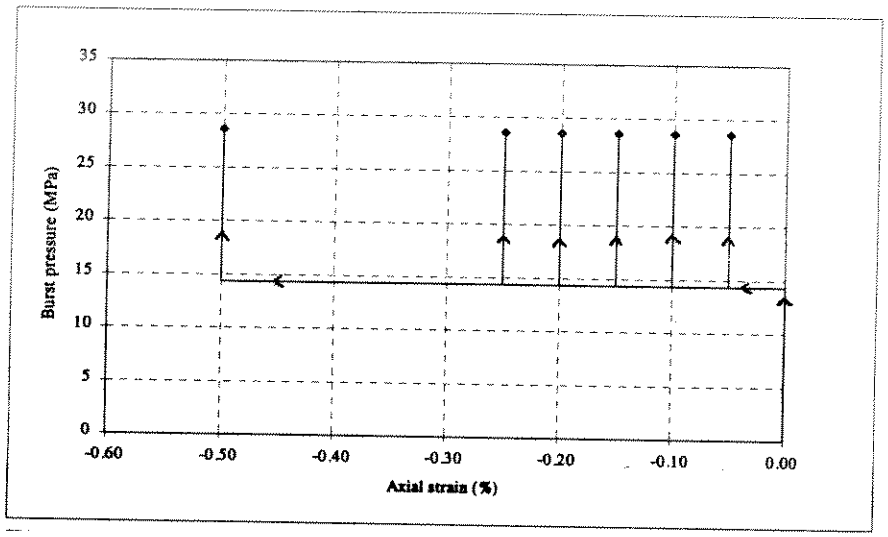

Figure 6-18 Interaction between Burst Pressure and Axial Strain for Circumferentially Corroded Pipe (Pipe-2H, D=914 mm, t=22 mm, d/t=0.6)

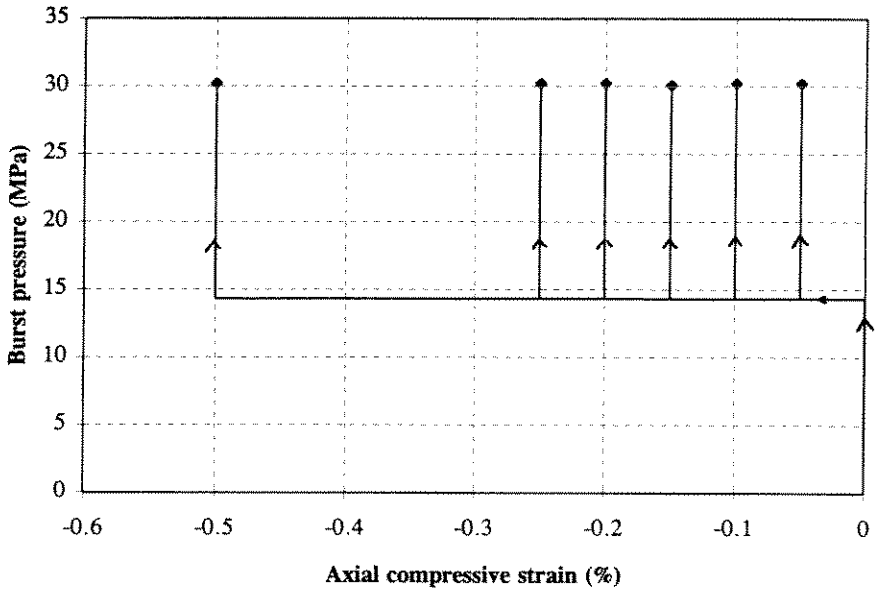

Figure 6-19 Interaction between Burst Pressure and Axial Strain for Circumferentially Corroded Pipe (Pipe-2K, D=914 mm, t=22 mm, d/t=0.3)

6.6 Local Buckling of Circumferentially Corroded Weld (Pipe)

6.6.1 Local Buckling of Pipes under Compression/Bending

Local buckling of pipes subjected to pure bending has been investigated by many researchers. The investigations show that pipe buckling is possible in two different modes: limit point type and bifurcation type of instability. Cross-sections of idealised pipes will deform by ovalizing under moment. As the deformation increases with increasing moment, it acts to reduce the moment-carrying capacity of the cross-section until a limit point is reached where the moment-curvature curve has zero slope. The loss of pipe stability beyond this point is called *limit point collapse*, which is caused by cross-section ovalization and reduced slope of the stress-strain relationship of the material. The pipe buckling associated with the axial mode of deformations (similar to buckling of compressed cylinders) is called *bifurcation buckling*. For D/t range of less than 35-40, limit point collapse occurs before bifurcation buckling. For larger pipes of D/t ratios, bifurcation buckling occurs earlier and in the plastic range.

Since typical pipe material stress-strain curves have the characteristic that a small difference in stress corresponds to a large difference in strain in the plastic range, using a strain criteria is considered more appropriate than a stress criterion.

A recent publication on limit-point collapse has been made by Bai et al(1994a). Substituting material properties for typical pipelines (linear yield stress σ_y = 327.13 MPa, hardening parameter n=18.83 and yield anisotropy parameter S=1.081), a simple (mean value) equation for critical strain may be obtained from Bai's formulae (Bai et al 1994a) as below:

$$\varepsilon_{cr} = 0.63\frac{t}{D} \qquad \textbf{(6.31)}$$

A theoretical study by Gellin (1980) indicates that the critical maximum axial stress for pipes in bending is close to the buckling stress for pipes under pure compression predicted by Batterman (1965). This was confirmed by Readdy (1979), who compared Batterman's prediction with his tests of pipes under pure bending. Recent experimental and numerical studies by Bai (1989) and Kyriakides and Ju (1992) indicated that buckling strain for pipes under pure bending can be 30% higher than buckling strain for pipes under pure compression.

Among many others listed in his literature, Batterman (1965) studies plastic buckling of axially compressed cylindrical shells analytically and experimentally. The analytical work has been based on both incremental theory and deformation theory. It has been found that the prediction due to deformation theory agrees well with experimental observation. His results based on deformation theory are summarised below:

A stress-strain relationship of the material is fitted by Ramberg-Osgood Curve

$$\varepsilon = \frac{\sigma}{E}\left(1+\frac{3}{7}\left(\frac{\sigma}{\sigma_R}\right)^{n-1}\right) \qquad \textbf{(6.32)}$$

The secant modulus E_s is

$$E_S = \frac{\sigma}{\varepsilon} = E\left(1 + \frac{3}{7}\left(\frac{\sigma}{\sigma_R}\right)^{n-1}\right)^{-1} \tag{6.33}$$

The tangent modulus E_t is

$$E_t = \frac{d\sigma}{d\varepsilon} = E\left(1 + \frac{3}{7}n\left(\frac{\sigma}{\sigma_R}\right)^{n-1}\right)^{-1} \tag{6.34}$$

According to Batterman's deformation theory, the half-wave length of plastic buckling is

$$L_d = \frac{1}{2}\frac{\pi\left[Rt(\lambda + 3\psi)\right]^{\frac{1}{2}}}{\left[3((3\psi + 2 - 4\nu)\lambda - (1 - 2\nu)^2)\right]^{\frac{1}{4}}} \tag{6.35}$$

and the buckling stress is given by

$$\sigma_d = \frac{2E}{\left[3((3\psi + 2 - 4\nu)\lambda - (1 - 2\nu)^2)\right]^{\frac{1}{2}}}\frac{t}{R} \tag{6.36}$$

in which

$$\psi = \frac{E}{E_S} = 1 + \frac{3}{7}\left(\frac{\sigma}{\sigma_R}\right)^{n-1} \tag{6.37}$$

and

$$\lambda = \frac{E}{E_t} = 1 + \frac{3}{7}n\left(\frac{\sigma}{\sigma_R}\right)^{n-1} \tag{6.38}$$

The poison's ratio ν is somewhat between 0.3 and 0.5. For buckling in fully plastic range, ν is close to 0.5. Assuming a poison's ratio of 0.5, Batterman's analytical prediction is identical to Gerard's equation (Gerard 1962), which is shown below:
The half-wave length of plastic buckling is

$$L_d = \frac{\pi}{2\sqrt{3}}\frac{(\lambda + 3\psi)^{\frac{1}{2}}}{(\psi\lambda)^{\frac{1}{4}}}\sqrt{Rt} \tag{6.39}$$

and the buckling stress is given by

$$\sigma_d = \frac{2E}{3(\psi\lambda)^{\frac{1}{2}}}\frac{t}{R} = \frac{2}{3}\sqrt{E_S E_t}\frac{t}{R} \qquad (6.40)$$

The buckling strain is estimated using

$$\varepsilon_d = \frac{\sigma_d}{E_S} = \frac{2}{3}\sqrt{\frac{E_t}{E_S}}\frac{t}{R} \qquad (6.41)$$

The procedure for iterative calculating buckling stress is:

1) To assume a stress σ
2) To calculate E_S, E_t, strain ε using Ramberg-Osgood Curve
3) To calculate σ_d
4) To calculate $\Delta\sigma$,
   if $\sigma_d > \sigma$, then $\Delta\sigma>0$;
   if $\sigma_d < \sigma$, then $\Delta\sigma<0$
5) Use $\sigma+\Delta\sigma$, start from 1) again until $\sigma-\sigma_d$ is close to 0.

For a typical pipeline, the following material parameters and geometry parameters are assumed:

- Radius R = 457 mm
- Wall-thickness t = 22 mm
- Young's modulus E = 206000 MPa
- Poison's ratio $\nu = 0.3$
- Material API 5LX60: σ_R = 395.8 MPa, n=19

The predicted half-wave length of plastic buckling for uncorroded pipes is L_d =196.9 (mm)and the predicted buckling stress for uncorroded pipes is σ_d = 440.6 (MPa). The buckling strain is calculated from the buckling stress and the Ramberg-Osgood curve ε_d = 0.0084.

Note that the axial length of a circumferential weld is typically 20 mm. The predicted L_d is 9.84 times of the length of the circumferential weld. *This means the weld is not sufficiently long to buckle in the weld !* Local buckling will therefore not actually occur in the weld.

When a pipeline is corroded, the buckling calculation should be done based on the remaining wall-thickness (which is t-d) and consequently the buckling strain can be lower.

Assuming a 80% of wall-thickness has been reduced due to corrosion, buckling calculation is done using the remaining wall-thickness of 4.4 (mm). The predicted half-wave length of plastic buckling for the corroded pipe is L_d = 13.4 (mm) and the predicted buckling stress for the corroded pipes is σ_d = 393.3 (MPa). The buckling strain is calculated from the buckling stress and the Ramberg-Osgood curve ε_d = 0.00264. Since L_d is smaller than the weld length, local buckling may actually occur. The critical strain given by Bai's formula for limit-point collapse ε_{cr} (= 0.63 t/D) is 0.0031. This means that for the pipeline considered, bifurcation buckling will occur before limit-point-collapse.

Local buckling is catastrophic and leads to containment leakage from the buckling pipe, because load-carrying capacity is reduced dramatically after the occurrence of local buckling. A procedure to calculate the global strain which lead to local buckling is

1) Assume a corrosion depth d
2) Calculate allowable strain in corroded area using Batterman's formulae,
   A safety factor is to be applied and the remaining wall-thickness (t-d) is to be used in the calculation.
   If the predicted half-wave length of plastic buckling for the corroded pipe L_d is longer than the length of the length of the circumferential weld, local buckling can not actually occur because the length of the weld is not sufficient. Local buckling check is not necessary.
3) Calculate stress in corroded region using Ramberg-Osgood curve from the allowable strain in 2)
4) Calculate stress in uncorroded section using

$$\sigma A = \sigma_{corr} A_{corr} \tag{6.42}$$

   where σ and A are stress and area at uncorroded section and σ_{corr} and A_{corr} are stress and area at corroded region
5) Calculate strain in uncorroded area, given stress (based on Ramberg-Osgood curve)
6) Check if calculated strain is identical to strain derived from global analyses
7) If 6) is not ok then start from 1).

6.6.2 Local Buckling of Pipes under Combined Loads

Kim (1992) theoretically studied the axi-symmetric plastic bifurcation buckling of pipes under combined uniform axial compression and internal pressure. The buckling stress for pipes under combined compression and internal pressure is predicted by

$$\sigma_d = \frac{t}{R}\sqrt{(a_{11}a_{22} - a_{12}^2)/3} \tag{6.43}$$

where

$$a_{11} = a[2\psi + 0.5(\lambda - \psi)S_{22}^2/\sigma_e^2] \tag{6.44}$$

$$a_{22} = a[2\psi + 0.5(\lambda - \psi)S_{11}^2/\sigma_e^2] \tag{6.45}$$

$$a_{12} = -a[1 - 2\nu - \psi + 0.5(\lambda - \psi)S_{11}S_{22}/\sigma_e^2] \tag{6.46}$$

$$S_{11} = 2\sigma - \sigma_h \tag{6.47}$$

$$S_{22} = 2\sigma_h - \sigma \tag{6.48}$$

$$\sigma_e^2 = \frac{1}{3}(S_{11}^2 + S_{11}S_{22} + S_{22}^2) \tag{6.49}$$

$$a = 2E / \left(3\psi\lambda - (1-2\nu)^2 + 2(1-2\nu)[\psi - 0.5(\lambda - \psi)S_{11}S_{22}/\sigma_e^2]\right. \tag{6.50}$$

σ_h denotes hoop stress due to internal pressure. Example calculations in Kim (1992) show that the buckling strain is improved by up to 30 % due to internal pressure, depending on the amount of internal pressure. Similar to Batterman's equation, iterative calculation is necessary to find buckling stress.

A number of factors exist that can influence the onset of local buckling and may have to be accounted for in predictive analyses. One of these factors is the presence of the girth welds that occur between the joints of pipe. The residual stresses, heat affected zones, and the geometric imperfections introduced by the weld would be expected to cause the initiation of local buckling at average strains of smaller magnitude than are applicable to plain pipe.

Yoosef-Ghodsi et al (1995) conducted a series of tests on specimens of full size pipe subjected to constant axial force, constant internal pressure and monotonically increasing curvature. The test specimens all had girth welds at mid-length and the bending curvature were continued until wrinkles of large amplitude had formed. All pressurised specimens developed bulging wrinkles while unpressurised specimens developed diamond pattern wrinkles. Local buckling was defined as the point at which load-carrying capacity is reduced (the softening point).

The experimental results indicate that, for the pipe associated with this test program, the initiation of wrinkling in girth-welded pipe occurs at strains approximately equal to 60 % of that for plain pipe.

As stated earlier, local buckling will not occur at only the girth weld zone in case the length of plastic buckling wave is longer than the girth weld length in the axial direction. In this case, local buckling can possibly occur at a longer area including both girth weld zone and the base material. The reduced wall-thickness can be a kind of imperfection/eccentricity which may reduce the local buckling strain significantly. It is a common knowledge that the effect of imperfection is not so significant for plastic buckling, as compared with elastic buckling. However, as the corrosion defect is usually deep in depth, it's effect on local buckling can be significant. This effect must be accounted for together with girth weld effect in an engineering assessment of local buckling of pipes with corroded girth welds.

6.7 Assessment of Cracks in Girth Welds

6.7.1 Possible Cracks in Girth Weld

Various types of imperfection are known to occur in girth butt welds. The most damaging types are cracks, inadequate penetration of the root bead, and lack of fusion. The imperfections are particularly damaging if they occur in a weld that undermatches the yield strength of the base material.

When evaluating the risk for unstable fracture of the girth welds, assumptions regarding types, dimensions and location of weld defects must be made. The most frequent type of planar/crack like defects in one-sided Shielded Metal Arc Welding (SMAW) are lack-of-fusion defects. Such defects can be located both near the surface or be surface breaking and may have gone undetected following NDT procedures according to API 1104. Examples of such near surface and surface breaking defects can be found in Karlsen (1974) which investigate some typical defects found during installation of the Ekofisk-Teesside pipeline (P2027A).

Based on these observations it is reasonable to assume that some defects, typically with a height equal to one weld pass, i.e. 3-4 mm and length around 150 mm may exist in the pipeline. These cracks will be assumed to be surface breaking or becoming surface breaking due to preferential corrosion of the root area of the girth weld.

6.7.2 Fracture of Cracked Girth Welds

The subsidence of an oil field (or soil movement) may lead to a longitudinal tensile strain in the pipelines. This strain can, combined with a possible initial weld defect in the weld-zone, be of a critical level with respect to the Unstable Fracture and Plastic Collapse (UFPC) failure mode.

Defects in girth weld can be addressed on one of three levels, depending upon the quality of affected welds, the availability of certain material data, and the difficulty of making repairs.

6.7.2.1 Level 1 Assessment - Workmanship Standards

Pipeline welding codes in the US and elsewhere establish minimum weld quality standards based on inspection of a welder's workmanship. The flaw acceptance criteria evolved through industry experience. Hence, most workmanship standards are similar, though not identical, in terms of allowable imperfection types and sizes. The advantage of workmanship standards is that they are time-tested, they are compatible with normal levels of NDE quality, they do not require material strength and toughness property data, and they are easy to apply. However, it has been recognised that some rejectable flaws may not necessary pose a real threat to pipeline integrity. A flawed girth weld that would be extremely costly to repair or replace should not be rejected solely on the basis of workmanship standards.

The only workmanship standards that are presently recognised by US gas pipeline regulations are those contained in API Standard 1104 (API 1988). Other workmanship standards one might apply to weldments are contained in other standards (i.e., ASME B&PV Code, CAN/CSA-Z184, BS4515).

6.7.2.2 Level 2 Assessment - Alternative Acceptance Standards

Alternative acceptance standards were developed to facilitate acceptance of flaws that do not meet workmanship standards. Incentives for alternative standards are usually economic, arising due to the inaccessibility or quantity of welds that would otherwise be repaired. Alternative standards recognise that the true severity of a flaw is dependent on material toughness and applied stress levels, and can only be determined using fracture mechanics principles.

The crack-tip opening displacement is most commonly used as the toughness measurement of welds. CTOD is established from destructive tests performed on weldments. If the pipeline is yet to be constructed, CTOD tests can be performed as part of the weld procedure qualification. If the pipeline is already in service and CTOD data are not available, the welding procedures, consumable, and base materials used in construction may be used to duplicate welds for the purpose of conducting CTOD tests. If any one of these elements is no longer available, it will be necessary to obtain a representative weld for testing. Alternatively, a lower-bound CTOD of 0.001 inch (0.025 mm) may be assumed in lieu of tests.

Three alternative criteria that are recognised by their respective national regulating agencies and that are often cited elsewhere are the appendix to API Standard 1104, Appendix K to CSA-Z184, and BSI PD-6493 (PD-6493 Level 1 is comparable to what is referred to herein as Level 2.). All three standards are based on the COD Design Curve approach developed by The Welding Institute which extends LEFM concepts into the elastic-plastic regime. In spite of their common origins, they differ in their treatment of residual stresses, summation of stress components, minimum toughness level, and factors of safety.

6.7.2.3 Level 3 Assessment - Detailed Analysis

Flaws that are not permitted by Level 2 assessment may be evaluated by detailed fracture mechanics analysis. PD 6493 provides an appropriate Level 3 procedure based on R-6 FAD methodology. PD 6493 Level 2 and Level 3 are both comparable to what is referred to herein as Level 3. In case accurate information about the whole stress-strain relationship for the weld material is lacking, the default Failure Assessment Diagram (FAD) specified in PD6493, based on yield stress and tensile stress of weld material, is applied to model the acceptance criteria against UFPC. The default FAD for level 3 is generally conservative. The internal pressure will have negligible influence on the UFPC capacity of transverse cracks, and is not accounted for in the analysis.

Glover et al (1992) presented a publication on assessment of pipeline girth welds using PD6493 and Appendix K to CSA-Z184.

The fatigue and fracture mechanics software program PROFRAC (DNVS 1993), can be applied in the assessment of the UFPC capacity, where the default FAD for level 3 is defined as Option 1. If more accurate information about the stress-strain relationship for the weld material is achieved, this information can be applied directly in the modelling of the FAD for level 3, defined as Option 2 in PROFRAC.

In the assessment of the UFPC capacity of the weld due to longitudinal strain of the pipe, it is assumed that there exist a semi-elliptical surface weld defect of depth a and total length 2c. In the determination of the stress intensity at the crack tip, established empirical expressions are applied to describe the stress distribution over the weld defect (geometry functions) for both the membrane and bending stress distribution (Newman and Raju 1981).

The critical stress levels with respect to UFPC failure can be obtained from FAD analysis, for the different pipelines as a function of the degree of corrosion wall-thickness reduction. The

corresponding critical strain level is estimated using Ramberg-Osgood (1943) curve for the stress-strain relationship.

6.7.3 Fracture of Corroded and Cracked Girth Welds

Corrosion of the weld material will lead to an increase in the stress level over the weld zone due to reduced local thickness and stress concentration when the pipeline is exposed to longitudinal tensile strain.

In a UFPC capacity modelling of the corroded weld due to longitudinal tension, it is assumed that the weld defect is present together with the reduced wall-thickness of the weld due to corrosion. Due to the high number of welds (weld lengths) being exposed to a similar high strain level, the combined effect of having a surface weld defect and a reduced weld thickness due to corrosion is considered realistic.

The thickness reduction due to corrosion is assumed only to affect the weld material, and not the base material, causing a high stress concentration. The corrosion reduction of the weld material will probably affect the weld only within the lower circumference of the pipe, but is for simplicity in the modelling assumed to be evenly distributed around the pipe circumference. It is further assumed that the weld defect is a semi-elliptical surface crack (defect depth a, total defect length 2c) located at the worst possible location with respect to the stress concentration, independently of the degree of corrosion, see Figure 6-21.

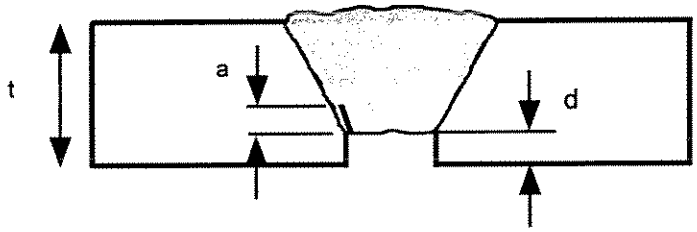

a is the weld defect, ,d is the corrosion depth, t is the pipe wall thickness.

Figure 6-20 Corroded Girth Weld

The corrosion results in a material reduction in the weld zone and thereby a stress concentration in the weld zone under longitudinal tension. To account for the stress concentration in the UFPC analysis, a finite element analysis is carried out in order to determine the stress distribution over the weld thickness.

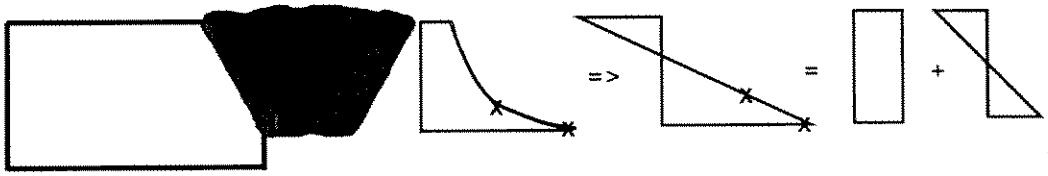

Figure 6-21 Stress Distribution in a corroded girth weld.

The stress distribution over the weld obtained from the finite element analysis is represented through a combined membrane and bending stress distribution over the weld thickness. The distribution of membrane and bending stresses are modelled in order to describe the stress distribution over the weld *defect* depth as accurately as possible, as shown in Figure 6-21. The stress magnification due to the shape of the weld will be insignificant due to relative large size of the weld defect, and is neglected in the analysis.

The critical stress levels with respect to UFPC failure can be obtained from FAD analysis, for the different pipelines as a function of the degree of corrosion wall-thickness reduction. The corresponding critical strain level is estimated using Ramberg-Osgood (1943) curve for the stress-strain relationship.

The UFPC analysis can be carried out considering the following parameters:

- stress-strain relationship of the pipeline material
- yield and tensile strength of the weld material
- CTOD value of the weld material
- depth of weld defect
- length of the weld defect
- residual stress

7 FATIGUE OF CORRODED PIPELINES UNDER CYCLIC LOADS

7.1 Introduction

In this chapter, the fatigue analysis of the corrosion features (pitting and girth weld corrosion) is described based on standard assessment methods PD6493 (BSI 1991). It is conservatively assumed that the corrosion is crack-like.

The analysis adopts the following philosophy:

(1) The size of the largest defect, $a_f * 2c_f$, tolerable at the maximum allowable operating pressure (MAOP) is determined.

(2) The initial size of defect, $a_i * 2c_i$, which could extend by fatigue to $a_f * 2c_f$ in a given number of years is determined using standard, accepted procedures (PD6493, 1991).

Note that a_i and a_f are initial and final defect depth, and $2c_i$ and $2c_f$ are initial and final defect length.

The fatigue analysis is carried out using pressure cycling data (compressor station inlet and outlet pressure fluctuation histories for a period) from the pipeline operator. Internal pressure cycle spectra are determined from this data. The most severe pressure spectrum is selected for the analysis.

The defect sizes ($a_f * 2c_f$) just tolerable at the MAOP are predicted using the following plastic collapse failure criteria:

(1) Axial Defects: B31G

The failure of the pipe body corrosion defects in ductile pipeline is controlled by plastic collapse mechanism and the critical defect size is associated with tensile properties.

(2) Circumferential Defects: Kastner's Criterion

A corroded girth weld would not fail in a brittle manner because a severe notch (e.g. a crack) is required to produce the conditions (particularly triaxiality) necessary for brittle fracture and corrosion is not a severe notch. Therefore corroded girth weld would failure by collapse mechanisms.

7.2 Internal Pressure Fluctuation

Cyclic stresses corresponding to internal pressure fluctuations only are considered.

Defects in the axial direction are assumed to experience cyclic hoop stresses:

$$\Delta\sigma_{AX} = \frac{\Delta PD}{2t} \tag{7.1}$$

where

- $\Delta\sigma$ = cyclic stress
- ΔP = internal pressure fluctuation
- D = pipe diameter
- t = pipe wall thickness at girth weld location

Defects in the circumferential direction are assumed to be subjected to the corresponding axial stress. The axial cyclic stress due to internal pressure is conservatively assumed to be 0.5 * hoop stress (which is obtained for unrestrained pipelines):

$$\Delta\sigma_{AX} = \frac{\Delta PD}{4t} \tag{7.2}$$

Other types cyclic axial stress (e.g. due to environmental loads) should be added for the defects in the circumferential direction.

7.3 Fatigue Assessment based on Fracture Mechanics

The fatigue calculations are performed by numerically integrating the Paris equation:

$$\frac{da}{dN} = C(\Delta K)^m \tag{7.3}$$

where

- da/dN = fatigue crack growth rate (mm per cycle)
- ΔK = cyclic stress intensity factor
- C, m = fatigue crack growth rate constants
- C = $2.3 * 10^{-12}$ and m=3 according to PD6493 (BSI 1991) for ferritic steels operating in a marine environment at temperature up to 20^0C assuming seawater entering the pipeline

and

$$\Delta K = Y\Delta\sigma\sqrt{\pi a} \tag{7.4}$$

where

- a = crack depth
- Y = geometry function dependent on crack shape and geometry
- $\Delta\sigma$ = stress range

The crack growth is found by integration of the Paris's equation. Substituting ΔK in the above equation in Paris's equation, it is obtained that

$$N = \frac{\int_{a_i}^{a_f} \frac{da}{\left(Y\sqrt{\pi a}\right)^m}}{C\Delta\sigma^m} \tag{7.5}$$

where a_f and a_i are the final and initial defect depths.
N is the number of stress cycles necessary to increase the defect from the entitle defect size a_i to the final defect size a_f.

The above equation can be used to determine the final defect size, a_f*2c_f, after any given period of time by progressively calculating the crack extension due to a stress history. The initial size of defect, a_i*2c_i, which could extend to a_f*2c_f in N years could also be determined.

In the following fatigue calculation examples are presented to illustrate fatigue assessment procedures.

The geometry, material data for the pipe considered are:

- Outside diameter D=323.85 mm
- Wall-thickness t=5.56 mm
- Yield stress σ_y=289.6 MPa
- Ultimate tensile stress σ_u=358.5 MPa

The MAOP for the pipe is 6.895 MPa.

Both longitudinal and circumferential surface corrosion defects are assumed. The burst strength for the longitudinally corroded pipe is calculated using the B31G criterion (ASME 1993). The maximum allowable axial stress for the pipe with girth weld corrosion is calculated using Kastner (1981) formula. In the burst strength calculation, the flow stress is taken as $1.15\sigma_y$. The following procedure is applied:

- The maximum depth at MAOP is determined.
- Initial depth is determined from crack propagation calculations.

The corrosion defects are conservatively considered as crack-like defects.

Since the corrosion defects are considered as crack like defects, the growth is calculated by Paris Equation. The Newman-Raju solution is used to calculate geometry function Y.

Crack growth is calculated from the following load history (1 year)

Δσ (MPa)	Number of cycles
200.	0.2
175.	0.3
150.	1
125.	2.5
100.	5
75.	25
50.	100
25.	500

The effective stress from this load history is

$$\Delta\sigma_{eff} = \left(\Sigma\left((\Delta\sigma_n)^m N_n\right)/\Sigma N_n\right)^{1/m} \qquad (7.6)$$

It is assume that all stress cycles contribute to crack propagation. The hoop stress and stress in the axial direction are calculated using Eq.(7.1) and Eq.(7.2) respectively.

The following tables give the calculated critical crack size at MAOP and the initial defect size which grows to critical size during 100 years.

Longitudinal Defects

Initial Defect Size ai*2ci	Critical Defect Size af*2cf
2.70*10	3.15*15.2
2.40*15	2.92*19.4
2.22*20	2.77*23.9
1.90*40	2.53*43.1
1.77*60	2.42*62.8
1.70*80	2.37*82.6
1.66*100	2.33*102.5

Circumferential Defects

Initial Defect Size ai*2ci	Critical Defect Size af*2cf
3.46*100	5.08*112.2
2.85*200	4.61*209.8
2.55*400	3.90*406.6
2.39*600	3.55*605.2
2.25*800	3.51*805.0

8 PROPOSED STRENGTH EQUATIONS

8.1 Proposed Strength Equations for Longitudinally Corroded Pipes

According to B31G (ASME 1993), pits depth exceeding 80 % of the wall-thickness is not permitted due to the possibility of a leak developing. From strength point of view, leak will not develop until the pit depth is closer to the wall-thickness. The 80 % limitation is mainly due to the fact that the accuracy of inspection tools is approximately 15-20 % of the wall-thickness.

If the ratio of maximum depth and wall-thickness, d/t, is between 10 % and 80 %, the following evaluation should be performed.

(1) The Safe Maximum Pressure Level P′ is

$$P' = \frac{1}{\gamma}\frac{2\sigma_{flow}t}{D}\frac{1 - Q\,AREA / AREA_0}{1 - M^{-1}\,AREA / AREA_0} \qquad (8.1)$$

where

P′ = Safe maximum pressure level
σ_{flow} = Flow stress of the material
t = Wall-thickness of the pipe
D = Outside diameter of the pipe
AREA = Exact area of the metal lost due to corrosion in the axial direction through-wall-thickness.
$AREA_0$ = Original area prior to metal loss due to corrosion within the effective area which is L*t
L = Defect length of corrosion profile
M = Folias factor
Q = Spiral correction factor
γ = Factor of safety

The predicted bursting pressure level P_b is γ P′.

γ = Factor of safety (needs to be calibrated). To obtain approximately the same level of safety as the NG-18 equation a preliminary factor of 1.85 should be used. This factor is derived as (1/0.72)·1.06·1.25=1.84, where σ_u=1.06·SMTS, and SMTS/SMYS = 1.25 (X60). The 0.72 factor is from the hoop stress formula.

The safe maximum pressure level must be less or equal to the Maximum Allowable Design Pressure, which is;

$$P = \frac{2 \cdot SMYS \cdot t}{D} \cdot F \qquad (8.2)$$

Where SMYS = Specified Minimum Yield Stress
F = Design factor which is normally 0.72

2) AREA, spiral correction factor Q, flow stress σ_{flow} and Folias factor M is calculated as follows:

(a) Effective Area AREA

-Complex Shaped Corrosion:

Two levels of AREA assessment are proposed:

(i) Level 1 :

For $L^2/(Dt)<30$: AREA=(2/3)Ld

where d is the maximum depth of corroded area

For $L^2/(Dt)>30$: AREA=0.85Ld

(ii) Level 2 : To calculate the exact area (AREA) of the corrosion profile using Simpson integration Method.

$$AREA = \frac{b-a}{6n}[y_a + 4y_1 + 2y_2 + 4y_3 + 2y_4 + \ldots + 4y_{2n-1} + y_b] \qquad \textbf{(8.3)}$$

in which 2n equal sub-intervals have been laid off on the x-axis (in longitudinal direction) by

$$a, x_1, x_2, \ldots, x_{2n-1}, b$$

and

$$y_a, y_1, y_2, \ldots, y_{2n-1}, y_b$$

are the respective ordinates(the reduction of the pipe wall-thickness) of these points.

-Closely Spaced Corrosion Pits:
A distance of t (Wall-thickness) is used as a criterion of pit separation for a colony of longitudinally oriented pits separated by a longitudinal distance or parallel longitudinal pits separated by a circumferential distance.

-Interaction of Longitudinal Grooves:
For defects inclined to pipe axis,

(a) If the distance x, between two longitudinal grooves of lengths L_1 and L_2, is greater than either L_1 or L_2, then the length of corrosion L is L_1 or L_2 which ever is greater.

(b) If the distance x, between two longitudinal grooves of lengths L_1 and L_2, is less than L_1 and less than L_2, then the length of corrosion L is the sum of x, L_1 and L_2, $L=L_1+L_2+x$.

For two longitudinal grooves separated by a circumferential distance x, the wall-thickness t could be used as grooves separation criterion.

(3) Spiral Correction Factor Q:

The spiral correction factor Q is

$$Q = \frac{1 - Q_1}{32}\frac{W}{t} + Q_1 \qquad (8.4)$$

in which W is defect width, and the coefficient Q_1 is a function of the spiral angle ψ ($\psi=90^0$ for longitudinal corrosion, $\psi=0^0$ for circumferential corrosion):

$Q_1 = 0.2$ for $0^0<\psi<20^0$
$Q_1 = 0.02\psi-0.2$ for $20^0<\psi<60^0$
$Q_1 = 1.0$ for $\psi>60^0$

For W/t>32, the value of Q must be taken as 1.0.

(4) Flow Stress σ_{flow}

The flow stress σ_{flow} is ultimate tensile stress σ_u for pipes under pure internal pressure or combined internal pressure and moderate tension. The effect of compressive axial stress can be accounted for by reducing the flow stress based on von Mises yield function. Tensile axial stress gives beneficial effect but the effect of tensile axial stress in negligible. If the ultimate tensile stress is not known, its value can be taken as SMTS.

Consideration should be given to factors affecting flow stress, e.g. fabrication process (e.g. hot rolled versus cold expanded), material ageing, possible size effect, installation process (e.g. reeling) and possible cracks in corrosion defect bottom. Use of the actual value of the flow stress is allowed, provided the value has been obtained through a reliable approach (e.g. material testing of the pipe in situ etc.).

(5) Folias factor M

The Folias factor is estimated as for $L^2/(Dt) \leq 50$

$$M = \sqrt{1 + \frac{2.51(L/2)^2}{Dt} - \frac{0.054(L/2)^4}{(Dt)^2}} \qquad (8.5)$$

and for $L^2/(Dt) > 50$

$$M = 0.032\frac{L^2}{Dt} + 3.3 \qquad (8.6)$$

(6) Corroded Welds

Corrosion in submerged-arc seams (longitudinal welds) should be handled in the same manner as corrosion in the body of the pipe. Corrosion in girth welds (circumferential) should be assessed using the Kastner's local collapse criterion.

The level-2 (or Level-3) FAD (Failure Assessment Diagram) implemented in PD6493 (1991)should be applied for assessing corroded welds. The corroded groove could be considered as a crack of the same depth and length. The effect of material's fracture toughness (in ductile

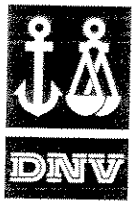

and low toughness pipe) could be taken into account in the assessment procedure of the material fracture toughness.

(7) Effect of Axial and Bending Loads

For corroded pipe under combined pressure, axial and bending loads, the flow stress in the circumferential direction could be calculated considering the effects of the longitudinal stress, using von Mises yield function.

(8) Safety Factor γ

Traditional safety factors are given based on engineering experience and judgement. Within RSTRENG projects (Kiefner and Vieth 1989, 1993), several modified B31G criteria and the RSTRENG2 program have been developed. In all cases, the safety factor is assumed to be 1/0.72 = 1.39, as the original B31G criterion.

8.2 Proposed Strength Equation for Circumferentially Corroded Pipes

Since the length of a girth weld defect is very short (typically of pipe wall-thickness), its influence on hoop rupture due to excessive internal pressure is negligible. The maximum allowable operating pressure for pipes under pure internal pressure is calculated using B31G.

The Safe Maximum Axial Tensile Stress σ_{AX}' is calculated using Kastner (1981) criterion

$$\sigma_{AX} = \frac{\sigma_{flow}}{\gamma} \frac{\eta[\pi - \beta(1-\eta)]}{\eta\pi + 2(1-\eta)\sin\beta} \qquad (8.7)$$

where

σ_{AX}' = safe maximum axial tensile stress
σ_{flow} = the flow stress
d = defect depth
t = wall-thickness
η = 1 - d/t
c = half defect (circumferential) length
R = pipe radius
β = c/R (in radians)
γ = Factor of safety

The predicted ultimate axial stress level is $\gamma\sigma_{AX}'$.

For pipes under combined internal pressure and axial tension, Eq.(8.7) is also valid and the axial stress is applied in the strength assessment. The influence of internal pressure on tensile strength of pipes under combined internal pressure and tension is negligible.

Eq.(8.7) is also valid for pipes under combined internal pressure, axial tension and bending, and the total axial tensile stress in the defect area is applied in the strength calculation.

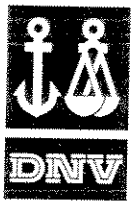

Strength of pipes under combined internal pressure and axial compression is dependent on the type of loading. Strain (deformation) type axial compression has no influence on the burst pressure. The interaction between internal pressure and (stress) load type axial compression is of von Mises type.

8.3 Comparison with the Test Database

Appendix A summarises test databases and the predictions due to alternative strength equations. In comparisons the characteristic strength is applied (no safety factor is used in the burst strength calculation).

8.3.1 Comparisons Between Strength Equations and the Test Database

The following figures show comparisons of alternative strength equations with the test database (consists AGA Database, NOVA Tests, British Gas Tests and Waterloo Tests). The x-axis is actual yield stress and the y-axis is the ratio of the tested burst pressure and the predicted strength.

Figure 8-1 Comparison of The *Proposed* Equation with The Test Database
Figure 8-2 Comparison of The *B31G* Strength Equation with The Test Database
Figure 8-3 Comparison of The *NG-18* Strength Equation with The Test Database
Figure 8-4 Comparison of The *Effective Area* Strength Equation with The Test Database
Figure 8-5 Comparison of The *0.85dL* Strength Equation with The Test Database

The B31G and modified B31G (Effective Area and 0.85dL) are applied exactly as stated in the B31G manual (ASME 1993) and Kiefner's RSTRENG project reports (Kiefner and Vieth (1989, 1993)). The NG-18 equation are, however, used based on recent knowledge since no standard/report describes how to use NG-18 equation. The difference between the NG-18 equation and the proposed equation is that in the NG-18 equation, flow stress is SMYS+10 ksi and the Folias factor is calculated as B31G, Eq. (3.9), and in the proposed criteria the flow stress is σ_u, and the Folias factor is calculated as Eq.(8.5) and Eq.(8.6)

It must be indicated other uncertainties, such as measurement uncertainties etc., are to some extent included in the comparisons and in the model uncertainty assessment. The actual COV can be smaller than what we obtained in Table 8-1. However, it is difficult for us to exclude measurement uncertainties from the experimental database.

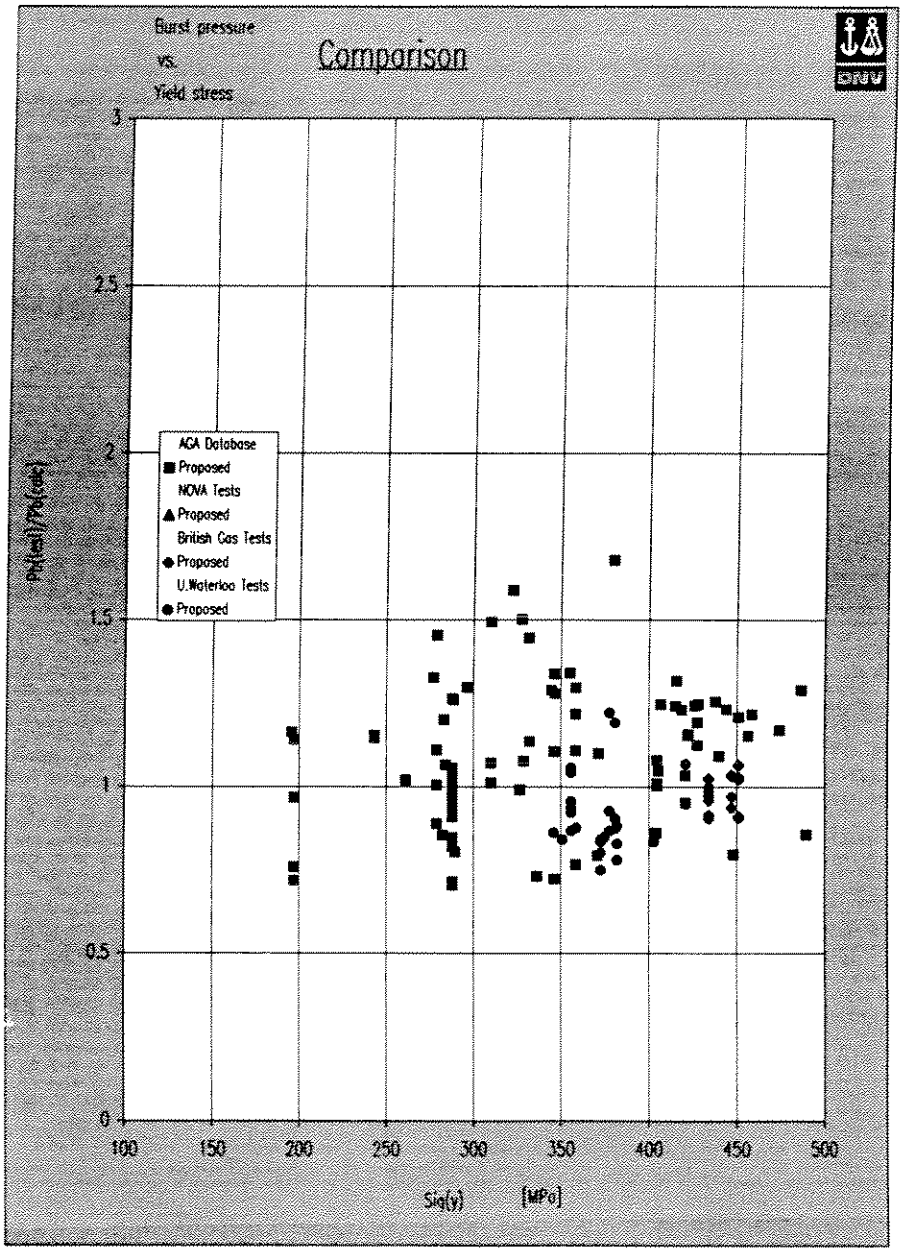

Figure 8-1 Comparison of The Proposed Equation with The Test Database

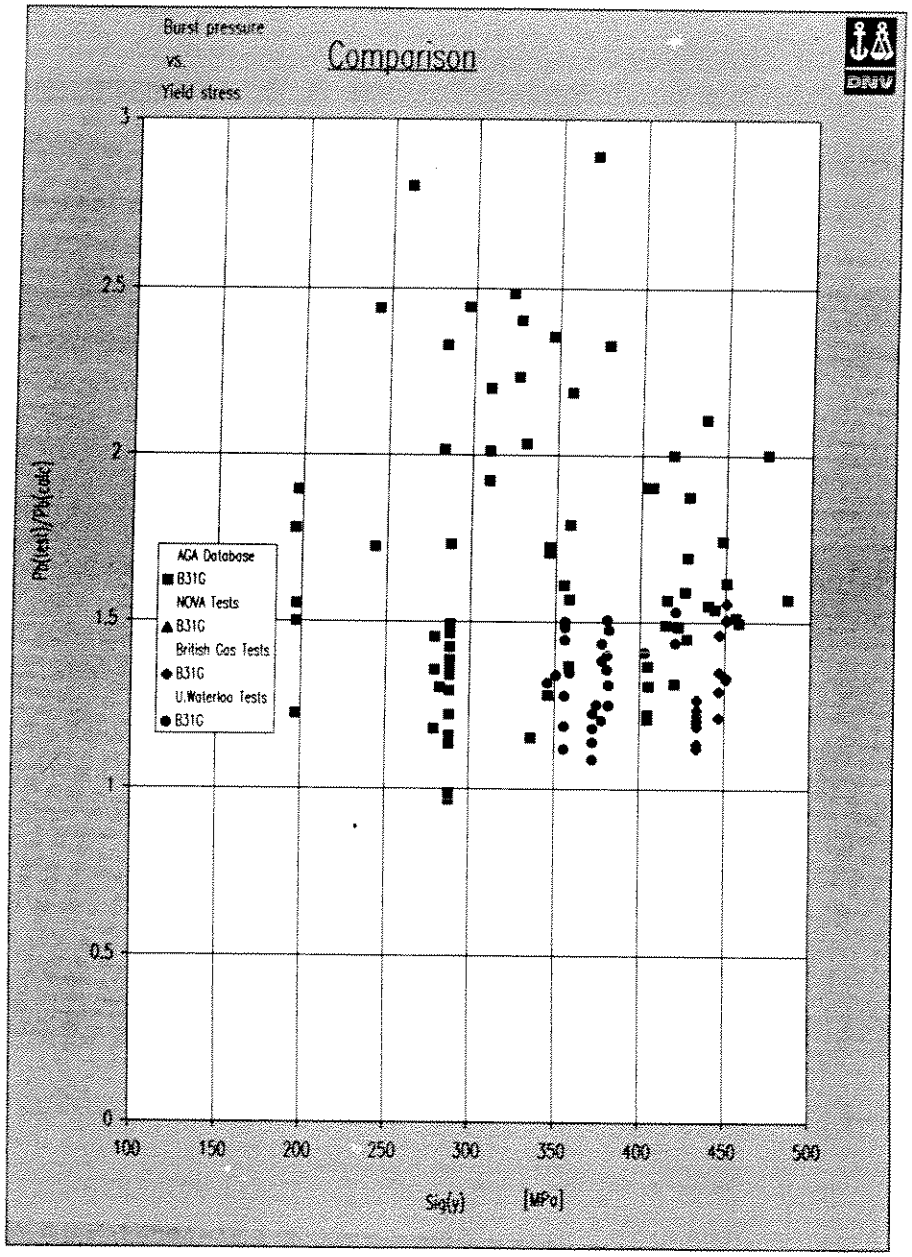

Figure 8-2 Comparison of The B31G Strength Equation with The Test Database

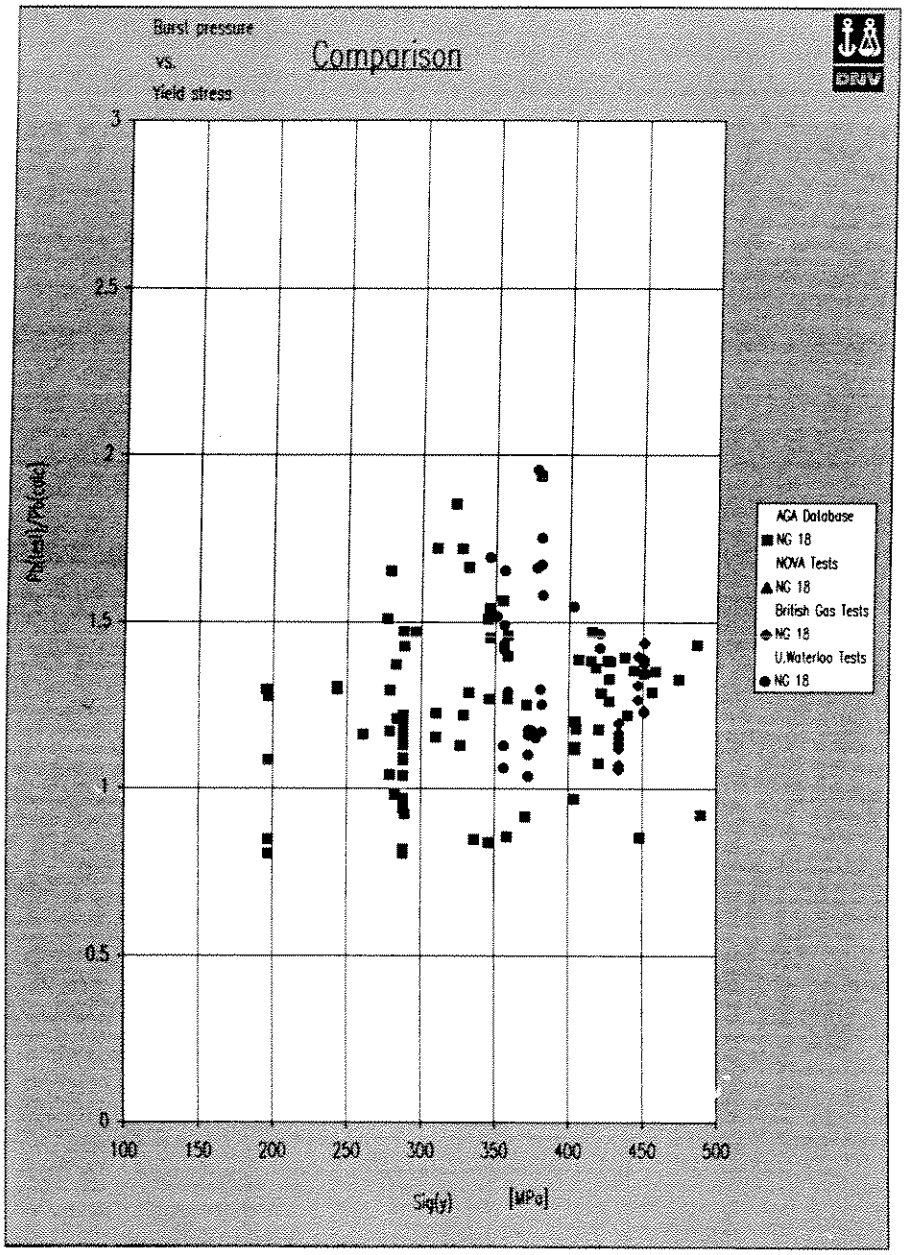

Figure 8-3 Comparison of The NG-18 Strength Equation with The Test Database

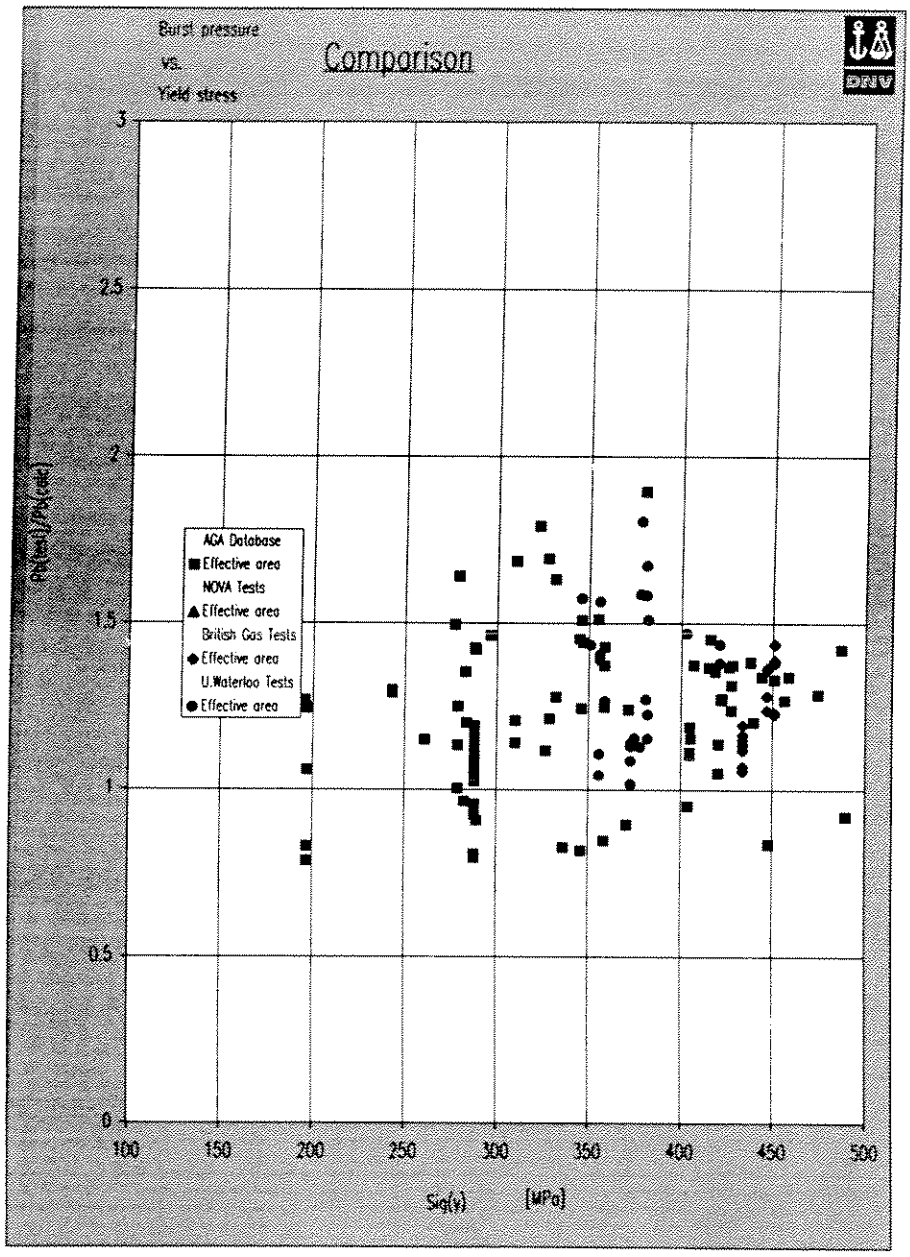

Figure 8-4 Comparison of The Effective Area Strength Equation with The Test Database

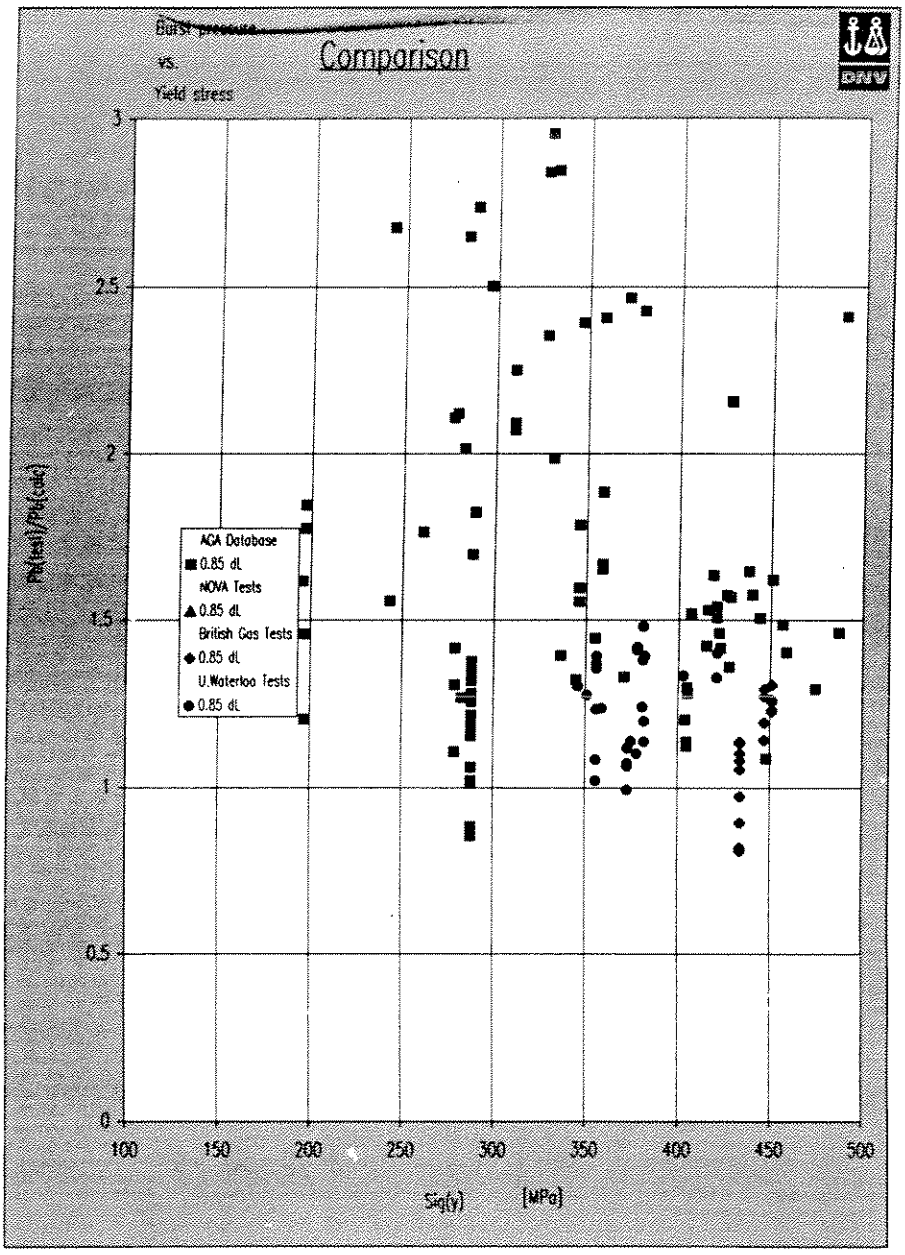

Figure 8-5 Comparison of The 0.85dL Strength Equation with The Test Database

8.3.2 Comparisons Between B31G and the Proposed Strength Equation

The following figures show comparisons of alternative strength equations with the test database (consists AGA Database, NOVA Tests, British Gas Tests and Waterloo Tests). The x-axis is actual yield stress and the y-axis is the ratio of the tested burst pressure and the predicted strength.

Figure 8-6 Comparison Between *B31G* and *Proposed* Equation as a Function of SMYS
Figure 8-7 Comparison Between *B31G* and *Proposed* Equation as a Function of SMTS
Figure 8-8 Comparison Between *B31G* and *Proposed* Equation as a Function of σ_y
Figure 8-9 Comparison Between *B31G* and *Proposed* Equation as a Function of d/t
Figure 8-10 Comparison Between *B31G* and *Proposed* Equation as a Function of $L^2/(Dt)$

Note that the B31G is a lower bound equation and the proposed equation is a mean value prediction.

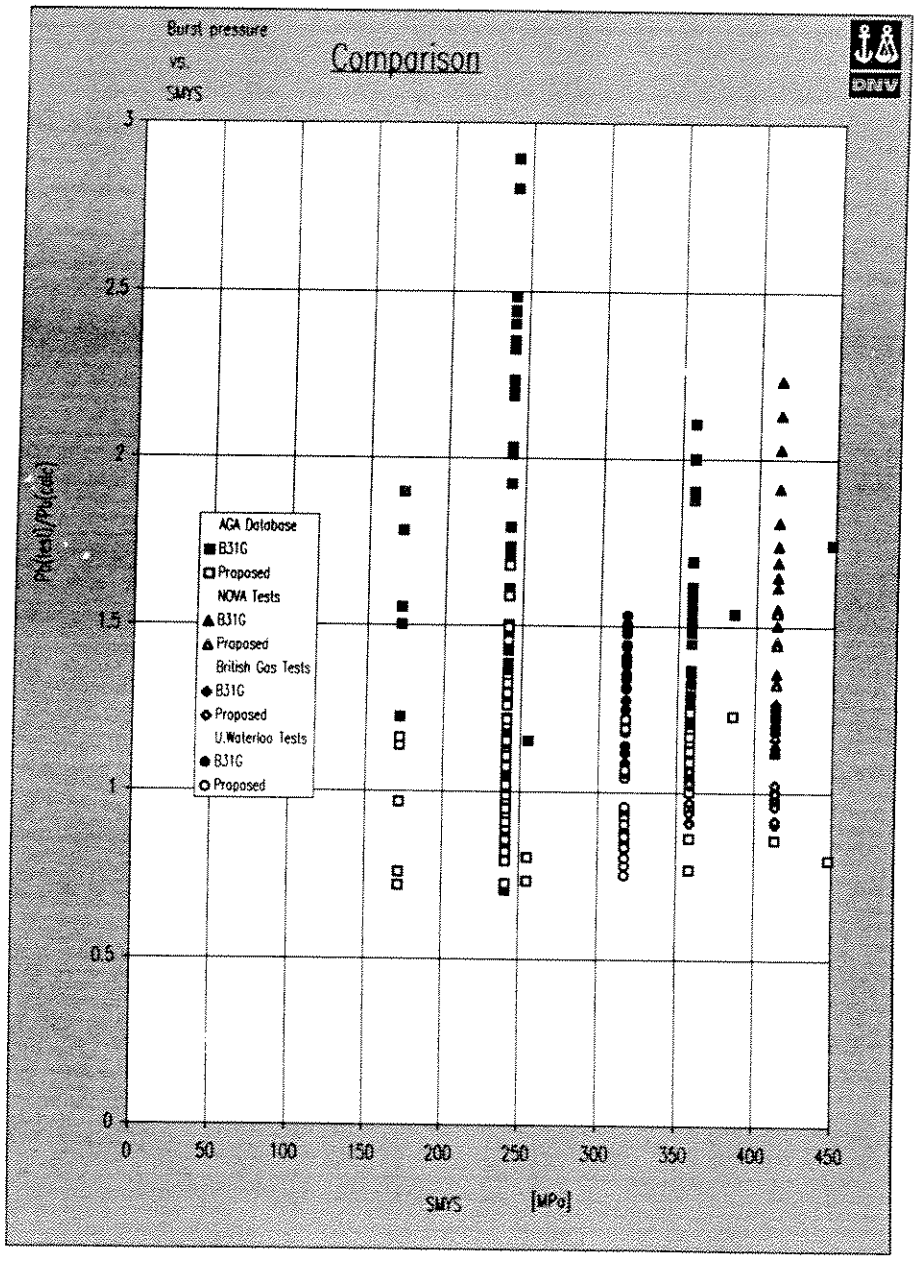

Figure 8-6 Comparison Between *B31G* and *Proposed* Equation as a Function of SMYS

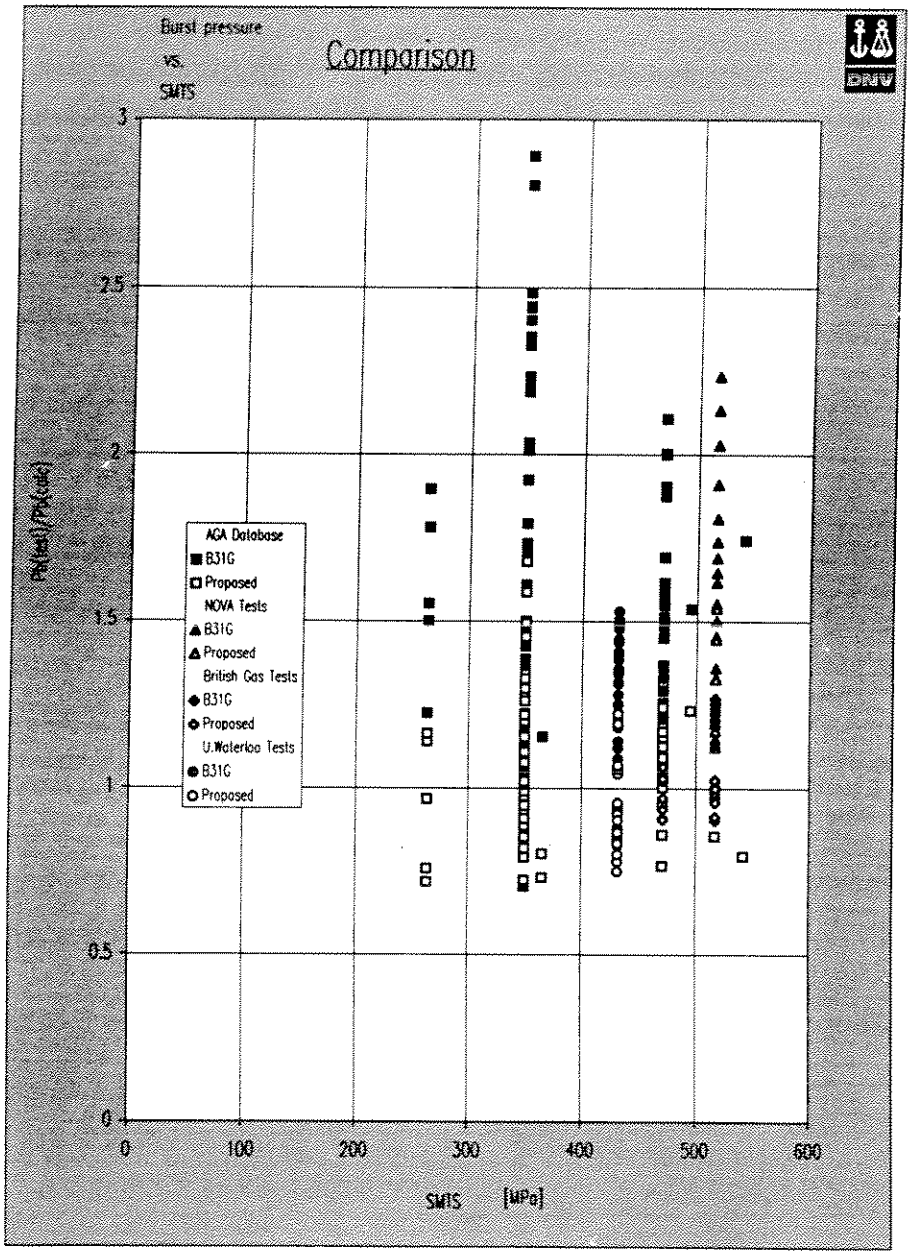

Figure 8-7 Comparison Between *B31G* and *Proposed* Equation as a Function of SMTS

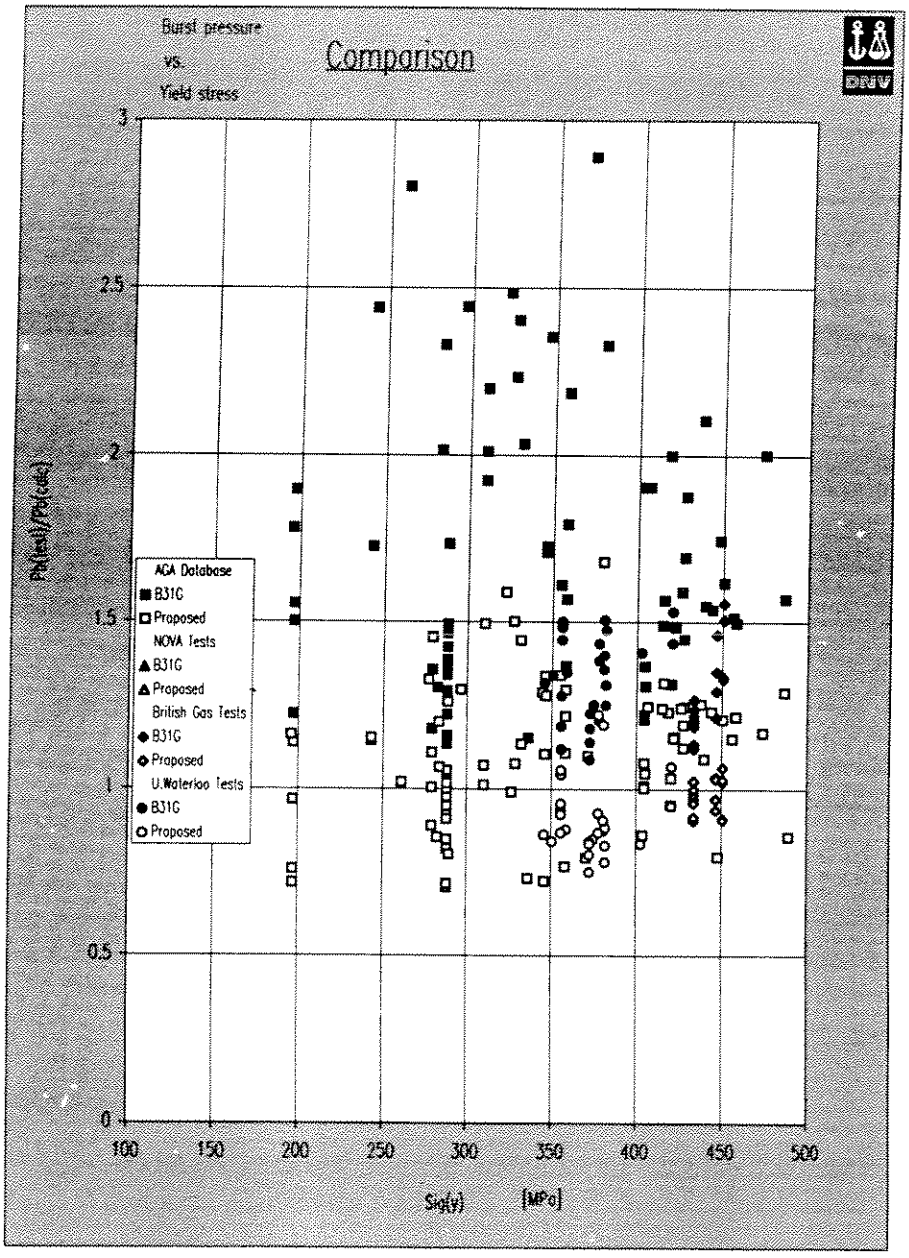

Figure 8-8 Comparison Between *B31G* and *Proposed* Equation as a Function of σ_y

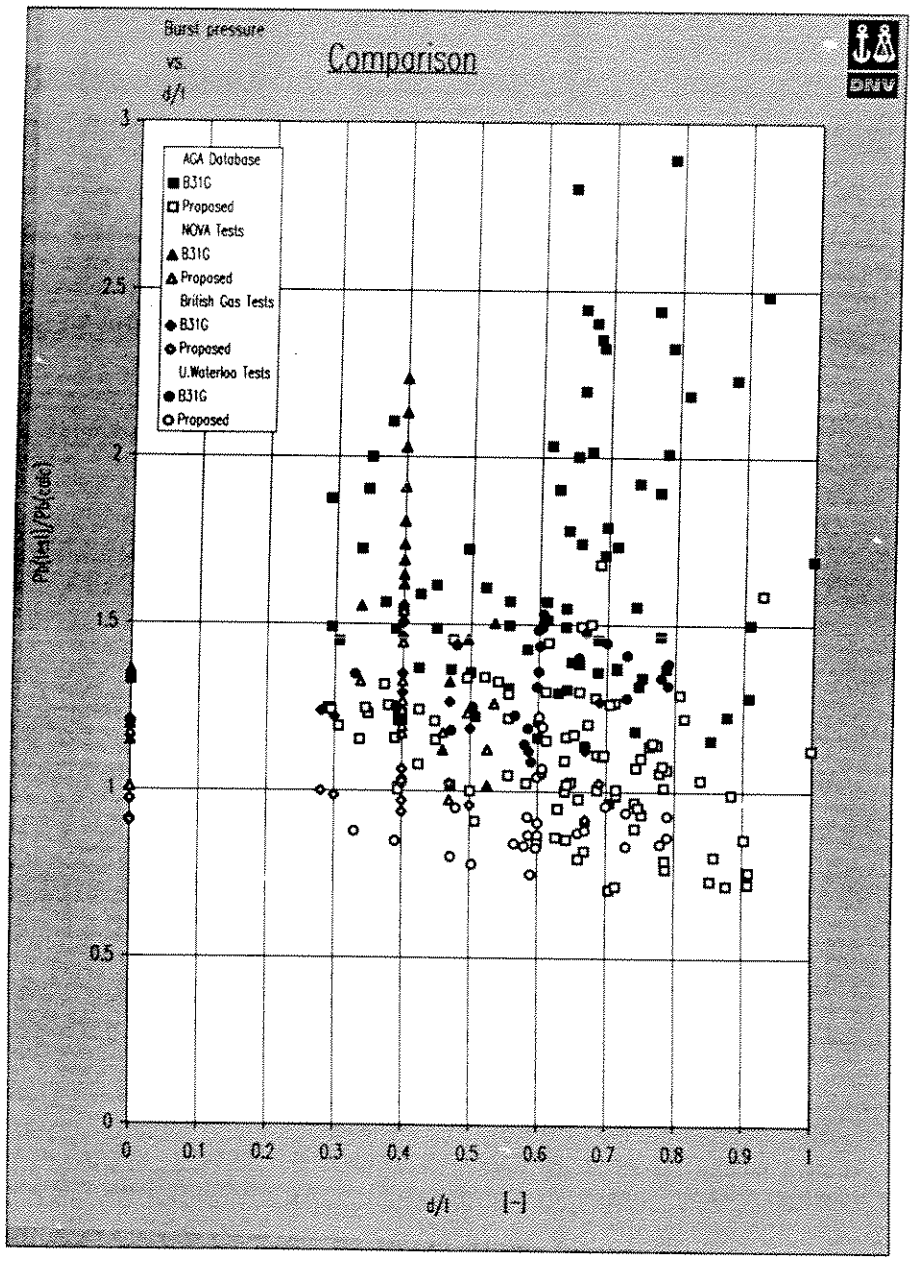

Figure 8-9 Comparison Between *B31G* and *Proposed* Equation as a Function of d/t

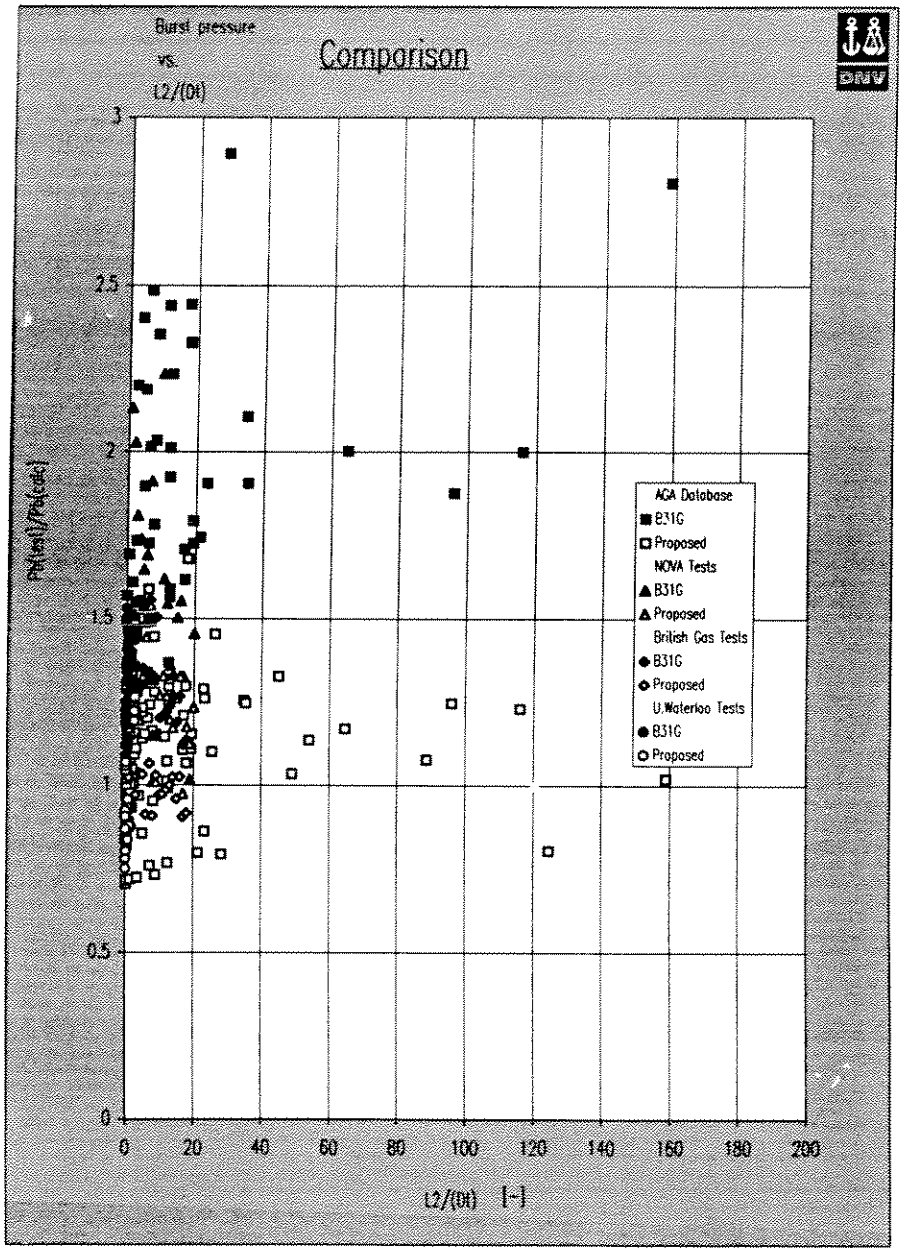

Figure 8-10 Comparison Between *B31G* and *Proposed* Equation as a Function of $L^2/(Dt)$

8.3.3 Comparison with All Available Tests

A model uncertainty parameter X_M is defined as

$$X_M = \frac{X_{TRUE}}{X_{PRED}} \tag{8.8}$$

where X_{TRUE} is the real strength and X_{PRED} the capacity predicted by a given criterion. X_{TRUE} is usually determined by laboratory tests or e.g. refined finite element analyses.

Table 8-1 shows the obtained statistics. In the table n is number of tests, μ and σ^2 denote mean value and standard deviation for X_M respectively.

Table 8-1 Statistics for Different Strength Equations and Test Databases

		B31G	NG18	B31G Eff.Area	B31G 0.85dL	Proposed
n	AGA Database	86	86	86	86	86
	NOVA Tests	20	20	20	20	20
	British Gas Tests	18	18	18	18	18
	U.Waterloo Tests	27	27	27	27	27
	Total	151	151	151	151	151
μ	AGA Database	2.01	1.24	1.22	1.67	1.09
	NOVA Tests	1.59	1.48	1.45	1.35	1.22
	British Gas Tests	1.33	1.24	1.23	1.12	0.98
	U.Waterloo Tests	1.37	1.39	1.35	1.25	0.92
	Total	1.76	1.30	1.27	1.49	1.07
σ^2	AGA Database	1.26	0.06	0.06	0.31	0.04
	NOVA Tests	0.13	0.10	0.10	0.07	0.04
	British Gas Tests	0.21	0.02	0.02	0.17	0.01
	U.Waterloo Tests	0.17	0.07	0.05	0.08	0.04
	Total	0.78	0.06	0.06	0.22	0.04
COV	AGA Database	0.56	0.20	0.20	0.33	0.19
	NOVA Tests	0.23	0.22	0.22	0.20	0.17
	British Gas Tests	0.35	0.11	0.10	0.36	0.10
	U.Waterloo Tests	0.30	0.19	0.17	0.22	0.21
	Total	0.50	0.19	0.19	0.31	0.18

Model uncertainty is due to imperfection or idealisation of a particular physical or analysis model, given that all the parameters entering the model are known in advance. Therefore, model uncertainty does not included any parameter uncertainty (which is uncertainty associated with a

particular random parameter). The model uncertainty parameter X_M, as defined, is introduced in order to account for modelling and methodology uncertainties and reflects a general confidence in the applied analytical modelling to describe a real life in-situ scenario.

It is at present assumed that the test results are associated with negligible measurement errors and with a very high confidence in modelling the real life scenario.

The mean value (MEAN) and coefficient of variation (COV) of the parameter X_M achieved for the alternative strength equations are shown in Table 8-1.

It is also shown that the obtained model uncertainty statistics are largely dependent on the test database used.

AGA database show large scatter.

The agreement between Tests and predictions is good for tests by British Gas, U. Waterloo.

The model uncertainty is then assessed using all available test data.

8.4 Maximum Allowable Depth/Area for Longitudinal Corrosion

8.4.1 Maximum Allowable Defect Depth and Length According to B31G

According to B31G (ASME 1993), the term MAOP represents maximum steady state operating pressure for pipeline within the scope of ASME B31.4 and ASME B31.11 and maximum allowable operating pressure for pipelines within the scope of ASME B31.8. If the established MAOP is equal to or less than P′, the corroded region may be used for service at the MAOP. If it is greater than P′, then a lower MAOP should be established not to exceed P′, or the corroded region should be repaired or replaced.

In the B31G, a criterion for the acceptance corroded length is given as below for a corroded area having a maximum depth 'd' of more than 10 %, but less than 80 % of the nominal wall-thickness.

$$L_{allow} = 1.12B\sqrt{Dt} \tag{8.9}$$

and where a constant 'B' is calculated using

$$B = \sqrt{\left(\frac{d/t}{1.1d/t - 0.15}\right)^2 - 1} \tag{8.10}$$

B may not exceed the value 4.
Equating the Safe Maximum Pressure Level P′ to the Design Operating Pressure P_D, the Maximum Allowable Corrosion Depth d_{allow} can be calculated from the B31G criterion

(a) For $A \leq 4$

$$d_{allow} = \frac{3t}{2}\left(\frac{1 - \frac{P_D}{1.1P}}{1 - \frac{P_D}{1.1P\sqrt{A^2+1}}}\right) \tag{8.11}$$

(b) For $A > 4$

$$d_{allow} = \left(1 - \frac{P_D}{1.1P}\right) t \tag{8.12}$$

in which the constant 'A' is given by $0.893L/(Dt)^{1/2}$.

8.4.2 Maximum Allowable Defect Area and Length (proposed criteria)

The maximum allowable defect area and length according to the proposed criterion are given in this section.

The Maximum Allowable Design Pressure P is

$$P = F\frac{2t}{D}SMYS \tag{8.13}$$

where F is the usage factor for intact pipe (which is 0.72 according to DNV (1981) pipeline rules).Equating the Safe Maximum Pressure Level P′ to the Maximum Allowable Design Pressure

$$\frac{1}{\gamma}\frac{2\sigma_{flow}t}{D}\frac{1 - Q\,AREA/AREA_0}{1 - M^{-1}\,AREA/AREA_0} = F\frac{2t}{D}SMYS \tag{8.14}$$

we may obtain the Maximum Allowable Effective Area $AREA_{allow}$ as

$$\frac{AREA_{allow}}{AREA_0} = \frac{F\gamma\frac{SMYS}{\sigma_{flow}} - 1}{F\gamma\frac{SMYS}{\sigma_{flow}}M^{-1} - Q} \tag{8.15}$$

in which γ is the safety factor used in the proposed residual strength criterion.

The Maximum Allowable Length L_{allow} is for $M_{allow} \leq 4.9$

$$L_{allow} = \sqrt{\frac{1.255}{0.0135} - \sqrt{\left(\frac{1.255}{0.0135}\right)^2 - \frac{\left(1 - M_{allow}^2\right)}{-0.0135/4}}}\sqrt{Dt} \tag{8.16}$$

and for $M_{allow} > 4.9$

$$L_{allow} = \sqrt{(M_{allow} - 3.3)/0.032} \quad \sqrt{Dt} \tag{8.17}$$

in which M_{allow} is again solved by equating the Safe Maximum Pressure Level P′ to the Maximum Allowable Design Pressure:

$$M_{allow} = \frac{F\gamma \dfrac{SMYS}{\sigma_{flow}}}{Q + \dfrac{AREA_0}{AREA}\left(F\gamma \dfrac{SMYS}{\sigma_{flow}} - 1\right)} \tag{8.18}$$

9 PROCEDURE FOR RELIABILITY-BASED CALIBRATION

9.1 General

In order to calibrate safety factors using reliability methods, it is necessary to make adequate uncertainty measures of model uncertainty, load uncertainty and parameter uncertainties.

To quantify the model uncertainty of limit states, different experimental databases have been compared with limit state functions. Mean values, COV and distribution function are to be proposed based on these comparisons. Load uncertainty is based on an modification to the value published by Sotberg and Leira (1994).

Parameter uncertainties concerning corrosion depth, length and area are estimated based on accuracy of inspection tools and future corrosion prediction. For instance a defect depth used in a residual strength assessment of internally corroded pipes is the sum of the defect depth from the pigging inspection and the increased depth calculated from future corrosion prediction by use of previous inspection results and a corrosion-rate formula

$$d(\text{used in strength calculation}) = d(\text{from pigging}) + d(\text{future growth}) \tag{9.1}$$

where

d_{PRED} = d(used in strength calculation) = The value used in a strength calculation using a residual strength criterion

d_p = d(from pigging) = The estimated corrosion depth at the time when the pipe is inspected

d_f = d(future growth) = The estimated increase of the corrosion depth, until a date the pipe is re-qualified, based on e.g. application of deWaard and Milliams formula (Shell formula)

The uncertainty associated with the estimation of corrosion depths is calculated using

$$X_d = \frac{d_{TRUE}}{d_{PRED}} = \frac{d_{TRUE}}{d_p + d_f} \tag{9.2}$$

In order to reasonably estimate statistical values of X_d, an assessment of the methods of pigging inspection and future corrosion prediction is necessary.

9.2 Safety Philosophy

9.2.1 Allowable Stress Format vs. ULS Design

Traditionally, an allowable stress format has been used as

$$\frac{R_n}{F.S.} \geq \sum Q_{ni} \tag{9.3}$$

where

R_n = Normal strength as given by an equation in a specification
Q_{ni} = Load effect (i.e. a computed stress or a force such as bending moment, shear force, axial force, etc.) determined from e.g., live load, dead load, wind load, etc.
F.S. = Factor of safety

or

$$\eta R_n \geq \Sigma Q_{ni} \tag{9.4}$$

η = Usage factor

Limit state design methods provides engineers with rational tools for achieving consistent levels of safety in the design of structural components. A partial safety factor approach (adopted in e.g. DNV rules) is

$$\frac{R_n}{\gamma_m} \geq \Sigma \gamma_{li} Q_{ni} \tag{9.5}$$

where γ_{li} = Load factors by which the characteristic loads are multiplied to obtain the design loads
γ_m = Material factor by which the characteristic strength Rn is divided to obtain the design strength

When the material factor γ_m is replaced by a resistance factor ϕ ($=1/\gamma_m$), this equation leads to LRFD (Load and Resistance Factor Design) format (adopted in e.g. API LRFD rules for fixed offshore platforms).

In general, the factor of safety F.S.>1.0, η<1.0, ϕ<1.0, γ_{li}>1.0 and γ_m>1.0, all serve the same purpose: to account for the uncertainties inherent in the determination of the nominal strength and the load effects due to natural variation in the loads, the material properties, the accuracy of the theory (knowledge uncertainty) etc. Their values are to be calibrated so that the implied safety level of a structure has a failure probability close to a target failure probability P_{fT}.

9.2.2 Mean Value versus Lower Bound

The B31G criterion was established based on lower bound formulae and the present proposed criterion is a mean value formulation. Lower bound equations should be replaced by mean value predictions for the following reasons (Faulkner et al 1987).

(a) lower bound equations give less consistency than mean value predictions do so far as reliability is concerned, especially where the sample size of validating test data is small.

(b) matching strength equations to weak test data will inevitably ignore the majority of the data which in turn is most relevant for the more likely levels of imperfection (defects).

(c) the very nature of predictions should be that on average they have the highest probability of being correct.

(d) for in-service assessments, design code equations are frequently used and by their nature lower bound expressions will have a higher probability of being wrong.

Alternatively, for the same reasons, median values or mpm (most probable maximum) values in extreme value predictions can be applied.

9.3 Inspection Tools

Inspection and testing will give important information on the status of the pipeline systems. The inspection results should be used with care when checking the residual strength of a pipeline system. Different inspection tools may give different results, both with respect to type of incidents reported and also the accuracy of information. The intelligent pigs are outlined in (1) - (3) and their accuracy is discussed in (4).

1. Magnetic Flux Leakage (MFL) pigs

The magnetic flux leakage technique consists of rings of permanent or electromagnets mounted on the pig body and in contact with the wall through a system of steel brushes. The magnet rings are the north and south poles which, when in contact with the pipe wall establish a magnetic field through the pipe wall. Any defect in the pipe wall between the poles will cause a disturbance or flux leakage in the magnetic field. Sensors supported on the pig body are located between the poles and detect any disturbances in the magnetic field. The magnetic flux leakage is measured by the sensors and recorded for later evaluation. The flux leakage technique is an interpretative measurement as opposed to a calibrated measurement. As such, the results are totally dependent on the interpretation of the recorded magnetic flux leakage signal.

An advanced MFL pig can generally detect the following types of defect and features:

- pitting corrosion
- general corrosion
- circumferential and transverse orientated defects
- girth welds
- valves, tees, taps, bends
- CP attachments
- discriminates between internal and external metal loss

Typical limitations for MFL pigs are:

- Pipe diameter/pig size: between 6" (152.4 mm) and 48" (1219.2 mm)
- Maximum pressure: between 70 and 207 bar
- Temperature: Maximum between 40 and 70 ^{0}C, Minimum between -17 and+4 ^{0}C
- Pig speed: Maximum between 0.25 and 4.4m/s, Minimum between 0.2 and 0.5 m/s
- Wall thickness: between 38 and 3 mm
- Minimum bend radius: usually 3D and in some cases 4D
- Pipeline length: between 200 - 300 km and up to 500 km

2. Ultrasonic (US) pigs

The ultrasonic pigs employ the pulse-echo technique of ultrasonic to measure wall thickness. The transducers transmit and receive acoustic pulses. The transducers are set in the pig away from the inside wall surface, at a so called stand-off distance. When the acoustic pulse meets the inside pipe wall surface a fraction of the energy will be reflected and the remainder will pass into the steel.

At the outside wall surface another acoustic reflection will occur. The transducer detects both reflections and calculates the wall thickness which is proportional to the difference in the duration of the two incoming pulses. With correct calibration of the transducers direct wall thickness measurements can be obtained. This technique also allows for discrimination between metal loss on internal and external pipe wall surface.

All ultrasonic pigs require a good acoustic conducting medium between sensor and reflective interfaces. A homogeneous liquid is a suitable medium. A gas or a multiphase liquid is not suitable as the acoustic signal will not propagate in a gas without attenuating significantly and a multiphase liquid will not allow precise calibration of the transducers.

An advanced US pig can generally detect the following:

- internal and external corrosion
- metal loss
- girth welds
- laminations

Typical limitations for US pigs are

- Pipe diameter/pig size: between 2" (50.8 mm) and 54" (1371.6 mm)
- Maximum pressure: between 100 and 138 bar
- Temperature: Maximum between 45 and 60 ^{0}C, Minimum between -10 and +4 ^{0}C
- Pig speed: Maximum between 1.0 and 4.4m/s, Minimum between 0.2 and 0.5 m/s
- Wall thickness: between 50 and 4 mm
- Minimum bend radius: usually 3D
- Pipeline length: up to 200 km

Detection accuracy varies, but typically it can be said that UT pigs specify features to within 10% of the wall thickness while MFL pigs specify features to within 20% of the wall thickness.

3. Eddy Current (EC) Pigs

EC pigs are relatively new on the market and have a potential for future use. As the name suggests, eddy currents set up by magnets on the pig, travel along or near the surface of the pipe wall and are detected using hall and coil sensors. This technique allows for the very accurate sizing of internal surface corrosion, to less than 1 mm, thereby permitting internal corrosion monitoring to be performed from early in the pipeline's life.

EC pigs can also detect surface cracking in the circumferential direction. As stated above, the tool employs Eddy Currents to permit the detection of the cracks.

4. Accuracy and Sensitivity of Pigs

The accuracy, limitation and sensitivity of the different MFL and US pigs vary considerably and therefore care needs to be taken when choosing an intelligent pig. One of the most important requirements when using intelligent pigs for pipeline condition monitoring is the pigs ability to provide repeatability, i.e. the ability to reproduce identical results from successive inspections in order to be able to identify defect development trends.

Typical accuracy and sensitivity for detection of different defects are given in Table 9.1 for magnetic flux pigs and ultrasonic pigs

Table 9-1 Typical Defect Identification and Sizing for MFL and US pigs

Feature	Parameter	2nd generation MFL pig	US pig
Pitting corrosion depth	Accuracy Size	+/- 0.1T-0.2T >=2T	+/- 0.5-1.0mm
General corrosion depth	Accuracy	+/- 0.1T-0.15T	
defect sizing accuracy	Axial Circumferential		
circumferential gouging	Accuracy Size	+/- 0.15T-0.2T >=3T	
axial gouging	Accuracy Size	+/- 0.1T-0.2T >=2T	
axial location		+/- 1.5 m	+/- 0.2m-0.3m
circumferential location		+/- 5 deg.	+/- 10-15 deg.

Notes: 1) T = nominal wall thickness
2) Blank box means no reliable information is available
3) All data are manufacturer supplied

It is generally accepted that US pigs are more accurate than MFL pigs for sizing of features but MFL pigs are better at detecting the full range of features.

9.4 Future Corrosion Prediction

External corrosion is efficiently prevented by the use of cathodic protection in combination with multi-layer coatings. For pipeline risers in the atmospheric/splash zone, external corrosion due to coating damage is a failure mechanism.

Internal corrosion is dependent of the containment as below:

1. Unprocessed Well Fluid

Unprocessed well fluid will always contain certain amounts of liquid water. Carbon dioxide, being a normal constituent of well fluid, will be dissolved in the water phase rendering it corrosive to ordinary CMn-steel line pipe material. Stainless steel linepipe or cladding, on the other hand, is fully resistant to *CO_2-Corrosion.*

At very high flow rates leading to annular flow, the water phase may become evenly distributed over the pipe surface. This will lead to a uniform corrosion attack, most probably combined with circumferential grooving of girth welds (*girth weld corrosion*).

CO_2-corrosion of CMn-steel pipelines can be controlled by the injection of corrosion retarding chemicals. The efficiency of such measures is verified by in-situ inspection while special probes and chemical analyses may be applied for control of the injection.

For CMn-steel pipelines carrying unprocessed hydrocarbons, any prediction of future corrosion should primarily be based on results from previous inspection by instrumented pigging. When estimating the future degradation, results from two or more pigging operations relatively recent in time (e.g. 0-5 years) should preferably be available. This will allow more accurate predictions by extrapolation of corrosion rates into the period of extended life. If such inspection data are available, the remaining life, can be assessed with higher certainty than was possible when estimating the initial life at the design stage when no experience data were at hand.

If economic and/or safety considerations based on inspection data indicate that the probability of achieving the extended life is not sufficiently high, then a chemical treatment program for corrosion control may be implemented (or modified if already applied). A prediction of future corrosion based on chemical injection, which would be an alternative to the installation of a new pipeline, should be based on a reliability analysis in which the estimated efficiency of the chemical treatment is expressed in probabilistic terms.

Shell has developed a prediction formula for CO_2-corrosion in gas/condensate systems ("deWaard/Milliams formula") (deWaard and Milliams 1975). This formula gives a relation between corrosion rate of "C-steel" and the temperature and CO_2-partial pressure of the gas phase. It has been widely used for predicting the corrosivity of gas/condensate flowlines during the initial design. For existing pipelines, experience data from pigging operations will give more reliable predictions of future corrosion. However, if major changes in CO_2-partial pressure and temperature during the remaining life are expected, then these may be taken into account by "calibrating" the Shell formula against inspection data.

The Shell formula (deWaard and Milliams 1975) is

$$\log V_{corr} = 5.8 - \frac{1710}{273+T} + 0.67 \log (P_{CO2}) \qquad \textbf{(9.6)}$$

where

V_{corr} = the corrosion rate (mm/year)
T = the temperature (^{0}C)
P_{CO2} = the partial pressure of CO_2 (bar)

The selection of physical parameters to be used in the basic CO_2-corrosion rate prediction according to deWaard et al (1991) and deWaard and Lotz (1993), does not normally involve any major uncertainties. The CO_2-content of reservoir fluids can be accurately determined during early well testing. Temperature and total pressure can usually be treated as deterministic parameters using design or maximum operating values.

Figure 9-1 shows the probability distribution assumed for model uncertainty X_{corr}, related to pitting corrosion and longitudinal grooving respectively. A Weibull distribution (W(μ, COV)) with mean value μ and COV has been selected for both damage models (Sydberger et al 1995). For the maximum pitting corrosion in any of the circumferential girth welds, a W(1.0; 0.45) distribution model is assumed such that the predicted value for V_{corr} based on Shell formula represents a 50% probability. For the probability distribution for longitudinal corrosion grooving, a W(0.4; 0.8) model is assumed such that this corresponds to a 90% probability that Shell formula prediction will not be exceeded at any point of the pipeline.

In Figure 9-2, a number of probability density functions for the inhibitor efficiency factor η is presented (Sydberger et al 1995). A Weibull distribution is applied for all cases with the distribution parameters estimated from engineering judgement and experience. The solid curve corresponds to a probability distribution where there is a 50% probability than an 85% efficiency is achieved. The other lines represent decreasing efficiencies down to 70% (with a 50% probability).

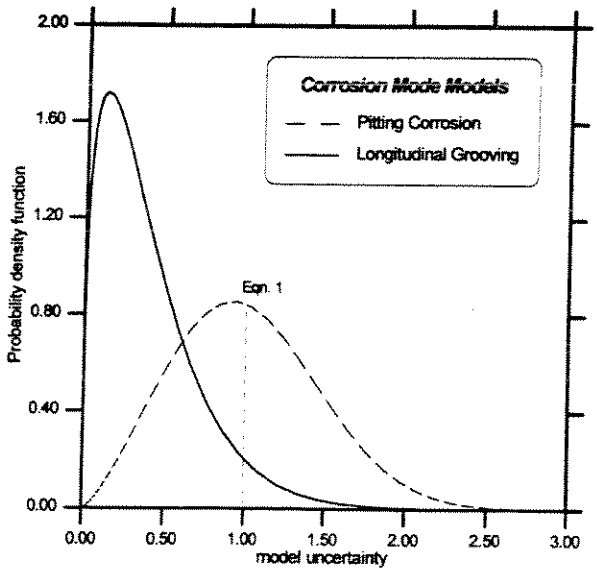

Figure 9-1 Assumed Model Uncertainty for Shell Formula at T=60^{0}C, P_{co2}=2 bar described as Probability Distribution for V_{corr}(real)/V_{corr}(Pred.) (From Fig.2 of Sydberger et al 1995)

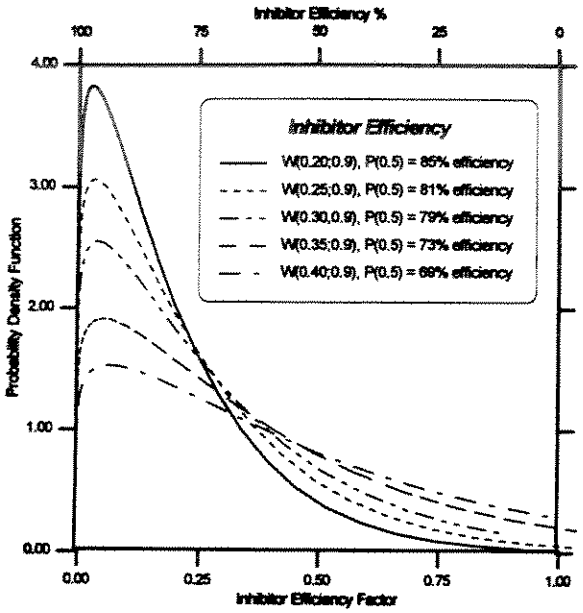

Figure 9-2 Probability Distributions for the 5 Cases of Inhibitor Efficiency(From Fig.3 of Sydberger et al 1995)

The predicted future growth of corrosion depth d_f is thus

$$d_f = V_{corr} \cdot t \cdot X_{\text{mod}} \cdot \eta \qquad (9.7)$$

2. Processed/Semi-Processed Oil

Stabilised crude oil, whether fully processed or semi-processed, will contain certain amounts of dispersed liquid water, and CO_2-corrosion may proceed. However, another relevant corrosion mechanism is bacterial corrosion, primarily by sulphate reducing bacteria (SRB). These may enter the pipeline via an upstream processing system.

CO_2-corrosion and bacterial corrosion may be controlled by injection of corrosion inhibitors and biocides respectively. However, such chemical treatment is normally to be combined with periodic cleaning by running special pigs through the pipeline. This is to remove various debris from the pipe wall which would otherwise retard the efficiency of such chemicals.

Bacterial corrosion as well as CO_2-corrosion in crude oil pipelines will occur as scattered shallow pits. Girth welds may become attacked preferentially.

Future corrosion prediction should preferably be based on inspection data. However, if the pipeline has been frequently cleaned by pigging, and these operations have confirmed that there

has been no separation of water in the pipeline, in-situ inspection may not be required. It is anticipated that the pigging program is continued during the extended life.

3. Processed (Dry) Gas

Processed gas (Export Gas) may be considered non-corrosive to CMn-steel pipelines provided that water has been removed so that the dew point is maintained well below the minimum operating temperature. However, liquid water or insufficiently dried gas may enter the pipeline due to processing up-sets or deliberate by-pass of the drying facilities. As the export gas will normally contain a significant amount of CO_2, corrosion damage may then occur.

Any corrosion attack will be confined to the "6 o'clock" position, as scattered shallow pits or grooves. Welds will be preferentially attacked. The corrosion during a period when liquid water persists may be estimated by means of the Shell formula mentioned above.

In case there are reasons to assume that a pipeline for dry gas has been operated under "wet" conditions for a significant period of time, then future corrosion prediction should be proceeded by an instrumented pigging to determine any corrosion damage.

4. Treated Seawater/Produced Water

Subsea pipelines for remove water injection are normally fabricated in CMn-steel linepipe as for hydrocarbon pipelines. Corrosion damage has been reported as circumferential grooving at girth welds and scattered pitting along the pipe. Pitting attack has been related to bacterial corrosion, while the circumferential girth weld corrosion may be caused by residual contents of oxygen or active chlorine. It has been suggested that the preferential weld corrosion is enhanced by galvanic interactions between the base material and weld metal/heat affected zone.

The potential corrosivity of any produced water for re-injection can be assessed by means of the Shell formula, provided that CO_2-content of the water is re-calculated to the equilibrium partial pressure of CO_2 in a hypothetic gas phase. The corrosion in treated seawater due to bacterial corrosion is not suitable for quantitative mathematical modelling.

In the case of corrosion due to residual contents of oxygen or active chlorine, corrosion under full mass transfer control can be calculated quantitatively if corrosion had occurred as uniform attack. However, practical experience show that corrosion damage will occur as preferential weld corrosion, probably due to galvanic effects. There are no models available for a quantitative description of such corrosion.

9.5 Reliability-based Calibration of Safety Factors

In the following, a calibration study is presented to illustrate an application of structural reliability methods.

Level of the reliability methods refers to the extent of information about the structural reliability problem that is provided and used. According to DNV Classification Note No.30.6 (DNV 1992), the levels of reliability methods are defined as:

- Level 1 methods are deterministic reliability methods that use only one "characteristic" value to describe each uncertain variable., e.g. LRFD format.
- Level 2 methods are reliability methods that use two values to describe each uncertain variables, i.e., its mean and variance, supplemented with a measure of correlation between the variables, usually the covariance, e.g. the first-order and second-moment method.
- Level 3 methods are reliability methods which use the joint probability distribution of all the uncertain variables to describe these variables, e.g FORM/SORM and Monte Carlo simulations.
- Level 4 methods are reliability methods that compare a structural prospect with a reference prospect according to the principles of engineering economic analysis under uncertainty, e.g. a decision analysis considering cost and benefits of construction, maintenance, repair, and consequences of failure.

9.5.1 Failure Probability Computation

A limit state function is defined such that it has a positive value when a pipeline is safe with respect to the failure mode and that it has a negative value when the pipeline fails by this failure mode. An overline is associated with the vector **x** in the limit state function to indicate that the vector is a set of random variables (uncertain parameters) describing the limit state, and the failure probability is defined as

$$P_f = P(g(\bar{x}) \leq 0) \tag{9.8}$$

To compute this probability where exact integration is generally infeasible, the First and Second Reliability Method (FORM/SORM) implemented in the probability analysis program PROBAN (Tvedt 1993), may be applied.

Details of FORM/SORM are available from standard text book, e.g. Madsen et al (1986). The procedures are summarised as below:

(1) To define an analytical limit state function,

(2) To evaluate uncertainty measures for the random variables involved in the limit state function, using probabilistic distributions,

(3) To transform the basic random variables into a vector of independent standard normal variables,

(4) To approximate the limit state function in the transformed space into a hyperplane (FORM), or a hyper-paraboloid (SORM),

(5) To compute the failure probability P_f corresponding to the approximate failure surfaces by finding the point in the failure set with the largest probability density (FORM) and also accounting for the limit state surface curvature at this point (SORM).

The reliability index β is related to the failure probability P_f by

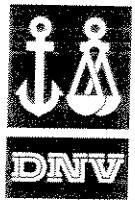

$$\beta = -\Phi^{-1}(P_f) \tag{9.9}$$

where $\Phi(\ )$ is the standard normal distribution function.

9.5.2 Procedure for Calibration of Partial Safety Factors

The objective is to use the results of the above Level 3 reliability analysis to develop a load and resistance factored design (LRFD) equation where bursting is taken as the failure criterion. This includes the following items:

- Specification of a target safety level.
- Specification of characteristic values for the variables.
- Calculation of Partial Safety Factors.
- Performing a safety check, formulated as a design equation, utilising the characteristic values and partial safety factors.

Such a design code equation is often referred to as a Level 1 reliability method.

The values of the partial safety factors must be calibrated to ensure that a design based on the design equation satisfies the safety level in terms of a considered target probability of failure.

The partial safety factors should be calibrated covering most of the design (operation) scenario as below:

- Formulation of limit state function based on the proposed design criterion
- Specification of characteristic values for the deterministic variables.
- Specification of the random variables including, characteristic value, mean value, COV and distribution type.
- Performing a reliability analysis, to obtain annual failure probability corresponding to each assumed set of partial safety factors for the design scenario considered, which cover most of the practical design cases.
- Evaluation of the partial safety factors corresponding to the target annual probability of failure.

9.5.3 Target Reliability

When dealing with reliability analysis of structural systems, an appropriate safety level in a given reference time period and for a given reference length of the pipeline should be selected; referred to as a target reliability level. The target reliability level should be evaluated based on information about the safety level implied by past and present rules and compared with historical data on reported failure. The comparison shall be done with due considerations to the fact that the observed failure rates include gross errors and the structural reliability does not. Furthermore, it should be related to the consequences of failure and failure type as well as the effect of inspection and repair. For pipeline operation, the target reliability is dependent of many factors e.g.:

- Consequence of failure
- Pipeline location
- Pipeline contents

The target safety level for dented and corroded pipeline should be defined in the same level as undamaged pipeline. The target safety level to be applied to the refined criteria need to be evaluated considering the implied safety level in the existing criteria. However, in the present calibration, an annual target reliability of 10^{-4} (safety index β=3.71), is adopted according to DNV classification notes (DNV 1992).

In general it is recommended that the reference length refer to the entire pipeline length. This requires consideration of the correlation from load, capacity and model uncertainties between individual failure element. At present, only one failure element is considered corresponding to full correlation.

In this study, an annual value of reliability is applied in the assessment of target reliability and reliability calculations.

9.5.4 Design Equation and Limit State Function

For the sake of simplicity only internal pressure is considered. The partial safety factor approach leads to

$$P_c \geq \gamma \; P_l \tag{9.10}$$

where P_c = Characteristic strength of the pipe according to a criterion
P_l = Characteristic load (internal pressure)
$\gamma = \gamma_l \gamma_m$ which may be referred to as an overall (partial) safety factor. γ is equivalent to the factor of safety F.S or the inverse of usage factor η.

A model uncertainty parameter X_M is introduced to reflect the confidence in the criterion for prediction of burst strength:

$$X_M = \frac{true\ burst\ strength}{predicted\ burst\ strength} \tag{9.11}$$

Normalised random variables are defined as

$$X_P = \frac{P_l}{2SMTS} \tag{9.12}$$

$$X_f = \frac{\sigma_{flow}}{SMTS} \tag{9.13}$$

$$X_A = \frac{AREA}{AREA_0} \tag{9.14}$$

$$X_L = \frac{L^2}{Dt} \tag{9.15}$$

$$X_t = \frac{t}{D} \tag{9.16}$$

The design equation for pipeline in operation, based on the proposed strength equation for longitudinal corrosion, is given by for $L^2/(Dt)<50$

$$\frac{1}{\gamma} X_{flow} X_t \frac{1 - X_A}{1 - (1 + 0.6275\, X_L - 0.003375\, X_L^2)^{-1/2} X_A} - X_P \geq 0 \tag{9.17}$$

and for $L^2/(Dt)>50$

$$\frac{1}{\gamma} X_{flow} X_t \frac{1 - X_A}{1 - (0.032\, X_L + 3.3)^{-1} X_A} - X_P \geq 0 \tag{9.18}$$

The limit state function is for $L^2/(Dt)<50$

$$g(\bar{x}) = X_M X_{flow} X_t \frac{1 - X_A}{1 - (1 + 0.6275\, X_L - 0.003375\, X_L^2)^{-1/2} X_A} - X_P \tag{9.19}$$

and for $L^2/(Dt)>50$

$$g(\bar{x}) = X_M X_{flow} X_t \frac{1 - X_A}{1 - (0.032\, X_L + 3.3)^{-1} X_A} - X_P \tag{9.20}$$

9.6 Uncertainty Measures

9.6.1 Uncertainty Modelling

Pipeline operation should be based on a rational treatment of the uncertainties in the loads, geometric and material parameters and models governing the structural collapse.

The probability distribution for a random variable represents the uncertainty of the variable. The results of a reliability analysis may be very sensitive to the tail behaviour of the probability distribution applies, implying that a proper procedure for the choice of distribution is required.

The process of establishing a probability distribution for a stochastic variable is:

(1) Collect experimental data (sample of measurement)

(2) Estimate sample statistics

The Method of Moment (MoM) can be applied to evaluate distribution parameters by assigning analytical moments to the sample moments. Usually estimates for the four moments estimators are applied as below:

the mean value

$$\mu = \frac{1}{n}\sum x_i \tag{9.21}$$

the standard deviation

$$\sigma^2 = \frac{1}{n-1}\sum (x_i - \mu)^2 \tag{9.22}$$

the coefficient of *skewness*

$$\delta = \left(\frac{n}{(n-1)(n-2)} \sum (x_i - \mu)^3 \right) / \sigma^3 \tag{9.23}$$

the coefficient of *curtosis*

$$\kappa = \left(\frac{n^2 - 2n + 3}{(n-1)(n-2)(n-3)} \sum (x_i - \mu)^4 + 3\sigma^4 \frac{(2n-3)(n-1)}{n(n-2)(n-3)} \right) / \sigma^4 \tag{9.24}$$

where n is the number of observations.

(3) Chose Distribution Models

Some of the distribution used in this report are:

Hermite Model

The Hermite distribution model is based on the four lowest statistical moments. It may e.g. be used with care to model weakly non-normal behaviour, see Winterstein (1988).

Gumbel Distribution

The Gumbel distribution is called the type I asymptotic distribution of the largest extreme used to model extreme values of variables which have initial distributions of the exponential type, see Madsen et al (1986).

Normal Distribution

The normal distribution is due to the central limit theorem widely used to describe linear physical phenomena as well as additive independent errors.

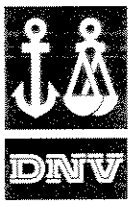

Lognormal Distribution
The lognormal distribution is one of the most widely used distributions to model resistance variables where the information is limited.

Mean value, coefficient of variation are specified for the chosen distribution parameters.

(4) Verify Fitted Distribution Parameters

A verification may be performed by plotting both the empirical and the fitted distribution function in a quantile plot or in a plot constructed so that the fitted model appear as a straight line.

9.6.2 Model Uncertainty

For a small amount of data available, the distribution parameter estimates can be uncertain themselves. This is called statistical uncertainty of the probabilistic distribution parameter. The statistical uncertainty is a function of the type of distribution fitted, the type of estimation technique applied, the value of the distribution parameters and the amount of underlying data.

A measure of the statistical uncertainty is established using simulation techniques (bootstrapping) (Efron and Tibshirani 1986) by use of the maximum likelihood method, linear least square regression, as below.

1. A set of parameter values is determined by fitting to the set of n test results by the Method of Moment (MoM).
2. These parameter values, and samples of n outcomes of the parent parameter values, and samples of n outcomes of the parent probabilistic distributions are generated.
3. For each sample, new parameter sets are estimated by MoM. The statistics of the sets of parameter values can then be established.
4. The resulting distribution including statistical uncertainty is then finally obtained from simulation.
5. A Hermite model (Winterstein 1988) is applied using the simulated 4 lower moments. A Hermite model with the 4 lower moments equal to 1.07, 0.19, 0.46, 3.0 respectively is applied for the model uncertainty. The mean bias, COV, skewness and curtosis for the Hermite model are estimated.

9.6.3 Load Uncertainty

The characteristic value of the normalised operating pressure X_P is obtained by substituting safety factors, characteristic values of the other parameters into the design equation.

In general, the annual maximum operating pressure is higher than the nominal operating pressure.

9.6.4 Parameter Uncertainties for Flow Stress to SMTS Ratio

In general flow stress σ_{flow} is approximately ultimate tensile strength of the material σ_u as discussed previously in this report. The ultimate tensile strength is defined as the stress at which the material loses its ultimate load-bearing capacity. The Specified Minimum Tensile Strength (SMTS) is defined as a statistical minimum of the ultimate tensile strength. The value of σ_u/SMTS is largely dependent of the steel grade and influenced by the pipe maker.

A random variable X_{flow} is defined as follow

$$X_f = \frac{\sigma_{flow}}{SMTS} = \frac{\sigma_u}{SMTS} \tag{9.25}$$

Uncertainty in X_{flow} is actually dependent of the material grade (SMYS or SMTS), pipe producer.

In the present project, a mean value, COV and distribution function are obtained from the experimental database in Appendix A.

In burst strength assessment within engineering re-qualification projects, material properties in longitudinal direction are usually used. Actually bursting of longitudinally corroded pipes is hoop collapse.

9.6.5 Parameter Uncertainties for Pipe t/D

The diameter D is considered as a deterministic parameter. The wall-thickness is assumed a normal variable with small COV.

9.6.6 Parameter Uncertainties for Corrosion Depth, Length and Area

In an assessment of existing corroded pipe, the remaining strength of the corroded pipe at the time being inspected is estimated considering the accuracy of the inspection tools. However, the residual strength criteria are also applied for the determination of the residual strength of the pipe in the future, until the end of its design/redesigned life limit. Therefore when parameter uncertainties are considered for corrosion depth, length and area, the conservatism introduced in pit separation, the inspection and future corrosion prediction should be taken into account.

Normalised Defect depth X_d
The normalised defect depth X_d is defined as

$$X_d = d / t \tag{9.26}$$

The normalised defect depth X_d is influenced by:

(1) Pit separation criterion

Pit separation criterion is normally conservative. The strengthen effect of the pipe wall between separated pits should be taken into account.

(2) Inspection Tools

As discussed in Section 9.3, the accuracy of inspection tools varies. When 2nd generation MFL pig is used, the accuracy is +/- 0.1T-0.2T. The accuracy is +/-0.5 - 1.0 mm for US pigs and EC pigs is even more accurate.

A "conservative estimates" based on inspection tools is the reported value from inspection plus 10% of nominal wall thickness. When no corrosion is reported, the pipeline is still assumed to contain corrosion up to 20% and 10% of nominal wall thickness with pitting corrosion and general corrosion, for longitudinal corrosion and girth weld corrosion respectively.

In the reliability calibration, the accuracy of the pit-depth measurement is given as 0.1t in which t is the nominal wall-thickness.

(3) Future Corrosion prediction

The accuracy of future corrosion prediction based on a combined use of previous inspected corrosion growth and Shell formula, can be good and the corrosion depth is conservatively over-estimated.

The potential corrosiveness of any water may be estimated from the operational temperature and the CO_2-content using the Shell formula. However, the formula should be calibrated against the recent inspection results.

"Extrapolated corrosion rate" refer to the same "conservative estimates" divided by the time of service from the first year of operation to the year of last inspection. Hence, the "extrapolated corrosion rate" and the calculated corrosion damage at some future time do not take into account any changes in operational parameters affecting fluid corrosivity. This may render a too pessimistic prediction of remaining life; i.e. if much of the damage has occurred during an initial period with poor operational control. Even when no corrosion was reported from inspection, maximum corrosion rates calculated based on the assumed detection limits of the equipment may give quite high accumulated corrosion damage when extrapolated 20-30 years.

The uncertainty in the corrosion depth prediction is the combination of the uncertainties associated with pit separation, inspection tools and future corrosion.

Normalised Defect Area X_A

The normalised defect area X_A is the ratio of metal loss area and its original area. Two kinds of inaccuracy are possible:

inaccuracy due to the calculation method for the area of metal loss: Traditionally, only one integration point is used and the area is calculated as the product of the maximum depth and corrosion length as the B31G criterion. Error due to insufficient knowledge of pits interaction does also belong to this type of inaccuracy.

inaccuracy due to use of measurement instruments: Extensive integration points may be used to measure the area. However, since the shape of corroded area is complex, and it is difficult to measure internal corrosion, there is certain error in the measurement of the depth of metal loss at individual integration points.

Similar to the discussions on corrosion depth, the uncertainty in the corroded area prediction is the combination of the uncertainties associated with pit separation, calculation of area, inspection tools and future corrosion. A lognormal distribution is thus assumed for X_A, and the mean value and COV are taken as 0.8 and 8% respectively.

Normalised Defect Length X_L

Both short corrosion and long corrosion are considered. Typical values of the normalised defect length X_L covering short corrosion and long corrosion are 10 and 200 respectively. The correlation coefficient ρ for defect area X_A and defect length X_L is taken as 0.80.

Similar to the discussions on corrosion depth, the uncertainty in the corroded area prediction is the combination of the uncertainties associated with pit separation, inspection tools and future corrosion. However, corrosion length is more easy to measure because of its large amount comparing to depth.

According to "Inspection Performance Specification - Feature Definition and Sizing Capability" of the British Gas pigs, the axial length of the rectangle can be measured to an accuracy of +50 mm and -20 mm of stated size.

Normal distribution is thus assumed for X_L, and the mean value and COV are taken as 0.9 and 5% respectively.

9.7 Implied Safety Level in the B31G Criterion

Reliability methods is applied to estimate the implied safety level of the ANSI/ASME B31G criterion. This is to use the B31G criterion as design equation, instead of the proposed design equation. This leads to calculating the mean value of the operating pressure using the B31G criterion instead of the proposed criterion. The limit states formulation are same for both the B31G and the proposed criterion.

The design equation for pipeline in operation, based on the B31G criterion, is given by for $L^2/(Dt)<20$

$$0.72\frac{1.1SMYS}{SMTS}X_t\frac{1-\frac{2}{3}X_d}{1-(1+0.79745\,X_L)^{1/2}\frac{2}{3}X_d}-X_P\geq 0 \qquad \textbf{(9.27)}$$

and for $L^2/(Dt)>20$

$$0.72\frac{1.1SMYS}{SMTS}X_t(1-X_d)-X_P\geq 0 \qquad \textbf{(9.28)}$$

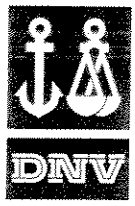

10 APPLICATIONS OF THE PROPOSED CRITERIA

Probabilistic assessment procedures need to be developed for pipeline operation, inspection and maintenance, since there are large uncertainties in the strength modelling, degradation estimation, inspection and measurement of damages (DNV 1994).

In this chapter, possible applications of the proposed criterion are discussed on the basis of deterministic analysis. Preliminary concept of probabilistic assessment is also given for information. A more extensive uncertainty modelling for the reliability analysis could be carried out in further study on this subject.

10.1 Decision of Operating Pressure, Repair and Replacement

Decision of operating pressure need to be made in many cases. For instance,

- If heavy corrosion occurs, the operating pressure need to be reduced.
- If there is a need for increased transportation capacity, the operating pressure of an in-service pipeline need to be uprated.
- If the planned service life of a pipeline is extended.

The operating pressure need to be determined considering possible damages and the integrity of pipes and connections over the whole length of the system.

Repair of the damages could be costly because repair methods require shut down periods and removal or replacement of a complete section of the pipe. For example, corrosion in the Trans Alaskan pipeline cost $ 1.5 billion to repair (Keen 1990). Replacing an existing pipeline is even more expensive. The Forties oil pipeline in the UK North Sea had to be replaced at a cost of $265 million because of weld corrosion caused by the presence of water in the oil (London 1991). There are therefore considerable economic incentives to continue operation of corroded pipe, provided an acceptable safety level is maintained.

One of the application of the proposed criterion is to be applied by operators, particularly field personnel, for making decisions on existing pipelines, when exposed for any purpose, as to whether any corroded region may be left in service or whether it needs to be repaired or replaced.

If it is necessary to uprate an in-service pipeline, existing standards require hydrostatic re-testing as the basis for demonstrating that the pipeline contains no damages which could fail at the operating pressure. However, hydrostatic re-testing could be costly, because it will interrupt transportation of oil and gas. It is difficult and time-consuming to locate and repair small leaks which occur during the test. While critical defects and possibly near-to critical defects may be burst out, sub-critical defects could not be detected and may grow due to highly applied pressure load (depending on testing procedure, test pressure and holding time).

An alternative method is to base the decision on an on-line inspection to obtain information on the damages in the pipeline followed by burst strength assessment using criteria and/or finite

element methods. Condition monitoring of existing pipeline by the on-line instrumented pigs has been applied by industry. However, consideration should be given to e.g.:

- the types of defects which can be detected and
- the quality for the possible inspection techniques.

Probabilistic methods could be applied for making decision on operating pressure. To develop the probabilistic methods, some work need to be done further, for instance,

- To evaluate the performance of the on-line instrumented pigs, for estimating the uncertainties associated with damage inspection, including detection of critical sections and measurement accuracy.
- To establish limit-states of dented and corroded pipe, including both formulae and their model uncertainty assessment.
- To calculate operating pressure using structural reliability methods.

10.2 Life Time Extension and Re-qualification of Ageing Pipelines

Many pipelines are about to reach the end of its design lifetime. At the same time, new technology has made it financially acceptable to take out more oil and gas from the reservoirs than first assumed in the design phase. In addition, new technology has been developed in the course of the pipeline's lifetime, and in certain cases this has revealed an unnecessarily conservative design.

Design conditions might need to be changed.

In these cases, reassessment (analysis of existing pipelines) or re-qualification (re-evaluation of suitability) is necessary. This is in order to assure the pipeline owner, operator and regulator that the authorities' safety criteria are satisfied and the pipeline does fit for its intended purpose.

When reliable information is available on all damage type, size and locations, i.e. through inspection, the re-qualification problem is simply: *Which action should be taken ?* - (1) To maintain operating condition, or (2) to reduce operating pressure, or (3) to repair/replace the pipeline ?

For reliability-based re-qualification, research is needed to estimate uncertainties associated with damage inspection and measurement, and model uncertainty of the criteria for estimating damages and capacity.

For estimating operating pressure and re-qualification of existing pipeline after damage, several levels of analyses of increasing detail and difficulty could be applied:

- Level 1: To use criteria for strength and loads available from rules or technical reports.
- Level 2: To apply a non-linear numerical procedure and conduct laboratory tests which accurately predicts strength and loads, *or* perform a hydrostatic re-testing.
- Level 3: Probabilistic design for a specific case accounting for uncertainties in loads, damage inspection and measurement and strength modelling.
- Level 4: To make optimum decisions based on balanced risks and costs.

Note that this classification of levels of re-qualification is similar to the levels of reliability methods outlined in Chapter 9.5.

In general, Level 1 procedure could be quite simple and reasonably accurate, if the criteria applied are updated based on latest knowledge and calibrated using reliability methods. The safety factors associated with Level 2 procedure could be smaller than those applied in Level 1 procedure, and can be obtained from Level 2 structural reliability analysis. When Level 3 procedure is applied, the target reliability level and uncertainty measures could be different comparing with those assumed in the rules (used in Level 1) and the specific safety factor could be obtained for the specific design case. In Level 4 procedure, economic consequences have been taken into account.

A method for making optimum decisions based on balancing risks and costs will rationalise decision-making for the re-qualification of existing pipelines. Costs connected with bad decisions can have extremely important long term consequences, for example through additional inspections, increased maintenance and repairs. Existing methods developed at DNV for other constructions (ships and platforms) could be applied for pipeline and give answers to questions like:

- How to use the results of a reliability analysis to quantify the safety of a damaged pipeline ?
- What level of safety should be used in the re-qualification process ?
- How can the demands of economy and safety be balanced in a re-qualification process ?
- How can rational decisions, based on evaluation of design costs, operational costs, maintenance policy and results from inspections, be made and defended at a later date ?
- How can expert evaluation be included in decisions based on reliability analysis of the pipeline's integrity ?

10.3 Assessment of Corrosion Allowance and Wall-thickness

North Sea pipelines are typically large diameter (36-40"), long (250-1000km) and used for transporting gas. The pipeline diameter and length are such that materials may be 30 % of the total installation cost and each additional millimetre of wall-thickness 1 % of the total cost (Kvernvold et al 1992). Wall-thickness need to be rationally determined based on refined criteria for strength modelling and degradation estimation. An useful application of the proposed criterion for pipeline design is the assessment of wall-thickness

A common practice for wall-thickness assessment, is to carry out yielding check (DNV 1981)

$$\sigma_{yp} = \eta_h \sigma_F k_t \qquad \textbf{(10.1)}$$

where η_h = Usage factor
σ_{yp} = Permissible hoop stress
σ_F = Specified minimum yield stress
k_t = Temperature derating factor
For material temperature below 120^0C, k_t=1.0.

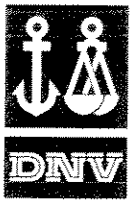

The proposed criterion could be applied for a more rational calibration of the usage factor η_h, together with criteria for dented and cracked pipeline. Calibration of the usage factor η_h is now carried out in SUPERB project. Their work can be improved if the criteria developed in the present project, are utilised instead of the existing criteria. The formulation used in calibration of safety factors for assessing strength of corroded pipeline, could be applied in the calibration of the usage factor η_h by only changing the design format to the yield check format.

The corrosion allowance wall-thickness is added to the value obtained from the yielding check.

Probabilistic methods could also be applied for the determination of the corrosion allowance wall-thickness, considering model uncertainties in the assessment of corrosion rate and burst strength. Since corrosion is an ageing pipeline problem, time-variant reliability methods could be applied to account for the degradation due to material loss.

When the design wall-thickness is less, the construction cost could be considerably reduced, for a long pipeline of several thousands kilo-metre length. However, this might imply that some years after installation the operating pressure will have to be lower (than desirable pressure) and repair cost will have to be higher (than thicker pipe). Decision of wall-thickness could be made based on optimisation of the total life-cycle cost.

11 REFERENCES

/1/ Andersen T.L. (1991):"Fracture Mechanics - Fundamentals and Applications," CRC Press.

/2/ Anderson T. L., Belloni A. and Willoughby A.A. (1988): "Plastic Collapse Analysis of Girth Weld repair Grooves in Pipe subjected to Offshore Laying Stresses," Int. J. Pres. Ves. & Piping, Vol. 31, pp.105-130.

/3/ Andrews R. M. (1992a): "The Effect of Corrosion on the Fracture and Fatigue Resistance of Welds in Pipelines," OMAE'92, Vol.V.A:Pipeline Technology, pp.195-202.

/4/ Andrews R. M. (1992b): "Pipeline Corrosion - Assessing the Damage," TWI Bulletin, Nov. & Dec. 1992 pp.124-126.

/5/ ANSI/ASME(1982): "B31.8, Code for Gas Transmission and Distribution Piping," American National Standards Institute and American Society of Mechanical Engineers, New York.

/6/ ASME(1993): "B31G, Manual for Determining the Remaining Strength of Corroded Pipelines, A Supplement to ASME B31 Code for Pressure Piping," American National Standards Institute and American Society of Mechanical Engineers, New York

/7/ API 1104 (1988): "Welding of Pipelines and Related Facilities," API 1104, 17th Ed., Sept. 1988.

/8/ ASME B&PV Code, Section VIII, Division I, Article UW-51, Radiographic Examination of Welded Joint; Appendix 4, Acceptance Standards for Radiographically Determined Rounded Indications in Welds; and Appendix 12, Ultrasonic Examination of Welds (UT).

/9/ Bai Y.(1989): "Load Carrying Capacity of Tubular Members in Offshore Structures,"Ph.D. Thesis, Hiroshima University, Hiroshima.

/10/ Bai Y., Igland R. and Moan T.(1993a): "Tube Collapse under Combined Pressure, Tension and Bending Loads," Int. J. of ISOPE, 3(2), pp.121-129.

/11/ Bai Y., Igland R. and Moan T.(1994a): "Ultimate Limit States of Pipes under Tension and Bending," Int. J. of ISOPE, 4(4), pp.312-319.

/12/ Bai Y., Skjolde M. and O. Astrup (1993b): "Residual Strength of Dented and Corroded Pipe, Project Report No.1, Finite Element Analysis Considering Ductile Fracture," DNV Report No.93-3531, Det Norske Veritas.

/13/ Bai Y., Moe E.T. and Mørk K.J.(1994b): "Probabilistic Assessment of Dented and Corroded Pipeline," Int. Conf. of ISOPE, Osaka, April 1994.

/14/ Batterman S.C.(1965) : "Plastic Buckling of Axially Compressed Cylindrical Shells," AIAA Journal, Vol.3, No.2, Jan. 1965.

/15/ Bjørnøy O. and Skjolde M. (1995): "Finite Element Analyses of Corroded Pipes," DNV Report No.95-3514, Det Norske Veritas.

/16/ British Gas Standard BGC/PS/P11: "Procedures for Inspection and Repair of Damaged Steel Pipelines,". Dec. 1983.

/17/ BS 4515: Specification for Field Welding of Carbon Steel Pipelines.

/18/ BSI (1991): "PD6493 - Guidance on Methods for Assessing the Acceptability of Flaws in Fusion Welded Structures," *Published Documents by British Standards Institute*.

/19/ Bubenik T.A., Olson R.J.. Stephens D.R. and Fransini R.B. (1992): "Analysing the Pressure Strength of Corroded Line Pipe," *OMAE'92, Vol.V(A): Pipeline Technology*, pp.225-231.

/20/ CAN/CSA (1986): "CAN/CSA-Z184-M86, Gas Pipeline Systems," *Canadian Standards Association*, 178 Rexdale Blvd, Rexdale, Ontario, Canada.

/21/ Centric (1995) : "Spectrum™ Solver, Solution Methods and Theory," *Manuals*, Centric Engineering Systems, Inc.

/22/ Chell, G.G. (1979) : "Elastic-plastic Fracture mechanics,"*Developments in Fracture Mechanics -1*, G.G. Chell Ed.

/23/ Chouchaoui B.A., Pick R.J. and Yost D.B. (1992): "Burst Pressure Predictions of Line Pipe Containing Single Corrosion Pits using the Finite Element Methods," *OMAE'92, Vol.V(A):Pipeline Technology*, pp.203-210.

/24/ Chouchaoui B.A. and Pick R.J. (1992a): "Residual Burst Strength of Pipe With Internal Corrosion Pits," *Proc. Int. Conf. on Pipeline Reliability, Calgary, June 1992*,II-8.

/25/ Chouchaoui B.A. and Pick R.J. (1992b): "Behaviour of Circumferentially Aligned Corrosion Pits," *Int. J. Pressure Vessels and Piping*, (Accepted).

/26/ Chouchaoui B.A. and Pick R.J. (1992c): "Behaviour of Longitudinally Aligned Corrosion Pits," *Int. J. Pressure Vessels and Piping*, (Accepted).

/27/ Chouchaoui B.A. and Pick R.J. (1993): "Interaction of Closely Spaced Corrosion Pits in Line Pipe," *OMAE'93, Vol.V:Pipeline Technology*, pp.203-214.

/28/ Clyne A.J. and Jones D.G. (1995): "The Integrity of Transmission Pipelines Containing Circumferential Girth Weld Defects," *To Be Presented At The Second International Conference on Pipeline Technology, Sept. 11th - 14th, 1995, Ostend, Belgium.*

/29/ Darlaston B.J.l. and Harrison R.P. (1977): "Ductile Failure of Thin Walled Pipes with Defects under Combinations of Internal Pressure and Bending," *3rd Int. Conf. on Pressure Vessel Technology,* Tokyo, Part II: Material and Fabrication, pp.669-676.

/30/ deWaard C. and Milliams D.E. (1975): *Corrosion 31, 5*, pp.177.

/31/ deWaard C., Milliams D.E. and Lotz U. (1991): *Corrosion 47, 12*, pp.976.

/32/ deWaard C. and Lotz U. (1993): "Prediction of CO_2 Corrosion of Carbon Steel," *Corrosion/93, Paper no. 69.*

/33/ DNV (1981): "Rules for Submarine Pipeline Systems 1981," Det Norske Veritas.

/34/ DNV (1992):"Structural Reliability Methods,"*Classification Notes No.30.6*, Det Norske Veritas.

/35/ DNVI (1994): "Reliability of Corroded Pipelines" A Proposal for Joint Industry Research Project, July 1994.

/36/ DNVS (1993): "PROFRAC - Fracture Mechanics Reliability Assessment of Welded Structures," *DNV Report 93-2049.*

/37/ Efron B and Tibshirani R (1986): "Bootstrap Method for Standard Error Confidence Intervals and Other Measures of Statistic Accuracy," *Statistical Sci.*, 1, pp.54-73.

/38/ Eiber R., Maxfy W.A., Duffey A.R. and Atterbury T.J. (1971) "Investigation of the Initiation and Extent of Ductile Pipe Rupture," *BMI-1908, Battelle Memorial Institute*, June 1971.

/39/ Ellinas C.P. and Williams K.A.J. (1989): "Reliability Engineering Techniques in Subsea Pipeline Design," *OMAE'89*, pp.335-346.

/40/ Faulkner D., Guedes Soares C. and Warwick D.M. (1987): "Modelling Requirements for Structural Design and Assessment," *Integrity of Offshore Structures-3*, Edited by Faulkner et al, Elsevier Applied Science, pp.25-54.

/41/ Folias E.S.(1964):"The Stresses in a Cylindrical Shell Containing an Axial Crack,"ARL 64-174, *Aerospace Research Laboratories*, October 1964, see also Folias E.S. (1965): "An Axial Crack in a Pressurelized Cylindrical Shell," *Int. J. of Fracture Mechanics*, Vol.1 (1), pp.104-113(1965).

/42/ Fu and Jones (1994): "Failure of Spiral Corrosion in Linepipe," *OMAE'94*, Vol.V, Pipeline Technology, pp.1-8.

/43/ Galambos T.V. (1988): "Guide to Stability Design Criteria for Metal Structures, "(written by the Structural Stability Research Council) *John Wiley & Sons, Inc.* pp.502-508.

/44/ Gellin S.(1980):"The Plastic Buckling of Long Cylindrical Shells under Pure Bending," *Int. J. Solids and Structures*, Vol.16, pp.397-407.

/45/ Gerard G. (1962): *Introduction to Structural Stability Theory*, McGraw-Hill International Book Company, New York.

/46/ Glover A.G. (1992): "Assessment of Pipeline Girth Welds Subjected to High Longitudinal Strain," OMAE'92, Vol.V-B, Pipeline Technology, pp.591-596.

/47/ Hahn G.T., Sarrate M. and Rosenfield A.R., (1969): Int. J. of Fracture Mechanics, Vol.5, pp.187-210.

/48/ Hopkins P. and Jones D.G. (1992): "A Study of the Behaviour of Long and Complex-shaped Corrosion in Transmission Pipelines," OMAE'92, Vol.V.A:Pipeline Technology,211-217.

/49/ Jones D.G., Turner T. and Ritchie D. (1992): "Failure Behaviour of Internally Corroded Linepipe," OMAE'92, Vol.V.A:Pipeline Technology, pp.219-224.

/50/ Karlsen, A.(1974): "Influence of Weld Defect on Low Cycle High Strength Fatigue Properties of Weld in Offshore Structures," DNV Report 84-5074-4, Nov. 1974.

/51/ Kastner E., Roehrich E., Schmitt W. and Steinbuch E. (1981): "Critical Crack Sizes in Ductile Piping," Int. J. Pres. Ves. and Piping, Vol.9, pp.197-219

/52/ Keen J. (1990): "Corrosion Forces Repairs to Oil Pipeline," USA Today, 5 Feb. 1990.

/53/ Kiefner J.F. (1969): "Fracture Initiation," in the 4th Symposium on Line Pipe Research, paper G, American Gas Association Catalogue No. L30075 (Nov. 18, 1969).

/54/ Kiefner J.F. and Duffy A.R. (1971): "Summary of Research to Determine the Strength of Corroded Areas in Line Pipe,"Presented to a Public Hearing at the U.S. Department of Transportation, July 20, 1971.

/55/ Kiefner J.F., Maxey W.A., Eiber R.JH. and Duffy A.R. (1973):"Failure Stress Levels of Flaws in Pressurized Cylinders,"Progress in Flaw Growth and Fracture Toughness Tests, ASTM STP 536s, American Society for Testing and Materials, pp.461-481.

/56/ Kiefner J.F. (1974):"Corroded Pipe: Strength and repair Methods," 5th Symposium on Line Pipe Research,Pipeline Research Committee of AGA (American Gas Association), Nov.20-22.

/57/ Kiefner J.F. and Vieth P.H. (1989):"A Modified Criterion for Evaluating the Remaining Strength of Corroded Pipe, RSTRENG" Project PR 3-805 Pipeline Research Committee, American Gas Association, Dec. 22, 1989.

/58/ Kiefner J.F. and Vieth P.H. (1990a): "New Method Corrects Criterion for Evaluating Corroded Pipe," Oil & Gas Journal, Aug.6, 1990.

/59/ Kiefner J.F. and Vieth P.H. (1990b): "PC Program Speeds new Criterion for Evaluating Corroded Pipe," Oil & Gas Journal, Aug.20, 1990.

/60/ Kiefner J.F. and Vieth P.H. (1993): "RSTRENG2 User's Manual" Project PR 218-9205 Pipeline Research Committee, American Gas Association, March 1993.

/61/ Kim H.O. (1992) "Plastic Buckling of Pipes under Bending and Internal Pressure," ISOPE'92, Vol.2, pp.46-51.

/62/ Klever F.J. (1992): "Burst Strength of Corroded Pipe: 'Flow Stress' Revisited," OTC7029, Proc. of Offshore Technology Conference, May 1992.

/63/ Klever F.J., Stewart G. and van der Valk A.C. (1995): "New Development in Burst Strength Predictions for Locally Corroded Pipelines," OMAE'95, Vol.V-B: Pipeline Technology.

/64/ Kvernvold O., Johnson R. and Helgerson T. (1992): "Assessment of Internal Pipeline Corrosion," OMAE'92, Vol.V-B: Pipeline Technology, pp.409-420.

/65/ Kyriakides, S. and Ju G.T. (1992): "Bifurcation and Localization Instabilities in Cylindrical Shells under Bending-I. Experiments," Int. J. Solids and Struc., Vol.29(9), pp.1117-1142.

/66/ London C.J., (1991): "The Forties Export Pipeline Project," Pipes and Pipelines International, May - June 1991, pp.7-13.

/67/ Maxey W.A., Kiefner J.F., Eiber R.J. and Duffy A.R. (1971): "Ductile Fracture Initiation, Propagation and Arrest in Cylindrical Vessels," Fracture Toughness, Proceedings of the 1971 National Symposium on Fracture Mechanics, Part II, ASTM STP 514, American Society for Testing and Materials, pp.70-81

/68/ Madsen, H.O., Krenk S. and Lind N.C. (1986): "Methods of Structural Safety," Prentice-Hall Inc., Englewood Cliffs, N.J.

/69/ Mandke J.S. (1990): "Corrosion Causes Most Pipeline Failure in Gulf of Mexico," Oil and Gas Journal, Oct. 29, 1990.

/70/ Miller A.G. (1985): "The Fracture of Cylinders with Defects under Bending and Combined Bending and Pressure," CEGB Report, TPRD/B/0725/N85.

/71/ Miller A.G. (1988): "Review of Limit Loads of Structures Containing Defects," Int. J. Pres. Ves. & Piping, **32**, pp.197-327.

/72/ Mok D.H.B., Pick R.J. and Glover A.G. (1990): "Behaviour of Line Pipe with Long External Corrosion,"Mat. Performance, 29(5), 75-79.

/73/ Mok D.H.B., Pick R.J., Glover A.G. and Hoff R. (1991): "Bursting of Line Pipe with Long External Corrosion,"Int. J. Pressure Vessel & Piping, 46, 159-216.

/74/ Morgan D. (1993): "Upgrading Russia's 140,000 km of Gas Pipeline," DNV Forum, Aut. 1993.

/75/ Newman J. and Raju I. (1981): "An Empirical Stress-Intensity Factor for the Surface Crack," Engineering Fracture Mechanics, 22(6), pp.185-192.

/76/ Petersen R.E. (1974): "Stress Concentration Factors," Wiley, New York.

/77/ Popelar C.H. (1993): "A Plane Strain Analysis Model for Corroded Pipelines,"OMAE'93, Vol.V: Pipeline Technology, pp.281-288.

/78/ Ramberg-Osgood (1943): "Description of Stress-Strain Curves by Three Parameters," NACA TN 902.

/79/ Reddy B.D.(1979): "An Experimental Study of the Plastic Buckling of Circular Cylinders in Pure Bending," Int. J. Solids and Strct., Vol.15, pp.669-683.

/80/ Schulze H.D., Togler G. and Bodmann E. (1980): "Fracture Mechanics Analysis on the Initiation and Propogation of Circumferential and Longitudinal Defects in Straight Pipes and Pipe Bends," Nuclear Engineering and Design, Vol.58, pp.19-31.

/81/ Shannon (1974): "The Failure Behaviour of Linepipe Defects," Int. J. Press Ves. & Piping, pp.243-255.

/82/ Sotberg T. and Leira B.J. (1994): "Reliability-based Pipeline Design and Code Calibration," OMAE'94, Vol.V:Pipeline Technology, pp.177-188.

/83/ Stewart G., Klever F. and Ritchie D. (1994): "An Analytical Model to Predict the Burst Capacity of Pipelines," OMAE'94, Vol.V:Pipeline Technology, pp.177-188.

/84/ Sydberger T., Edwards J.D. and Mørk K.J. (1995): "A Probabilistic Approach to Prediction of CO_2-Corrosion, and Its Application to Life Cycle Cost Analyses of Oil and Gas Equipment," Corrosion 95, Paper no.65.

/85/ Tvedt L (1993): "PROBAN Version 4, Theory Manual" DNV Report 93-2056, Det Norske Veritas Research AS, Høvik, Norway.

/86/ Verley R. (1994), letter dated 24 May 1994.

/87/ Wang Y.S. (1991): "An Elastic Limit Criterion for the Remaining Strength of Corroded Pipes," OMAE'91, Vol.V:Pipeline Technology, pp.179-186.

/88/ Watanabe M., Mukai Y., Kaga S. and Fujihara S. (1977): "Mechanical Behaviour on Bursting of Longitudinally and Circumferentially Notched AISI 304 Stainless Steel Pipes by Hydraulic and Explosion Tests," 3rd Int. Conf. on Pressure Vessel Technology, Tokyo, Part II: Material and Fabrication, pp.677-683.

/89/ Wilkowski G.M. and Eiber R.J. (1981): "Evaluation of Tensile Failure of Girth Weld Repair Grooves in Pipe subjected to Offshore Laying Stresses," J. Energy Resources Technology, **103,** pp.48-55.

/90/ Wiloughby A.A. (1982): "A Survey of Plastic Collapse Solutions used in the Failure Assessment of Part Wall Defects," Welding Institute Report 191/1982.

/91/ Winterstein SR (1988): "Nonlinear Vibration Models for Extremes and Fatigue," J. of Engng Mech., ASCE, 114(10), pp.1772-1790.

/92/ Yoosef-Ghodsi N., Kulak G.L. and Murray D.W. (1995): "Some Test Results for Wrinkling of Girth-Welded Line Pipe," OMAE'95, Vol.V:Pipeline Technology, pp.379-387.

12 APPENDIX A EXPERIMENTAL DATABASES - TABLES

Table A-1 **Experimental Databases for Longitudinally Corroded Pipes under Internal Pressure**

Test No. 1 - No. 86: **AGA Database (U.S. Units)**
Test No. 87 - No. 106: **NOVA (Mok et al) Tests (SI Units)**
Test No. 107 - No. 124: **British Gas Tests (SI Units)**
Test No. 125 - No. 151: **U. Waterloo Tests (SI Units)**

Column 1: Test No.
Column 2: Out-Diameter
Column 3: Wall-thickness
Column 4: SMYS
Column 5: SMTS
Column 6: Yield stress σ_y
Column 7: Ultimate stress σ_u
Column 8: Ultimate strain ε_u
Column 9: Defect length L (projected length for spiral corrosion)
Column 10: Defect depth d
Column 11: Defect area A
Column 12: Defect width W
Column 13: Spiral angle
Column 14: Burst pressure P_b
Column 15: Source of the information
Column 16: Reference Name in the original source
Column 17: d/t
Column 18: $L^2/(Dt)$
Column 19: D/t

APPENDIX A EXPERIMENTAL DATABASES - TABLES

No	Dia	t	SMYS	SMTS	σ(y)	σ(u)	ε(u)	L	d	A	W	Angle	Pb	Source	Ref.	d/t	L^2/Dt	D/t
[-]	[mm]	[mm]	MPa	MPa	MPa	MPa	[-]	[mm]	[mm]	[mm^2]	[mm]	[deg]	[MPa]			[-]	[-]	[-]
1	762.0	9.40	359	471	405	na	na	64	3.71	150	na	90	11.19	Aga	1	0.39	0.56	81
2	762.0	9.40	359	471	405	na	na	57	3.71	141	na	90	11.17	Aga	2	0.39	0.46	81
3	762.0	9.40	359	471	405	na	na	108	3.99	188	na	90	11.72	Aga	3	0.42	1.63	81
4	762.0	9.53	359	471	440	na	na	140	6.10	305	na	90	11.52	Aga	4	0.64	2.69	80
5	762.0	9.53	359	471	406	na	na	121	5.31	390	na	90	10.52	Aga	5	0.56	2.01	80
6	609.6	9.27	241	350	279	na	na	76	6.88	375	na	90	7.59	Aga	6	0.74	1.03	66
7	609.6	9.27	241	350	279	na	na	121	6.38	521	na	90	8.03	Aga	7	0.69	2.58	66
8	609.6	9.27	241	350	279	na	na	133	6.38	606	na	90	8.41	Aga	8	0.69	3.15	66
9	609.6	9.40	241	350	288	na	na	44	6.63	165	na	90	7.17	Aga	9	0.71	0.34	65
10	609.6	9.53	241	350	288	na	na	108	7.16	459	na	90	8.03	Aga	10	0.75	2.01	64
11	609.6	9.27	241	350	288	na	na	51	6.63	194	na	90	7.03	Aga	11	0.72	0.46	66
12	609.6	9.27	241	350	288	na	na	57	5.56	185	na	90	8.38	Aga	12	0.60	0.58	66
13	609.6	9.27	241	350	288	na	na	64	5.84	231	na	90	9.10	Aga	13	0.63	0.71	66
14	609.6	9.27	241	350	288	na	na	70	6.63	290	na	90	9.10	Aga	14	0.72	0.86	66
15	609.6	9.65	241	350	288	na	na	95	6.38	350	na	90	9.21	Aga	15	0.66	1.54	63
16	609.6	9.40	241	350	288	na	na	51	4.78	150	na	90	9.31	Aga	16	0.51	0.45	65
17	609.6	9.40	241	350	288	na	na	76	6.10	312	na	90	9.48	Aga	17	0.65	1.01	65
18	609.6	9.53	241	350	288	na	na	95	6.10	237	na	90	9.92	Aga	18	0.64	1.56	64
19	609.6	9.27	241	350	288	na	na	44	6.63	175	na	90	10.00	Aga	19	0.72	0.35	66
20	609.6	9.53	241	350	288	na	na	57	6.38	204	na	90	8.28	Aga	20	0.67	0.56	64
21	609.6	9.53	241	350	288	na	na	57	7.42	254	na	90	10.28	Aga	21	0.78	0.56	64
22	609.6	9.53	241	350	288	na	na	64	5.56	175	na	90	10.48	Aga	22	0.58	0.69	64
23	609.6	9.53	241	350	288	na	na	51	4.78	132	na	90	10.48	Aga	23	0.50	0.44	64
24	609.6	9.53	241	350	288	na	na	57	4.50	163	na	90	10.48	Aga	24	0.47	0.56	64
25	609.6	9.65	241	350	288	na	na	127	6.88	574	na	90	10.41	Aga	25	0.71	2.74	63
26	762.0	9.53	359	471	428	na	na	70	9.53	253	na	90	12.03	Aga	26	1.00	0.67	80
27	762.0	9.53	359	471	423	na	na	140	3.71	208	na	90	12.69	Aga	27	0.39	2.69	80
28	762.0	9.53	359	471	428	na	na	114	2.92	206	na	90	13.07	Aga	28	0.31	1.80	80
29	762.0	9.53	359	471	457	na	na	102	5.84	272	na	90	12.24	Aga	29	0.61	1.42	80
30	762.0	9.53	359	471	487	na	na	41	5.31	118	na	90	14.76	Aga	30	0.56	0.23	80
31	762.0	9.53	359	471	459	na	na	51	5.31	135	na	90	13.79	Aga	31	0.56	0.36	80
32	508.0	8.26	241	350	283	na	na	146	5.31	372	na	90	7.93	Aga	32	0.64	5.09	62
33	508.0	8.26	241	350	283	na	na	165	5.56	317	na	90	11.69	Aga	33	0.67	6.50	62
34	406.4	7.87	172	264	197	na	na	114	5.84	355	na	90	7.59	Aga	34	0.74	4.08	52
35	406.4	7.87	172	264	197	na	na	127	6.10	393	na	90	8.76	Aga	35	0.77	5.04	52
36	406.4	7.87	172	264	197	na	na	152	7.16	474	na	90	5.66	Aga	36	0.91	7.26	52
37	406.4	7.87	172	264	197	na	na	70	6.91	225	na	90	6.14	Aga	37	0.88	1.52	52
38	406.4	7.87	172	264	196	na	na	159	5.05	454	na	90	8.90	Aga	38	0.64	7.88	52
39	609.6	10.59	241	350	346	na	na	330	7.37	1266	na	90	9.62	Aga	39	0.70	16.89	58
40	609.6	10.41	241	350	323	na	na	203	9.65	1152	na	90	11.45	Aga	40	0.93	6.50	59
41	609.6	10.06	241	350	346	na	na	146	9.14	603	na	90	6.41	Aga	41	0.91	3.48	61
42	609.6	11.28	241	350	346	na	na	210	5.59	874	na	90	13.10	Aga	42	0.50	6.39	54
43	609.6	9.30	241	350	372	na	na	381	6.99	630	na	90	10.10	Aga	43	0.75	25.61	66
44	609.6	9.25	241	350	359	na	na	330	6.45	1000	na	90	8.72	Aga	44	0.70	19.35	66
45	609.6	9.02	241	350	359	na	na	165	7.34	443	na	90	10.38	Aga	45	0.81	4.96	68
46	609.6	8.10	241	350	328	na	na	140	5.49	303	na	90	11.94	Aga	46	0.68	3.95	75
47	609.6	8.43	241	350	310	na	na	114	5.59	330	na	90	12.08	Aga	47	0.66	2.54	72
48	609.6	9.53	241	350	371	na	na	406	7.49	1860	na	90	5.12	Aga	48	0.79	28.44	64
49	609.6	9.53	255	366	337	na	na	229	8.13	1028	na	90	5.43	Aga	49	0.85	9.00	64
50	508.0	7.92	241	350	345	na	na	305	6.40	1734	na	90	4.92	Aga	50	0.81	23.08	64

APPENDIX A EXPERIMENTAL DATABASES - TABLES

No [-]	Dia [mm]	t [mm]	SMYS MPa	SMTS MPa	σ(y) MPa	σ(u) MPa	ε(u) [-]	L [mm]	d [mm]	A [mm^2]	W [mm]	Angle [deg]	Pb [MPa]	Source	Ref.	d/t [-]	L^2/Dt [-]	D/t [-]
51	508.0	7.75	241	350	380	na	na	267	5.33	910	na	90	11.54	Aga	51	0.69	18.07	66
52	609.6	9.17	241	350	327	na	na	267	8.10	506	na	90	8.90	Aga	52	0.88	12.73	66
53	609.6	9.17	241	350	284	na	na	318	7.24	364	na	90	10.17	Aga	53	0.79	18.03	66
54	609.6	9.02	241	350	347	na	na	216	6.17	283	na	90	12.01	Aga	54	0.68	8.48	68
55	609.6	9.42	241	350	310	na	na	267	7.01	668	na	90	9.36	Aga	55	0.74	12.38	65
56	609.6	9.42	241	350	310	na	na	267	7.39	515	na	90	9.36	Aga	56	0.78	12.38	65
57	609.6	9.45	241	350	332	na	na	559	7.21	659	na	90	11.03	Aga	57	0.76	54.21	65
58	609.6	9.25	241	350	332	na	na	216	5.69	745	na	90	11.34	Aga	58	0.62	8.27	66
59	609.6	9.30	241	350	297	na	na	318	6.15	397	na	90	12.47	Aga	59	0.66	17.79	66
60	609.6	9.30	241	350	355	na	na	102	4.85	468	na	90	10.92	Aga	60	0.52	1.82	66
61	609.6	9.35	241	350	329	na	na	711	7.32	661	na	90	10.55	Aga	61	0.78	88.77	65
62	508.0	7.19	241	350	261	na	na	762	4.62	1533	na	90	7.52	Aga	62	0.64	159.01	71
63	508.0	6.96	241	350	279	na	na	305	3.30	378	na	90	11.99	Aga	63	0.47	26.28	73
64	508.0	7.90	241	350	243	na	na	216	6.07	156	na	90	11.68	Aga	64	0.77	11.62	64
65	508.0	7.90	241	350	243	na	na	279	2.67	203	na	90	11.68	Aga	65	0.34	19.45	64
66	508.0	6.76	241	350	277	na	na	394	3.66	509	na	90	10.39	Aga	66	0.54	45.16	75
67	508.0	7.85	241	350	289	na	na	305	5.54	254	na	90	12.52	Aga	67	0.71	23.30	65
68	762.0	9.45	359	471	419	na	na	914	3.30	1126	na	90	12.72	Aga	68	0.35	116.13	81
69	762.0	9.55	359	471	359	na	na	305	5.84	1205	na	90	10.45	Aga	69	0.61	12.77	80
70	762.0	9.53	359	471	416	na	na	305	3.56	773	na	90	12.52	Aga	70	0.37	12.80	80
71	762.0	9.70	359	471	438	na	na	508	3.68	789	na	90	13.12	Aga	71	0.38	34.90	79
72	762.0	9.55	359	471	407	na	na	508	3.30	977	na	90	12.31	Aga	72	0.35	35.46	80
73	762.0	9.60	359	471	428	na	na	838	2.79	994	na	90	13.21	Aga	73	0.29	96.03	79
74	762.0	9.63	359	471	451	na	na	356	4.32	684	na	90	12.24	Aga	74	0.45	17.24	79
75	762.0	9.68	359	471	359	na	na	305	7.62	665	na	90	7.72	Aga	75	0.79	12.60	79
76	762.0	9.60	359	471	422	na	na	203	4.32	437	na	90	11.86	Aga	76	0.45	5.64	79
77	762.0	9.58	359	471	426	na	na	305	4.06	658	na	90	12.34	Aga	77	0.42	12.73	80
78	762.0	9.47	359	471	415	na	na	229	2.79	439	na	90	12.69	Aga	78	0.29	7.24	80
79	609.6	9.53	255	366	290	na	na	851	8.18	3505	na	90	5.54	Aga	79	0.86	124.69	64
80	762.0	9.27	359	471	404	na	na	406	5.82	1441	na	90	6.81	Aga	80	0.63	23.38	82
81	762.0	9.53	359	471	474	na	na	686	6.22	3615	na	90	6.84	Aga	81	0.65	64.80	80
82	762.0	9.53	386	495	444	na	na	191	3.81	350	na	90	13.59	Aga	82	0.40	5.00	80
83	508.0	6.60	359	471	421	na	na	406	5.54	1612	na	90	5.76	Aga	83	0.84	49.23	77
84	914.4	8.38	448	542	448	na	na	406	5.54	1368	na	90	5.34	Aga	84	0.66	21.55	109
85	762.0	7.57	414	517	490	na	na	1600	6.83	4553	na	90	5.62	Aga	85	0.90	443.96	101
86	558.8	5.03	359	471	421	na	na	152	3.76	315	na	90	5.71	Aga	86	0.75	8.26	111

APPENDIX A EXPERIMENTAL DATABASES - TABLES

No [-]	Dia [mm]	t [mm]	SMYS MPa	SMTS MPa	σ(y) MPa	σ(u) MPa	ε(u) [-]	L [mm]	d [mm]	A [mm²]	W [mm]	Angle [deg]	Pb [MPa]	Source	Ref.	d/t [-]	L²/Dt [-]	D/t [-]
87	508.0	6.35	414	517	na	na	na	381	2.54	-	25	20	14.55	Nova	1	0.40	45.00	80
88	508.0	6.35	414	517	na	na	na	381	2.54	-	25	30	13.85	Nova	2	0.40	45.00	80
89	508.0	6.35	414	517	na	na	na	381	2.54	-	25	45	12.35	Nova	3	0.40	45.00	80
90	508.0	6.35	414	517	na	na	na	191	2.54	-	25	20	15.85	Nova	4	0.40	11.31	80
91	508.0	6.35	414	517	na	na	na	381	2.54	-	25	90	11.25	Nova	5	0.40	45.00	80
92	508.0	6.35	414	517	na	na	na	1016	2.54	-	25	90	11.55	Nova	6	0.40	320.00	80
93	508.0	6.35	414	517	na	na	na	381	2.54	-	25	90	13.05	Nova	7	0.40	45.00	80
94	508.0	6.35	414	517	na	na	na	457	0.00	-	25	90	13.05	Nova	8	0.00	64.74	80
95	508.0	6.35	414	517	na	na	na	152	0.00	-	25	90	13.05	Nova	9	0.00	7.16	80
96	508.0	6.35	414	517	na	na	na	650	2.54	-	25	20	15.25	Nova	10	0.40	130.98	80
97	508.0	6.35	414	517	na	na	na	508	2.54	-	25	90	11.05	Nova	11	0.40	80.00	80
98	508.0	6.35	414	517	na	na	na	508	2.54	-	25	90	10.55	Nova	12	0.40	80.00	80
99	508.0	6.35	414	517	na	na	na	∞	0.00	-	25	90	15.45	Nova	13	0.00	na	80
100	508.0	6.40	414	517	na	na	na	∞	0.00	-	25	90	15.25	Nova	14	0.00	na	79
101	508.0	6.40	414	517	na	na	na	900	3.43	-	25	90	8.00	Nova	15	0.54	249.14	79
102	508.0	6.40	414	517	na	na	na	900	2.16	-	25	90	11.80	Nova	16	0.34	249.14	79
103	508.0	6.40	414	517	na	na	na	103	3.01	-	102	0	12.50	Nova	17	0.47	3.26	79
104	508.0	6.40	414	517	na	na	na	205	2.94	-	204	0	9.80	Nova	18	0.46	12.93	79
105	508.0	6.40	414	517	na	na	na	205	3.37	-	394	90	8.45	Nova	19	0.53	12.93	79
106	508.0	6.40	414	517	na	na	na	1000	3.18	-	25	90	8.40	Nova	20	0.50	307.58	79
107	610.0	12.34	359	471	451	577	na	3048	4.94	-	na	90	14.44	British	Ves. 1-1	0.40	1234.2	49
108	610.0	12.34	359	471	447	564	na	610	4.94	-	na	90	14.00	British	Ves. 2-1	0.40	49.43	49
109	610.0	12.34	359	471	447	564	na	305	4.94	-	na	90	15.45	British	Ves. 2-2	0.40	12.36	49
110	610.0	12.34	359	471	447	564	na	305	4.94	-	na	90	16.46	British	Ves. 2-3	0.40	12.36	49
111	610.0	12.34	359	471	447	564	na	152	4.94	-	574	90	18.45	British	Ves. 2-4	0.40	3.07	49
112	610.0	12.34	359	471	451	577	na	∞	0.00	-	574	90	21.30	British	Ring 1-1	0.00	na	49
113	610.0	12.34	359	471	451	577	na	∞	4.94	-	574	90	14.90	British	Ring 1-2	0.40	na	49
114	610.0	12.34	359	471	451	577	na	∞	0.00	-	574	90	21.20	British	Ring 2-1	0.00	na	49
115	610.0	12.34	359	471	451	577	na	∞	4.94	-	574	90	14.40	British	Ring 2-2	0.40	na	49
116	914.0	22.00	414	517	434	563	na	∞	0.00	-	574	90	26.30	British	1	0.00	na	42
117	914.0	22.00	414	517	434	563	na	∞	0.00	-	574	90	26.40	British	2	0.00	na	42
118	914.0	22.00	414	517	434	563	na	∞	6.60	-	574	90	18.70	British	3	0.30	na	42
119	914.0	22.00	414	517	434	563	na	∞	6.16	-	574	90	19.50	British	4	0.28	na	42
120	914.0	22.00	414	517	434	563	na	∞	10.34	-	574	90	14.70	British	5	0.47	na	42
121	914.0	22.00	414	517	434	563	na	∞	11.00	-	574	90	13.00	British	6	0.50	na	42
122	914.0	22.00	414	517	434	563	na	∞	15.18	-	574	90	8.60	British	7	0.69	na	42
123	914.0	22.00	414	517	434	563	na	∞	14.74	-	574	90	8.10	British	8	0.67	na	42
124	914.0	22.00	414	517	434	563	na	∞	14.74	-	574	90	8.20	British	9	0.67	na	42

APPENDIX A EXPERIMENTAL DATABASES - TABLES

No [-]	Dia [mm]	t [mm]	SMYS MPa	SMTS MPa	σ(y) MPa	σ(u) MPa	ε(u) [-]	L [mm]	d [mm]	A [mm²]	W [mm]	Angle [deg]	Pb [MPa]	Source	Ref.	d/t [-]	L²/Dt [-]	D/t [-]
125	324.0	5.93	317	432	378	502	0.111	47	4.68	-	43	90	13.49	Waterloo	F1	0.79	1.15	55
126	324.0	6.07	317	432	381	542	0.191	59	4.01	-	53	90	14.29	Waterloo	F4	0.66	1.77	53
127	324.0	5.84	317	432	382	570	0.179	33	3.91	-	21	90	16.29	Waterloo	F5	0.67	0.58	55
128	324.0	5.99	317	432	351	543	0.065	26	4.67	-	20	90	15.36	Waterloo	F7	0.78	0.35	54
129	324.0	6.00	317	432	403	575	0.175	29	4.38	-	30	90	16.09	Waterloo	F14A	0.73	0.43	54
130	324.0	6.07	317	432	421	520	0.107	41	2.91	-	34	90	16.95	Waterloo	F17	0.48	0.85	53
131	324.0	5.58	317	432	346	516	0.212	35	4.41	-	31	90	13.00	Waterloo	F18	0.79	0.68	58
132	324.0	6.14	317	432	375	509	0.185	29	2.39	-	24	90	15.78	Waterloo	F20	0.39	0.42	53
133	324.0	6.16	317	432	356	463	0.041	37	4.50	-	30	90	14.29	Waterloo	F25	0.73	0.69	53
134	324.0	5.95	317	432	356	514	0.188	39	4.17	-	27	90	15.57	Waterloo	F29	0.70	0.79	54
135	324.0	6.02	317	432	359	529	0.157	50	1.99	-	24	90	16.12	Waterloo	F32B	0.33	1.28	54
136	324.0	6.40	317	432	382	570	0.179	20	3.23	-	19	90	16.64	Waterloo	S1co	0.50	0.19	51
137	324.0	6.01	317	432	382	570	0.179	19	3.60	-	19	90	16.22	Waterloo	S2co	0.60	0.19	54
138	324.0	6.30	317	432	373	522	0.179	20	3.57	-	19	90	15.95	Waterloo	S3co	0.57	0.19	51
139	323.0	6.31	317	432	373	522	0.160	20	3.73	-	20	90	14.16	Waterloo	S4co	0.59	0.20	51
140	324.0	6.16	317	432	356	514	0.188	20	3.73	-	20	90	18.85	Waterloo	S1cc	0.61	0.20	53
141	324.0	6.27	317	432	356	514	0.188	20	3.76	-	20	90	19.13	Waterloo	S2cc	0.60	0.20	52
142	324.0	6.25	317	432	356	514	0.188	20	3.79	-	20	90	19.27	Waterloo	S3cc	0.61	0.20	52
143	324.0	6.18	317	432	421	520	0.107	20	3.75	-	20	90	19.44	Waterloo	S4cc	0.61	0.20	52
144	325.0	6.45	317	432	373	522	0.160	21	3.05	-	22	90	15.81	Waterloo	S110	0.47	0.21	50
145	324.0	6.40	317	432	373	522	0.160	39	3.72	-	20	90	13.87	Waterloo	S210	0.58	0.75	51
146	325.0	6.45	317	432	356	463	0.041	20	3.79	-	21	90	14.84	Waterloo	S310	0.59	0.19	50
147	324.0	6.35	317	432	356	463	0.041	20	3.72	-	21	90	15.53	Waterloo	S410	0.59	0.19	51
148	322.0	6.27	317	432	381	542	0.191	20	3.77	-	21	90	17.61	Waterloo	S11c	0.60	0.20	51
149	324.0	6.29	317	432	378	502	0.111	72	3.79	-	21	90	15.11	Waterloo	S21c	0.60	2.57	52
150	324.0	6.24	317	432	381	542	0.191	72	3.79	-	21	90	15.67	Waterloo	S31c	0.61	2.57	52
151	324.0	6.16	317	432	378	502	0.111	20	3.70	-	20	90	15.25	Waterloo	S41c	0.60	0.20	53

13 APPENDIX B COMPARISON, TEST RESULTS AND PREDICTIONS

The formulas and input parameters used for the predictions of the burst capacities listed in the table on the next pages are given in this section. The predictions are normalized by dividing the experimetal test result by the equation predictions.

The input parameters are those given in the table in Section 12.

The B31G formulas

The maximum allowable design pressure is

$$P = \frac{2\,SMYS\,t}{D} \tag{13.1}$$

A constant 'A' is calculated from

$$A = 0.893\left(\frac{L}{\sqrt{Dt}}\right) \tag{13.2}$$

The safe maximum pressure level P′ for the corroded area is

(a) For $A \leq 4$

$$P' = 1.1P\left(\frac{1-\frac{2}{3}\left(\frac{d}{t}\right)}{1-\frac{2}{3}\left(\frac{d}{t\sqrt{A^2+1}}\right)}\right) \tag{13.3}$$

except that P′ may not exceed P.

(b) For $A > 4$

$$P' = 1.1P\left(1-\frac{d}{t}\right) \tag{13.4}$$

except that P′ may not exceed P

The NG-18 surface-flaw equation

The predicted hoop stress level at failure is calculated as

$$\sigma_p = \sigma_{flow} \frac{1 - AREA / AREA_0}{1 - M^{-1}(AREA / AREA_0)} \quad (13.5)$$

, and when L = ∞,

$$\sigma_p = \sigma_{flow} (1 - \frac{d}{t}) \quad (13.6)$$

The Folias factor M is

$$M = \sqrt{1 + \frac{0.8 L^2}{Dt}} \quad (13.7)$$

The burst pressure is calculated as

$$P = \frac{\sigma_p \cdot 2t}{D} \quad (13.8)$$

AREA = A from table when available, else A = L · t
$AREA_0$= L · t
σ_{flow} = SMYS + 69 MPa

Modified B31G Criterion, Effective Area

$$P_b = \left(\frac{2t}{D}\right)(SMYS + 69) \frac{1 - AREA_{eff} / AREA_0}{1 - M^{-1}(AREA_{eff} / AREA_0)} \quad SI\ Unit \quad (13.9)$$

$AREA_{eff}$ = A from table when available, else A = L · t

$AREA_0$ = L · t

L_{eff} = L from table

for $L_{eff}^2/(Dt) \leq 50$

$$M = \left(1 + \frac{1.255}{2}\frac{L_{eff}^2}{Dt} - \frac{0.0135}{4}\frac{L_{eff}^4}{(Dt)^2}\right)^{1/2} \quad (13.10)$$

For $L_{eff}^2/(Dt) > 50$

$$M = 0.032\frac{L_{eff}^2}{Dt} + 3.3 \quad (13.11)$$

Modified B31G Criterion, 0.85 dLArea

$$P_b = \left(\frac{2t}{D}\right)(SMYS + 69)\frac{1 - 0.85\frac{d}{t}}{1 - M^{-1}\left(0.85\frac{d}{t}\right)} \qquad SI\ Unit \tag{13.12}$$

for $L_{eff}^2/(Dt) \le 50$

$$M = \left(1 + \frac{1.255}{2}\frac{L_{eff}^2}{Dt} - \frac{0.0135}{4}\frac{L_{eff}^4}{(Dt)^2}\right)^{1/2} \tag{13.13}$$

For $L_{eff}^2/(Dt) > 50$

$$M = 0.032\frac{L_{eff}^2}{Dt} + 3.3 \tag{13.14}$$

L_{eff} = L from table

Proposed criterion

$$P = \frac{2\sigma_{flow}t}{D}\frac{1 - Q\,AREA / AREA_0}{1 - M^{-1}\,AREA / AREA_0} \tag{13.15}$$

σ_{flow} = σ_u when available, else σ_{flow} = SMTS
AREA = A when available, else
$L^2/Dt < 30$ AREA = 2/3 L · t
$L^2/Dt \ge 30$ AREA = 0.85 L · t
$AREA_0$ = L · t
when L = ∞, AREA/ $AREA_0$ = d/t
γ = 1.0 when compared to the tests in the database

$$Q = \frac{1 - Q_1}{32}\frac{W}{t} + Q_1 \tag{13.16}$$

Q_1 = 0.2 for $0^0 < \psi < 20^0$
Q_1 = 0.02ψ-0.2 for $20^0 < \psi < 60^0$
Q_1 = 1.0 for $\psi > 60^0$

ψ = Angle (deg), 90 = longitudinal, 0 = circumferential

The Folias factor is estimated for $L^2/(Dt) \leq 50$

$$M = \sqrt{1 + \frac{2.51(L/2)^2}{Dt} - \frac{0.054(L/2)^4}{(Dt)^2}} \qquad \textbf{(13.17)}$$

and for $L^2/(Dt) > 50$

$$M = 0.032\frac{L^2}{Dt} + 3.3 \qquad \textbf{(13.18)}$$

No.	Source	Test	Test results/Equation predicted results				
			B31G	NG18	B31G Eff.Area	B31G 0.85dL	Proposed
		[MPa]	[MPa]	[MPa]	[MPa]	[MPa]	[MPa]
1	AGA Database	11.19	1.27	1.12	1.11	1.14	1.01
2	AGA Database	11.17	1.26	1.11	1.10	1.12	1.00
3	AGA Database	11.72	1.37	1.20	1.19	1.30	1.08
4	AGA Database	11.52	1.55	1.22	1.20	1.58	1.09
5	AGA Database	10.52	1.31	1.18	1.15	1.28	1.05
6	AGA Database	7.59	1.18	1.04	1.00	1.11	0.89
7	AGA Database	8.03	1.36	1.17	1.13	1.31	1.00
8	AGA Database	8.41	1.45	1.29	1.25	1.41	1.11
9	AGA Database	7.17	0.97	0.81	0.80	0.85	0.71
10	AGA Database	8.03	1.34	1.08	1.05	1.32	0.93
11	AGA Database	7.03	0.99	0.82	0.81	0.88	0.72
12	AGA Database	8.38	1.16	0.97	0.96	1.02	0.85
13	AGA Database	9.10	1.29	1.09	1.07	1.15	0.95
14	AGA Database	9.10	1.36	1.15	1.12	1.25	0.99
15	AGA Database	9.21	1.38	1.13	1.10	1.28	0.98
16	AGA Database	9.31	1.25	1.04	1.03	1.06	0.91
17	AGA Database	9.48	1.38	1.19	1.16	1.26	1.03
18	AGA Database	9.92	1.49	1.14	1.13	1.37	1.00
19	AGA Database	10.00	1.37	1.15	1.13	1.21	1.01
20	AGA Database	8.28	1.13	0.94	0.93	1.01	0.82
21	AGA Database	10.28	1.46	1.22	1.19	1.35	1.05
22	AGA Database	10.48	1.42	1.17	1.15	1.26	1.02
23	AGA Database	10.48	1.39	1.14	1.13	1.17	1.00
24	AGA Database	10.48	1.39	1.16	1.15	1.18	1.02
25	AGA Database	10.41	1.73	1.47	1.42	1.70	1.26
26	AGA Database	12.03	1.69	1.26	1.24	2.15	1.12
27	AGA Database	12.69	1.48	1.28	1.27	1.41	1.15
28	AGA Database	13.07	1.46	1.33	1.31	1.36	1.19
29	AGA Database	12.24	1.51	1.29	1.27	1.48	1.15
30	AGA Database	14.76	1.65	1.43	1.42	1.46	1.29
31	AGA Database	13.79	1.54	1.35	1.34	1.40	1.21
32	AGA Database	7.93	1.30	0.98	0.96	1.27	0.85
33	AGA Database	11.69	2.02	1.37	1.35	2.01	1.20
34	AGA Database	7.59	1.55	1.08	1.06	1.46	0.97
35	AGA Database	8.76	1.90	1.27	1.24	1.85	1.14
36	AGA Database	5.66	1.50	0.85	0.83	1.78	0.76
37	AGA Database	6.14	1.22	0.81	0.79	1.20	0.72
38	AGA Database	8.90	1.78	1.29	1.27	1.62	1.16
39	AGA Database	9.62	1.71	1.27	1.24	1.79	1.10
40	AGA Database	11.45	2.48	1.85	1.79	3.29	1.59
41	AGA Database	6.41	1.28	0.84	0.82	1.55	0.72
42	AGA Database	13.10	1.73	1.54	1.51	1.60	1.34
43	AGA Database	10.10	5.02	1.25	1.24	2.47	1.10
44	AGA Database	8.72	1.79	1.27	1.25	1.88	1.11
45	AGA Database	10.38	2.19	1.40	1.37	2.41	1.22
46	AGA Database	11.94	2.40	1.72	1.69	2.35	1.50
47	AGA Database	12.08	2.20	1.72	1.68	2.09	1.49
48	AGA Database	5.12	2.89	0.92	0.89	1.33	0.79
49	AGA Database	5.43	1.15	0.85	0.83	1.39	0.73
50	AGA Database	4.92	3.09	1.51	1.45	1.32	1.29
51	AGA Database	11.54	2.33	1.94	1.89	2.43	1.68

52	AGA Database	8.90	2.23	1.13	1.12	2.84	0.99
53	AGA Database	10.17	2.33	1.21	1.20	2.65	1.06
54	AGA Database	12.01	2.35	1.45	1.44	2.39	1.28
55	AGA Database	9.36	1.92	1.22	1.21	2.07	1.07
56	AGA Database	9.36	2.01	1.15	1.14	2.25	1.01
57	AGA Database	11.03	5.66	1.29	1.28	2.84	1.13
58	AGA Database	11.34	2.03	1.66	1.63	1.99	1.44
59	AGA Database	12.47	2.44	1.47	1.46	2.50	1.30
60	AGA Database	10.92	1.61	1.56	1.51	1.44	1.34
61	AGA Database	10.55	5.96	1.22	1.21	2.95	1.07
62	AGA Database	7.52	2.80	1.16	1.15	1.77	1.02
63	AGA Database	11.99	3.14	1.65	1.64	2.12	1.45
64	AGA Database	11.68	2.44	1.29	1.29	2.68	1.14
65	AGA Database	11.68	1.72	1.30	1.30	1.56	1.15
66	AGA Database	10.39	3.21	1.51	1.49	2.11	1.33
67	AGA Database	12.52	5.18	1.43	1.42	2.74	1.26
68	AGA Database	12.72	2.00	1.36	1.35	1.63	1.23
69	AGA Database	10.45	1.57	1.46	1.43	1.67	1.29
70	AGA Database	12.52	1.56	1.47	1.45	1.53	1.32
71	AGA Database	13.12	2.11	1.39	1.38	1.65	1.25
72	AGA Database	12.31	1.90	1.39	1.37	1.52	1.25
73	AGA Database	13.21	1.88	1.38	1.37	1.57	1.25
74	AGA Database	12.24	1.62	1.34	1.33	1.62	1.21
75	AGA Database	7.72	1.37	0.86	0.85	1.65	0.77
76	AGA Database	11.86	1.49	1.28	1.27	1.46	1.15
77	AGA Database	12.34	1.59	1.38	1.37	1.57	1.24
78	AGA Database	12.69	1.49	1.38	1.37	1.42	1.24
79	AGA Database	5.54	4.47	0.92	0.91	1.82	0.80
80	AGA Database	6.81	1.90	0.97	0.95	1.20	0.86
81	AGA Database	6.84	2.00	1.32	1.29	1.29	1.17
82	AGA Database	13.59	1.54	1.35	1.34	1.50	1.23
83	AGA Database	5.76	3.48	1.17	1.14	1.54	1.03
84	AGA Database	5.34	1.74	0.85	0.84	1.09	0.80
85	AGA Database	5.62	6.39	0.92	0.92	2.41	0.86
86	AGA Database	5.71	1.31	1.07	1.05	1.51	0.95
87	NOVA Tests	14.55	2.13	1.88	1.84	1.70	1.17
88	NOVA Tests	13.85	2.03	1.79	1.75	1.61	1.21
89	NOVA Tests	12.35	1.81	1.59	1.56	1.44	1.24
90	NOVA Tests	15.85	1.74	1.91	1.87	1.75	1.19
91	NOVA Tests	11.25	1.65	1.45	1.42	1.31	1.33
92	NOVA Tests	11.55	1.69	1.55	1.55	1.41	1.44
93	NOVA Tests	13.05	1.91	1.68	1.65	1.52	1.54
94	NOVA Tests	13.05	1.26	1.08	1.08	1.08	1.01
95	NOVA Tests	13.05	1.26	1.08	1.08	1.08	1.01
96	NOVA Tests	15.25	2.23	2.02	1.99	1.83	1.27
97	NOVA Tests	11.05	1.62	1.45	1.42	1.31	1.33
98	NOVA Tests	10.55	1.54	1.38	1.36	1.25	1.27
99	NOVA Tests	15.45	1.49	1.28	1.28	1.28	1.19
100	NOVA Tests	15.25	1.46	1.25	1.25	1.25	1.17
101	NOVA Tests	8.00	1.50	1.36	1.35	1.16	1.26
102	NOVA Tests	11.80	1.55	1.43	1.42	1.33	1.33
103	NOVA Tests	12.50	1.33	1.46	1.41	1.32	0.97
104	NOVA Tests	9.80	1.12	1.29	1.26	1.15	1.17
105	NOVA Tests	8.45	1.02	1.24	1.20	1.06	1.12
106	NOVA Tests	8.40	1.45	1.33	1.32	1.16	1.23
107	British Gas Tests	14.44	1.51	1.37	1.38	1.26	1.02

108	British Gas Tests	14.00	1.46	1.26	1.24	1.14	0.94
109	British Gas Tests	15.45	1.21	1.31	1.28	1.19	0.97
110	British Gas Tests	16.46	1.29	1.39	1.37	1.27	1.03
111	British Gas Tests	18.45	1.35	1.40	1.36	1.29	1.03
112	British Gas Tests	21.30	1.47	1.23	1.23	1.23	0.91
113	British Gas Tests	14.90	1.56	1.44	1.44	1.31	1.06
114	British Gas Tests	21.20	1.46	1.23	1.23	1.23	0.91
115	British Gas Tests	14.40	1.50	1.39	1.39	1.26	1.03
116	British Gas Tests	26.30	1.32	1.13	1.13	1.13	0.97
117	British Gas Tests	26.40	1.33	1.14	1.14	1.14	0.97
118	British Gas Tests	18.70	1.22	1.15	1.15	1.08	0.99
119	British Gas Tests	19.50	1.24	1.17	1.17	1.10	1.00
120	British Gas Tests	14.70	1.27	1.19	1.19	1.05	1.02
121	British Gas Tests	13.00	1.19	1.12	1.12	0.97	0.96
122	British Gas Tests	8.60	1.27	1.19	1.19	0.90	1.02
123	British Gas Tests	8.10	1.12	1.06	1.06	0.81	0.91
124	British Gas Tests	8.20	1.13	1.07	1.07	0.82	0.92
125	U.Waterloo Tests	13.49	1.38	1.95	1.80	1.42	0.93
126	U.Waterloo Tests	14.29	1.40	1.67	1.58	1.38	0.88
127	U.Waterloo Tests	16.29	1.47	1.58	1.51	1.39	0.88
128	U.Waterloo Tests	15.36	1.34	1.52	1.43	1.27	0.84
129	U.Waterloo Tests	16.09	1.41	1.55	1.47	1.33	0.84
130	U.Waterloo Tests	16.95	1.44	1.42	1.38	1.33	0.95
131	U.Waterloo Tests	13.00	1.32	1.69	1.57	1.30	0.86
132	U.Waterloo Tests	15.78	1.31	1.17	1.15	1.14	0.85
133	U.Waterloo Tests	14.29	1.28	1.49	1.40	1.23	0.94
134	U.Waterloo Tests	15.57	1.45	1.65	1.56	1.39	0.96
135	U.Waterloo Tests	16.12	1.37	1.29	1.26	1.23	0.88
136	U.Waterloo Tests	16.64	1.33	1.17	1.15	1.14	0.78
137	U.Waterloo Tests	16.22	1.38	1.25	1.23	1.20	0.83
138	U.Waterloo Tests	15.95	1.29	1.16	1.14	1.12	0.84
139	U.Waterloo Tests	14.16	1.14	1.04	1.02	0.99	0.75
140	U.Waterloo Tests	18.85	1.56	1.43	1.40	1.36	1.05
141	U.Waterloo Tests	19.13	1.56	1.41	1.39	1.35	1.04
142	U.Waterloo Tests	19.27	1.57	1.43	1.41	1.37	1.06
143	U.Waterloo Tests	19.44	1.61	1.46	1.44	1.40	1.07
144	U.Waterloo Tests	15.81	1.26	1.10	1.09	1.07	0.80
145	U.Waterloo Tests	13.87	1.14	1.17	1.13	1.06	0.84
146	U.Waterloo Tests	14.84	1.18	1.06	1.04	1.02	0.87
147	U.Waterloo Tests	15.53	1.25	1.13	1.11	1.08	0.92
148	U.Waterloo Tests	17.61	1.43	1.29	1.27	1.24	0.91
149	U.Waterloo Tests	15.11	1.44	1.66	1.59	1.41	1.22
150	U.Waterloo Tests	15.67	1.51	1.75	1.67	1.48	1.19
151	U.Waterloo Tests	15.25	1.26	1.15	1.13	1.10	0.87

14 APPENDIX C ALTERNATIVE STRENGTH EQUATIONS

Comarison of predicted σ_{ax} / σ_{flow} based on alternative strength equations for pipes with circumferential defects under axial tensile load.

The equations considered are Kastner's local collapse criterion, Schulze's global collapse criterion, Chell method, and B31G.

Pipe:	**Diameter**	**D**	**914.0 mm**
	Thickness	**t**	**22.0 mm**
	Defect depth	**d**	**variable**
	Defect width	**2*beta**	**15 degree**
	Defect length		**20 mm** (width of the weld)

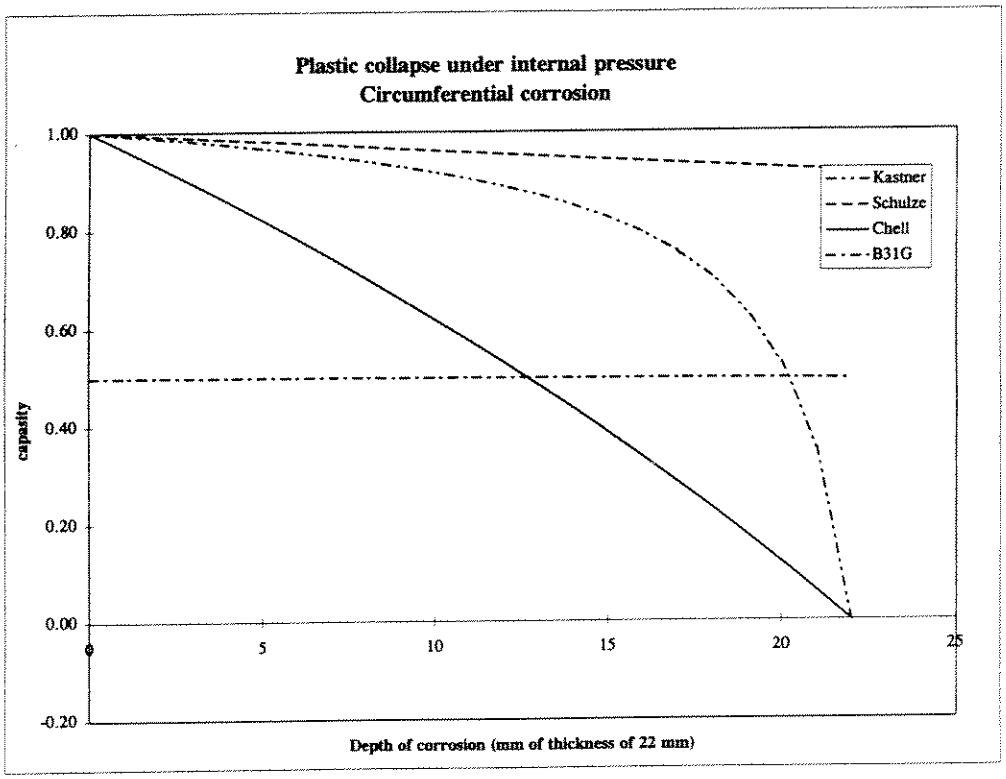

The capacity is calculated as (axial stress) / (sigma flow).
For B31G, 1.1*SMYS is used as sigma flow, and sigma axial is taken as (P*D)/(4*t)

Pipe:	**Diameter**	**D**	**914.0 mm**
	Thickness	**t**	**22.0 mm**
	Defect depth	**d**	**variable**
	Defect width	**2*beta**	**30 degree**
	Defect length		**20 mm** (width of the weld)

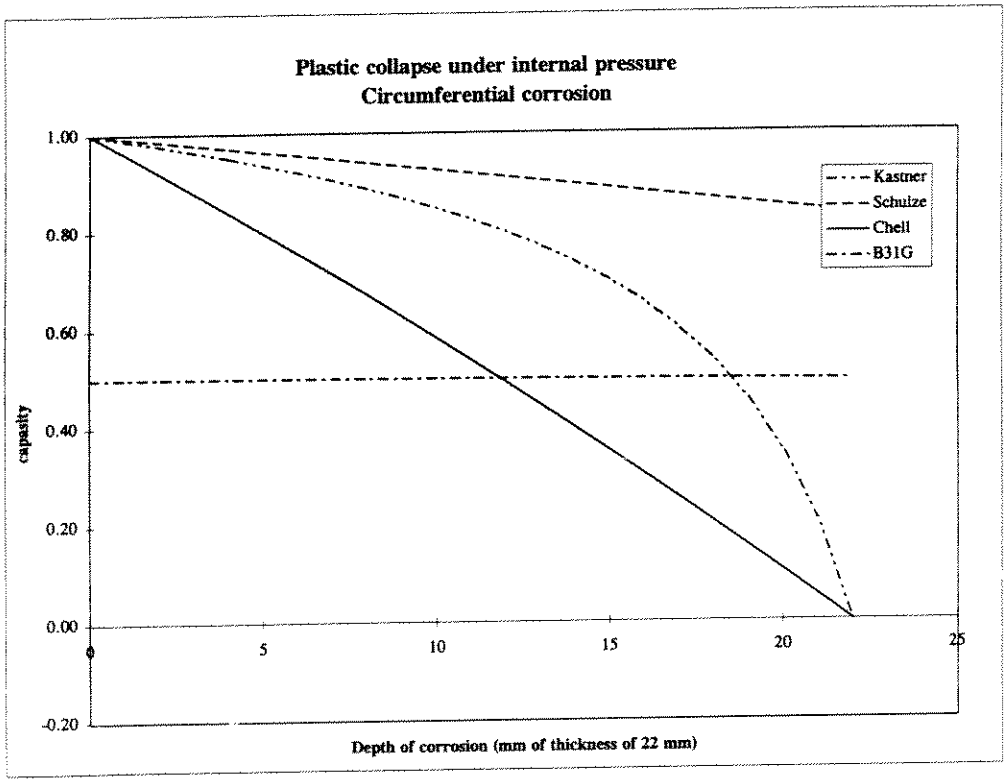

The capacity is calculated as (axial stress) / (sigma flow).
For B31G, 1.1*SMYS is used as sigma flow, and sigma axial is taken as (P*D)/(4*t)

Pipe:	**Diameter**	**D**	**914.0 mm**
	Thickness	**t**	**22.0 mm**
	Defect depth	**d**	**variable**
	Defect width	**2*beta**	**60 degree**
	Defect length		**20 mm** (width of the weld)

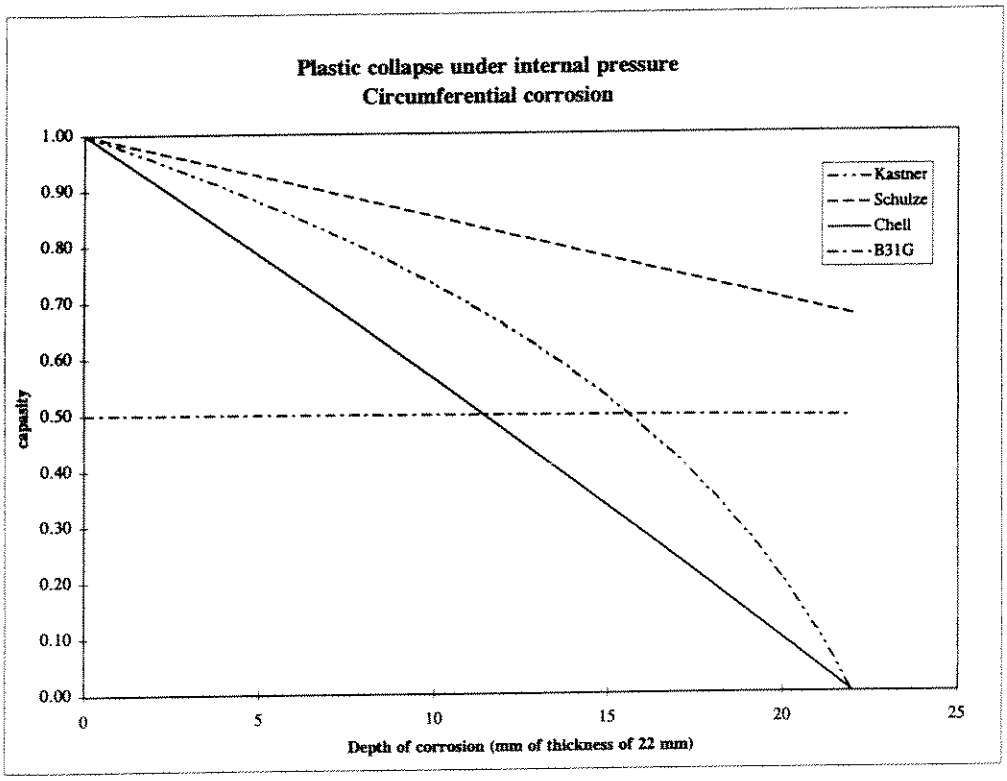

The capacity is calculated as (axial stress) / (sigma flow).
For B31G, 1.1*SMYS is used as sigma flow, and sigma axial is taken as (P*D)/(4*t)

Pipe:	**Diameter**	**D**	**914.0 mm**
	Thickness	**t**	**22.0 mm**
	Defect depth	**d**	**variable**
	Defect width	**2*beta**	**120 degree**
	Defect length		**20 mm** **(width of the weld)**

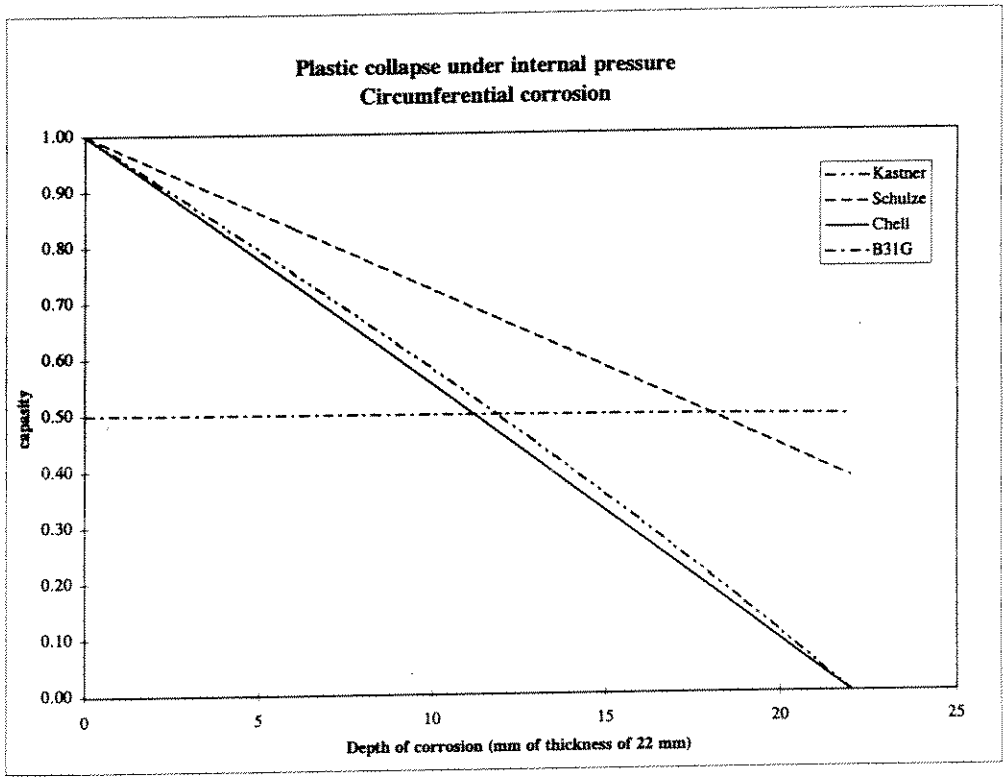

The capacity is calculated as (axial stress) / (sigma flow).
For B31G, 1.1*SMYS is used as sigma flow, and sigma axial is taken as (P*D)/(4*t)

Pipe:	**Diameter**	**D**	**914.0 mm**
	Thickness	**t**	**22.0 mm**
	Defect depth	**d**	**variable**
	Defect width	**2*beta**	**240 degree**
	Defect length		**20 mm** (width of the weld)

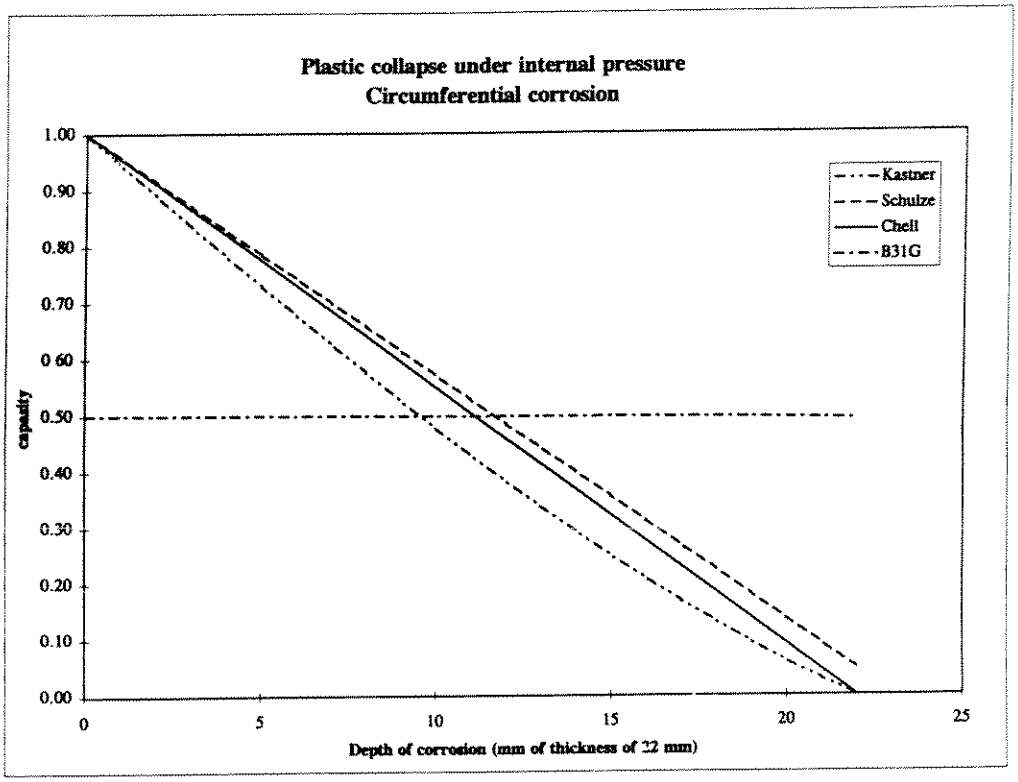

The capacity is calculated as (axial stress) / (sigma flow).
For B31G, 1.1*SMYS is used as sigma flow, and sigma axial is taken as (P*D)/(4*t)

Pipe:	**Diameter**	**D**	**914.0 mm**
	Thickness	**t**	**22.0 mm**
	Defect depth	**d**	**variable**
	Defect width	**2*beta**	**360 degree**
	Defect length		**20 mm** (width of the weld)

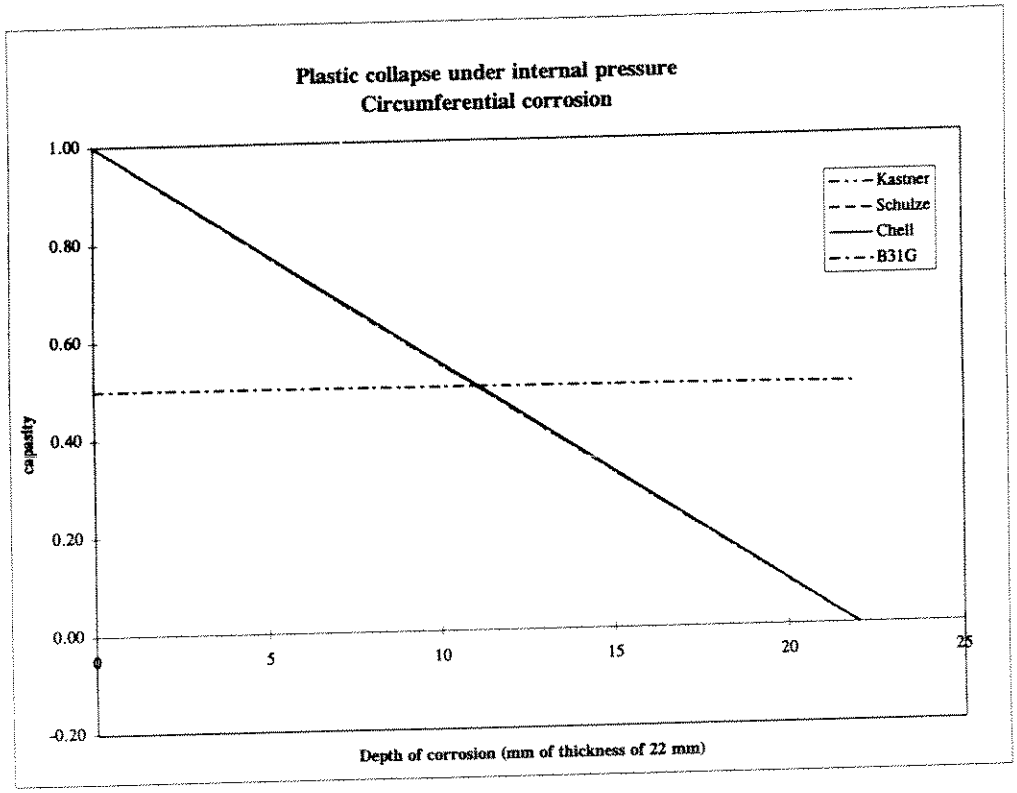

The capacity is calculated as (axial stress) / (sigma flow).
For B31G, 1.1*SMYS is used as sigma flow, and sigma axial is taken as (P*D)/(4*t)

Pipe:	**Diameter**	**D**	**914.0 mm**	
	Thickness	**t**	**22.0 mm**	
	Defect depth	**d**	**4.4 mm**	
	Defect width	**c**	**variable**	
	Defect length		**20 mm**	**(width of the weld)**
	d/t=	**0.20**		

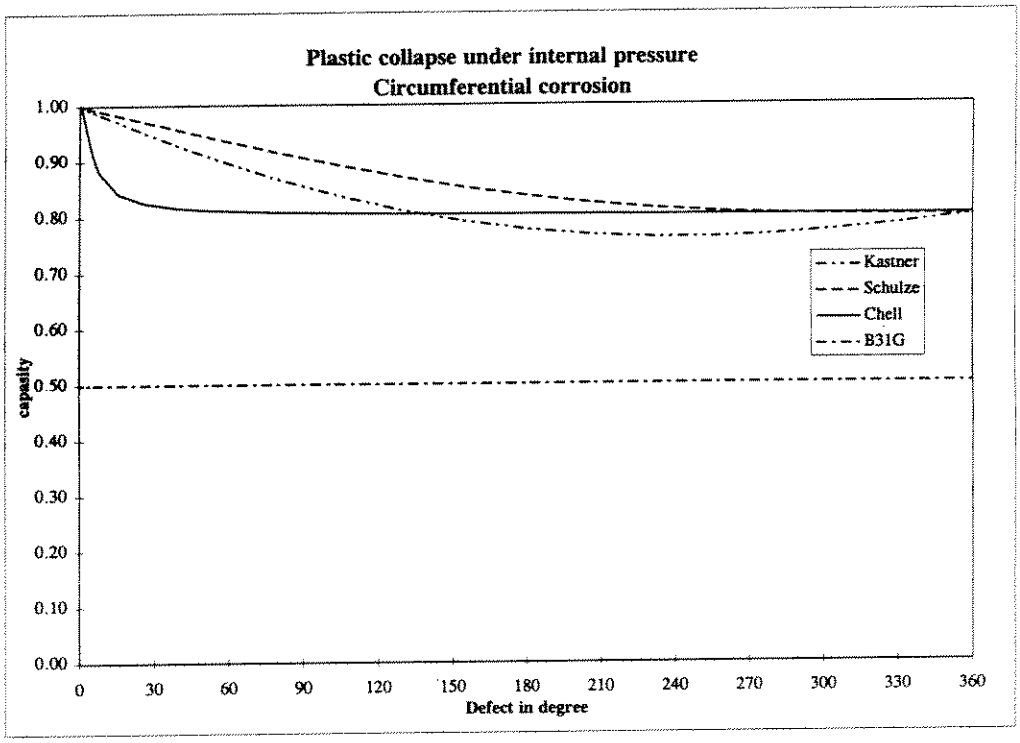

The capacity is calculated as (axial stress) / (sigma flow).
For B31G, 1.1*SMYS is used as sigma flow, and sigma axial is taken as (P*D)/(4*t)

Pipe:	**Diameter**	**D**	**914.0 mm**	
	Thickness	**t**	**22.0 mm**	
	Defect depth	**d**	**6.6 mm**	
	Defect width	**c**	**variable**	
	Defect length		**20 mm**	**(width of the weld)**
	d/t=	**0.30**		

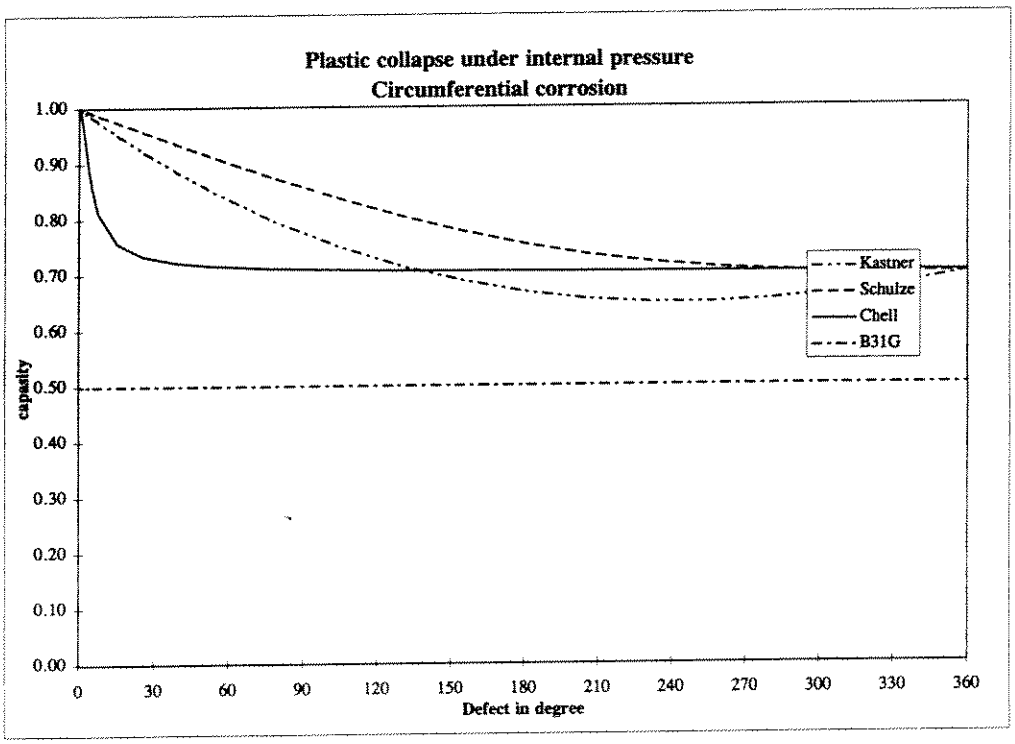

The capacity is calculated as (axial stress) / (sigma flow).
For B31G, 1.1*SMYS is used as sigma flow, and sigma axial is taken as (P*D)/(4*t)

Pipe:	**Diameter**	**D**	**914.0 mm**	
	Thickness	**t**	**22.0 mm**	
	Defect depth	**d**	**8.8 mm**	
	Defect width	**c**	**variable**	
	Defect length		**20 mm**	**(width of the weld)**
	d/t=	**0.40**		

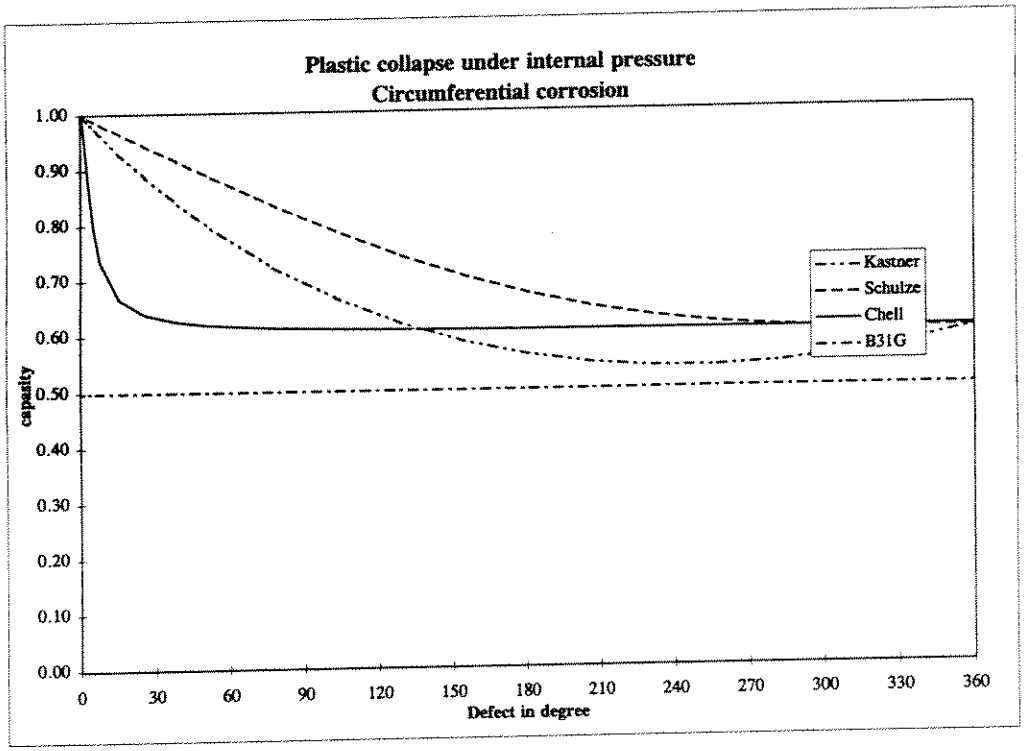

The capacity is calculated as (axial stress) / (sigma flow).
For B31G, 1.1*SMYS is used as sigma flow, and sigma axial is taken as (P*D)/(4*t)

Pipe:	**Diameter**	**D**	**914.0 mm**
	Thickness	**t**	**22.0 mm**
	Defect depth	**d**	**13.2 mm**
	Defect width	**c**	**variable**
	Defect length		**20 mm** (width of the weld)
	d/t=	**0.60**	

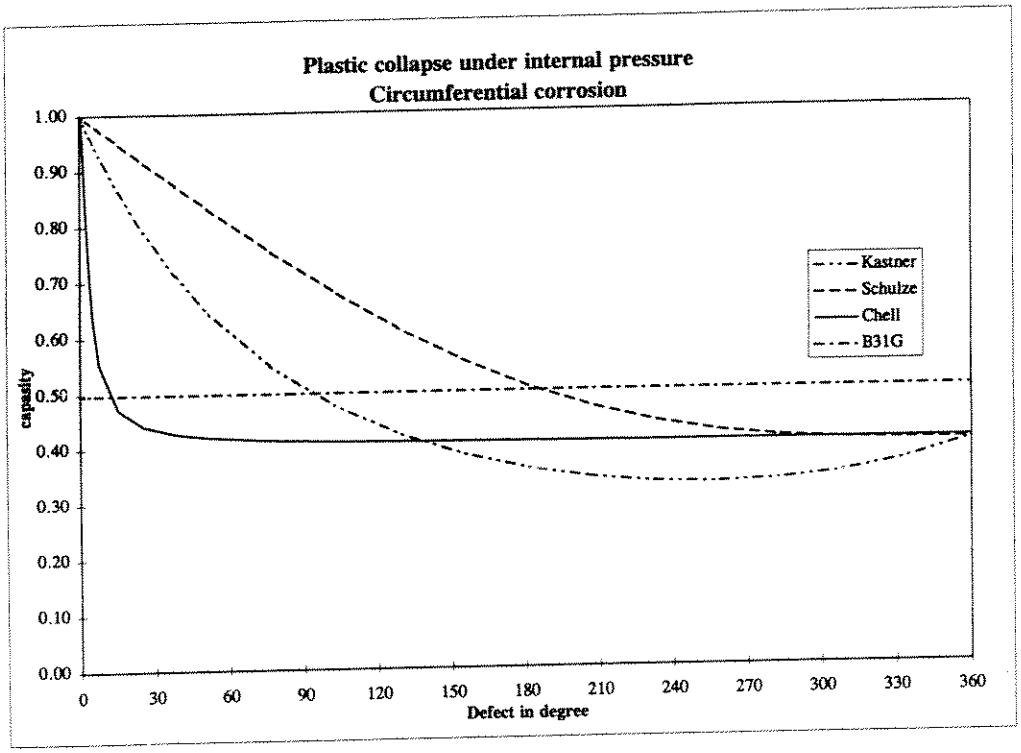

The capacity is calculated as (axial stress) / (sigma flow).
For B31G, 1.1*SMYS is used as sigma flow, and sigma axial is taken as (P*D)/(4*t)

Pipe:	**Diameter**	**D**	**914.0 mm**
	Thickness	**t**	**22.0 mm**
	Defect depth	**d**	**17.6 mm**
	Defect width	**c**	**variable**
	Defect length		**20 mm** (width of the weld)
	d/t=	**0.80**	

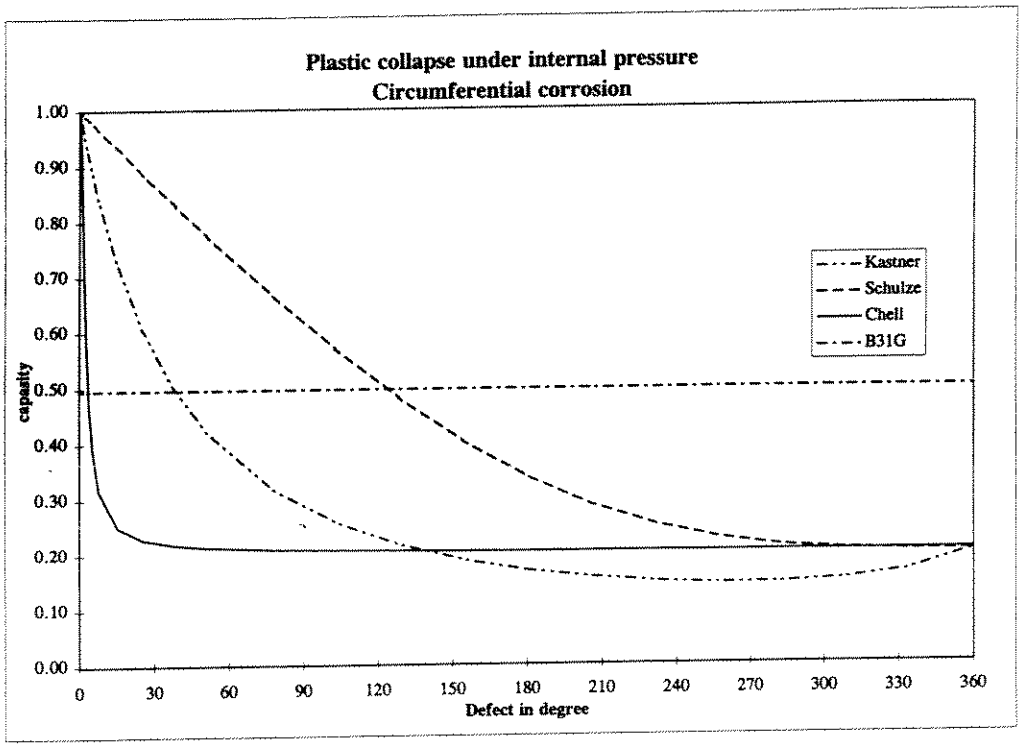

The capacity is calculated as (axial stress) / (sigma flow).
For B31G, 1.1*SMYS is used as sigma flow, and sigma axial is taken as (P*D)/(4*t)